Regulation *of* Gene Expression *during* Oocyte Maturation *and* Early Embryo Development

Bo Yu

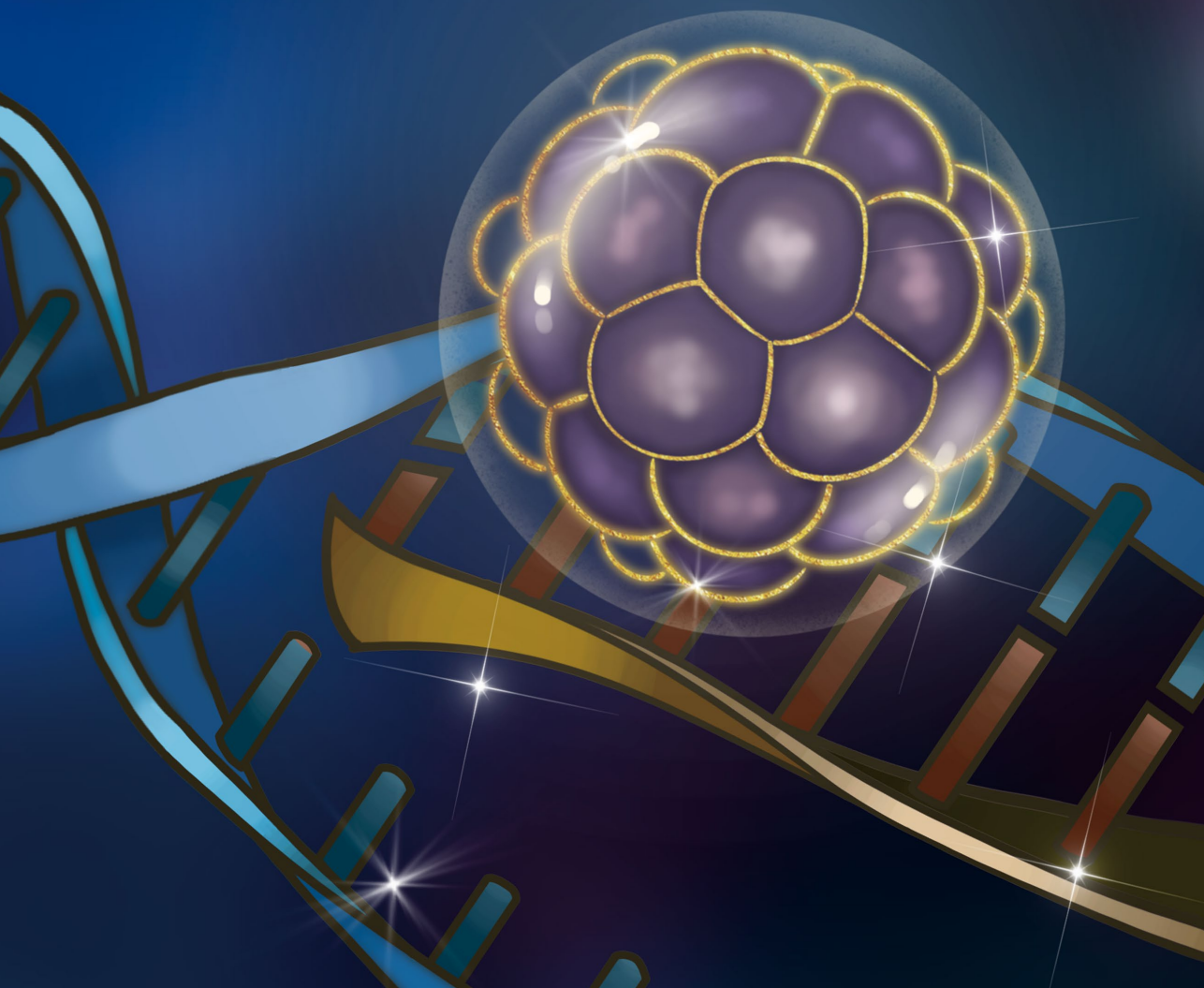

Regulation of gene expression during oocyte maturation and early embryo development

Bo Yu

2022

Regulation of gene expression during oocyte maturation and early embryo development

Regulatie van genexpressie gedurende eicelrijping en vroeg embryonale ontwikkeling

(met een samenvatting in het Nederlands)

Proefschrift

ter verkrijging van de graad van doctor aan de
Universiteit Utrecht
op gezag van de
rector magnificus, prof.dr. H.R.B.M. Kummeling,
ingevolge het besluit van het college voor promoties
in het openbaar te verdedigen op

woensdag 23 februari 2022 des ochtends te 10.15 uur

door

Bo Yu

geboren op 3 oktober 1990
te Wuhan, China

Promotor:

Prof. dr. T.A.E. Stout

Copromotor:

Dr. B.A.J. Roelen

This research is funded by the China Scholarship Council (CSC No. 201606300033)

Content

Chapter 1

General introduction

How can an oocyte give rise to all of the differentiated cells of the fetus and adult, including information on position? The journey starts with fertilization of the oocyte by a spermatozoon to form the single cell zygote. The zygote's genome is a combination of the maternal pronucleus (from the oocyte) and the paternal pronucleus (from the spermatozoon) and contains all the genetic information needed to build the embryo and give rise to all kinds of cell. The zygote undergoes multiple rounds of rapid cell division, although the resulting increase in cell number is not accompanied by an increase in the overall volume of the embryo. In fact, the size of the blastomeres roughly halves at each of these early cleavage divisions. During this period, the blastomeres are considered autonomous and remain uncommitted to any fate. After a series of cleavage divisions that do not need to be synchronized, the embryo has divided into approximately 16 cells and begins to resemble a small mulberry-like ball, known as a morula (Latin, morus: mulberry). At this stage, the first cell lineage specification is initiated: outer cells adhere tightly to each other and form a uniform epithelial layer named the trophectoderm (TE), while the inner cells form the inner cell mass (ICM), with the division heralding the formation of the blastocyst. The TE will contribute to the future placenta. A second cell lineage specification then takes place within the ICM with the formation of the hypoblast and epiblast to respectively establish the yolk sac and the embryo proper.

Almost all cells in a mammal, with the exception for instance of red blood cells, contain essentially the same genome. However, cell type and function become increasingly differentiated as embryonic development progresses, a divergence achieved by regulation of gene expression. Therefore, precise regulation of gene expression is essential for embryonic development and cell fate determination.

Gene expression

In order to understand how gene expression is regulated during oocyte maturation and early embryo development, it is important to first briefly overview how genes are expressed in eukaryotic cells. Gene expression is the process of creating a functional gene product by reading genetic information from the DNA; this consists of two major steps—transcription and translation (Figure 1). Gene expression starts with transcription of the DNA template of a gene into an exact pre-mRNA molecule. To initiate transcription, RNA polymerase binds to a specific DNA sequence known as a promoter and forms a closed polymerase-promoter complex. Subsequently, the complex unwinds approximately 14 base

pairs of the DNA duplex. As a result, part of the promoter DNA, the transcription bubble, is unwound and becomes single stranded. In the transcription bubble, RNA polymerase moves along the single DNA strand to produce complementary RNA molecules, called primary RNA transcripts or pre-mRNAs. The pre-mRNAs must undergo several posttranscriptional processing steps before they can be transferred from the nucleus to the cytoplasm and further translated into a protein. To protect RNA molecules from degradation, both ends of a pre-mRNA need to be chemically modified; the addition of a methylated guanosine 'cap' to the 5′ end and a string of adenosine residues to the 3′ end. Meanwhile, the pre-mRNA undergoes RNA splicing by removing intron sequences and ligating exons

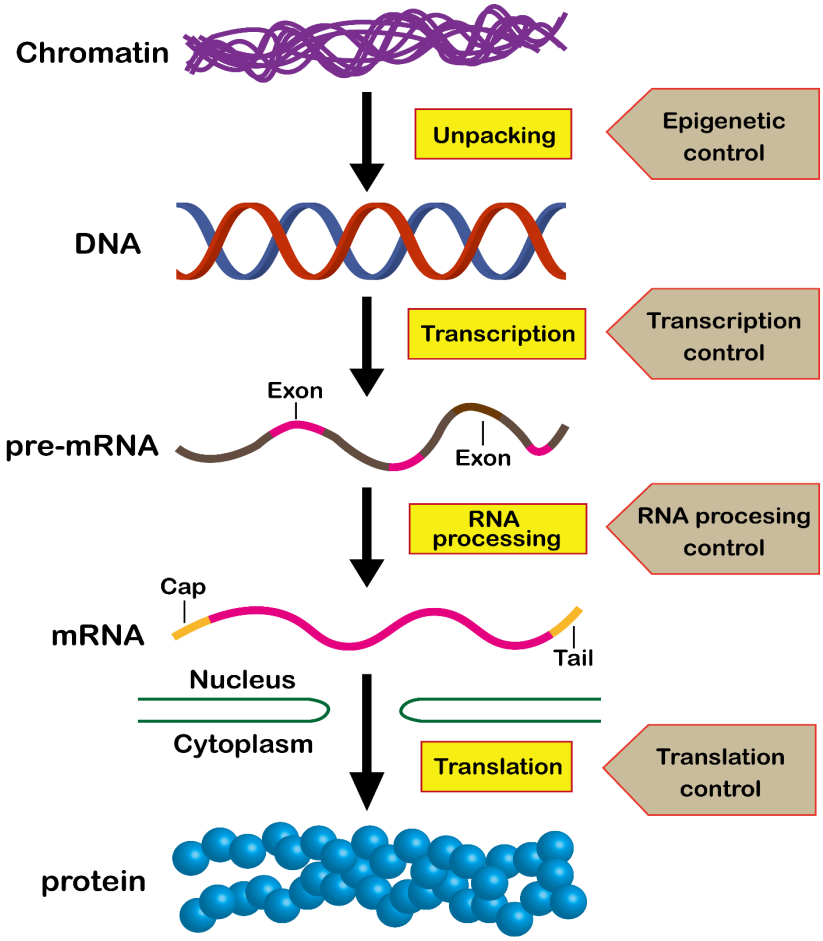

Figure 1. The process of gene expression, and its regulation.

together in an appropriate way (Figure 1). After post-modification, mature and functional mRNAs are transported from the nucleus to the cytoplasm for translation.

Translation is the process by which the genetic information carried in a mature mRNA molecule is converted into a protein, and comprises three distinct steps— initiation, elongation and termination. To initiate transcription, the ribosome and the first tRNA are assembled by eukaryotic initiation factors at the start codon of the target mRNA. After the initiation step, the genetic code of the mRNA is read in triplets by the ribosome and other tRNAs with anticodon matching the mRNA codons, new amino acids are assembled with the formation of peptide bonds during the elongation process. Termination occurs when a stop codon is reached in the A site of the ribosome, which is mediated by release factors. The small and large subunits of ribosome dissociate, releasing the completed gene product (Jackson *et al.* , 2012).

Therefore, there are two main points at which gene expression can be regulated, transcription and translation. However, unlike somatic cells, oocytes and early embryos rely exclusively on regulation of maternal mRNA to achieve changes in gene expression.

Maternal mRNA regulation

In mammals, oocytes initiate meiosis during fetal life and become arrested at the diplotene stage of meiosis I in primordial follicles within the ovary. During this stage, the nucleus of the oocyte is referred to as a germinal vesicle (GV) because the chromosomes are decondensed and the nucleus is relatively large and vesicular. Following puberty, primordial follicles are selectively recruited to develop and oocyte meiosis resumes. The first visible sign of meiosis resumption is germinal vesicle breakdown (GVBD), with the chromatin becoming condensed. As a result, the oocyte is transcriptionally silenced after GVBD and transcription remains inactive throughout oocyte maturation, fertilization, and early embryonic development up to the time of zygotic genome activation (ZGA). As a result, the oocyte and early embryo rely completely on the temporal and spatial activation of maternal transcripts to regulate gene expression during oocyte maturation and early development (Figure 2).

Maternal mRNAs are transcribed and accumulate in the oocyte during oogenesis (Vastenhouw *et al.* , 2019). However, in organisms such as *Drosophila*, maternal transcripts are produced by somatic nurse cells and are transported to the oocyte through microtubules (Cooley and Theurkauf, 1994, Pokrywka and

Stephenson, 1995). After transcription, most maternal mRNAs are translationally repressed and stored for subsequent activation at the appropriate time (Winata and Korzh, 2018). The predominant method for regulating translation activation and repression in oocytes is cytoplasmic polyadenylation and deadenylation.

A long poly(A) tail is closely associated with an increase in mRNA stability and translatability. Unlike in somatic cells, newly synthesized maternal mRNAs are deadenylated and therefore have a short poly(A) tail, at least in mouse, *Xenopus*, and zebrafish oocytes (Esencan *et al.* , 2019, Winata and Korzh, 2018). These maternal mRNAs are in a translationally inactive state and are stored in cytoplasmic granules in preparation for oocyte maturation and early embryonic development (Winata and Korzh, 2018). Interestingly, mRNAs with short poly(A) tails are thought to be less stable and to be easily degraded, which makes them inappropriate subjects for storage in anticipation of oocyte meiosis resumption. In fact, maternal mRNA appears to be very stable with a half-life measured in days, as opposed to the hours measured in most somatic cells (Esencan *et al.*, 2019, Medvedev *et al.* , 2008). These studies raise important questions about how maternal mRNAs with short poly (A) tails maintain their stability for a relatively long period of time and whether the methods of maternal mRNA storage in oocytes follow the same pattern in different species.

Because the genome is transcriptionally silent during and after nuclear maturation, the oocyte starts to recruit stored maternal mRNAs to initiate translation by regulating the mRNA poly(A) tail length. One of the best

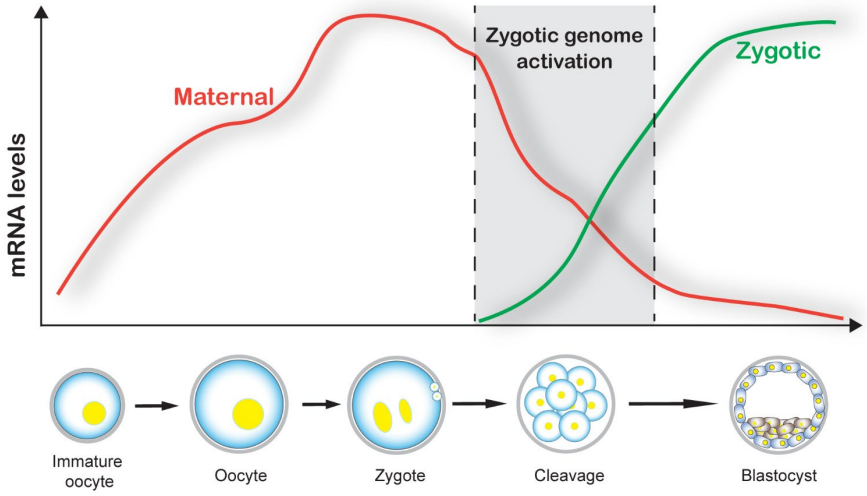

Figure 2. Maternal and zygotic mRNA levels during embryonic development.

characterized examples of the regulation of maternal gene expression is the translational control of cyclin B1 during oocyte maturation. Cyclin B1 is the regulatory subunit of maturation promoting factor (MPF), which plays an essential role in the mouse oocyte's entry into metaphase I from prophase I (Jones, 2004). The cytoplasmic polyadenylation element (CPE) is the main cis-acting element required to regulate cytoplasmic polyadenylation for translational activation and repression, and is located in the 3' untranslated region (UTR) of certain mRNAs including mouse cyclinB1 (*CCNB1*) mRNA (Kotani *et al.* , 2013). It has been demonstrated that elongation of the poly(A) tail is closely correlated with the activation of cyclin B1 translation in the mouse (Kotani *et al.*, 2013). After induction of oocyte maturation in mice, dormant RNA granules are disassembled and the cyclin B1 mRNA is released into the cytoplasm for translational activation (Kotani *et al.*, 2013). In the mouse, *Drosophila* and *Xenopus*, CPE-binding protein (CPEB) then binds to the CPE sequence of the CCNB1 mRNA and recruits cleavage and polyadenylation specificity factor (CPSF) (Dickson *et al.* , 2001, Kim and Richter, 2007, Kotani *et al.*, 2013). In *Xenopus*, CPSF carries the poly(A) polymerase to the mRNA to induce cytoplasmic polyadenylation (Dickson *et al.*, 2001, Monti, 2017). The poly(A) tail of the mRNA is then elongated by poly(A) polymerase after recruitment of poly(A)-binding protein (PABP). PABP also stimulates translation initiation by promoting dissociation of Maskin from eIF4E, resulting in formation of the eIF4E–eIF4G complex (in *Xenopus*: (Barragán-Iglesias *et al.* , 2018, Cao and Richter, 2002). The 40S ribosomal subunit is then recruited to the 5' cap of cyclin B1 mRNA for subsequent translational activation. Considering that cyclin B1 is translated at different times during oocyte maturation, accurate timing of cyclin B1 activation in *Xenopus* is achieved by specific factors in cytoplasmic polyadenylation such as Pumilio and Musashi (Charlesworth *et al.* , 2013).

Although studies on transcription of individual genes have revealed how maternal mRNA is recruited for regulation of gene expression, it is still unknown whether transcription of other mRNAs follows the same pattern as described above. Using genome-wide analysis, recent studies have shown how maternal mRNA expression is regulated. The global switch in maternal mRNA translation occurs at around the exit from prophase I, at the time of GVBD (Luong et al. , 2020), after which the oocyte is transcriptionally silent. Subsequently, most maternal mRNAs are polyadenylated, as the oocytes enter the MI stage. But the maternal mRNAs in oocytes then undergo global deadenylation between the MI and MII stages (Yang *et al.* , 2020). It has been proposed that there is a strong correlation between poly-A tail length and translational activity during oogenesis

and early development (Lim *et al.* , 2016, Subtelny *et al.* , 2014). Meanwhile, the majority of translationally activate mRNAs have at least one CPE sequence, and all the translationally activated mRNAs have interacted with CPEB1 (Luong *et al.*, 2020). It has been demonstrated that poly(A) tail length of maternal mRNAs changes markedly from the immature oocyte to an activated egg in *Drosophila* (Lim *et al.*, 2016).

When determining levels of gene expression, quantitative reverse transcription polymerase chain reaction (qRT-PCR) is frequently used. This technique is based on the generation of cDNA from isolated mRNA. In general, two methods are used for the generation of cDNA, priming with random sequences or oligo(dT) sequences. Reverse transcription using oligo(dT)s is dependent on and starts at the poly(A) tail, whereas reverse transcription using random primers does not depend on poly(A) RNA. Therefore, it is possible that different methods used for reverse transcription may lead to different results for mRNA abundance measurements in oocytes.

Developmental epigenetics

As development proceeds, the embryo needs to switch from maternal products to transcription from an activated nuclear genome, since maternal products are not sufficient for further embryonic development (Despic and Neugebauer, 2018, Lee *et al.* , 2014). Therefore, a subset of maternal mRNA and proteins is gradually degraded, and zygotic genome products are generated; a phenomenon referred to as maternal to zygotic transition (MZT), zygotic genome activation (ZGA) or embryonic genome activation (EGA) (Despic and Neugebauer, 2018, Hamm *et al.* , 2015). Since all cells share the same original DNA sequence passed down from the zygote, embryonic cells destined to assume a different phenotype need to govern their own different pattern of gene expression that defines that cell type by a process called epigenetics.

By definition, epigenetics is the process of heritable changes that affect gene activity and expression without changing the original DNA sequence. DNA methylation is one of the major epigenetic mechanisms operating to guide and restrict differentiation during embryonic development (Messerschmidt *et al.* , 2014). DNA methylation is catalyzed by DNA methyltransferases and results in the addition of a methyl (CH3) group to the 5′-carbon of cytosines in the DNA molecule. This epigenetic modification is known for its role in repressing gene expression by blocking the binding sites for transcription factors or by recruiting additional proteins involved in gene silencing (Moore *et al.* , 2013). There are

two major episodes of DNA methylation operating during embryonic development. The first round of genome-wide DNA demethylation and remethylation takes place in primordial germ cells (PGCs) (Rivera and Ross, 2013). The DNA of newly formed PGCs is highly methylated, and it has undergone drastic demethylation by the time the PGCs have reached the genital ridge (Messerschmidt *et al.*, 2014, Rivera and Ross, 2013, Zeng and Chen, 2019a). During the formation of oocytes and spermatozoa from PGCs, de novo methylation of DNA occurs (Zeng and Chen, 2019b). The second wave of global DNA demethylation and remethylation then starts following fertilization. The paternal pronucleus firstly undergoes active demethylation in the zygote, followed by passive demethylation of the maternal genome during the following cell divisions (Seisenberger *et al.* , 2013, Zeng and Chen, 2019b). At around the morula and early blastocyst stage, both maternal and paternal genomes are equally demethylated and have reached their lowest methylation levels (Marcho *et al.* , 2015, Zeng and Chen, 2019b). Soon after global demethylation, de novo DNA methylation is initiated, coinciding with the formation of ICM and TE (Bergsmedh *et al.* , 2011, Combes and Whitelaw, 2010).

Another major epigenetic mechanism active during embryonic development is histone tail modification (Bannister and Kouzarides, 2011). In general, histone acetylation corresponds with higher levels of gene transcription and histone methylation is correlated with either silencing or activation of transcription (Canovas and Ross, 2016). Among a wide range of histone tail modifications, methylation of lysine (K) residues on histone 3 (H3) is the most extensively studied (O'Neill, 2015). Trimethylation of histone H3 at lysine 27 (H3K27me3) is associated with repression of gene expression, and is mediated by polycomb repressive complex 2 (PRC2). In contrast, H3K4me3 is commonly related to activation of transcription by recruitment of nucleosome remodeling complexes (Bernstein *et al.* , 2005, Santos-Rosa *et al.* , 2002). Asymmetric distribution of H3K27me3 and H3K4me3 at specific chromatin regions ensures precise regulation of gene expression, which is associated with the initiation of lineage determination in the blastocyst (Canovas and Ross, 2016, Dahl *et al.* , 2010, Gao *et al.* , 2010). H3K27me3 is also involved in repression of X-linked genes in X-chromosome inactivation (XCI), which is an epigenetic modification characteristic of female cells.

In mammals, gender is genetically determined by the absence or presence of a Y chromosome, with females having two copies of the X chromosome and males having one X and one Y chromosome. Having two copies of the much

larger X chromosome in females can potentially lead to double doses of X-linked genes, compared with males. To achieve dosage compensation in female mammals, cells inactivate one of the two X chromosomes via the process known as XCI. As a result, most genes on that X chromosome are silenced. In mammals, this epigenetic process is thought to be initiated during preimplantation development; however, the timing and mechanisms may differ between mammalian species.

Most studies on the initiation of mammalian XCI have used mice as a model. A major effector of XCI is the long non-coding RNA, *XIST*, which is a component of the X-chromosome inactivation center (XIC). *XIST* RNA is transcribed from the XIC of the future inactive X chromosome and progressively coats in cis the entire X chromosome. Meanwhile, *XIST* RNA recruits polycomb repressive complexes to repress X-linked gene expression, together with H3K27me3 (Brockdorff, 2017, de Napoles *et al.* , 2004a, Plath *et al.* , 2003). In the mouse, other key effectors like *Tsix*, *Jpx* and *Ftx* are also involved in regulation of XCI. As a result, most genes on the inactive X chromosome are not expressed, although a small number of X-linked genes do escape inactivation. It has been reported that 3–15% of X-linked genes escape transcriptional repression in the inactive X chromosome of mice, while this percentage is 15-30% in women (Balaton and Brown, 2016, Berletch *et al.* , 2015, Calabrese *et al.* , 2012).

Even though XCI in mammals is initiated during female embryonic development, the timing and strategies of the initiation appear to differ among species (Escamilla-Del-Arenal *et al.* , 2011) (Figure 3). The X chromosome is active in both the oocyte and X-bearing sperm, and they remain active after fertilization. In female mouse embryos, at around the 2 to 4 cell stage the paternal X chromosome only (Xp) starts to express *XIST* and becomes inactivated in every embryonic cell (van den Berg *et al.* , 2011a). In human and rabbit embryos, however, *XIST* expression is not imprinted, and starts relatively late at the blastocyst and morula stages, respectively (Okamoto *et al.* , 2011). Moreover, in human and rabbit embryos *XIST* is expressed and accumulates on both maternal and paternal X chromosomes in some, but not all, cells of the early embryo. In mouse embryos reaching the late blastocyst stage, the Xp remains inactive in TE cells but is reactivated in the ICM cells (Figure 3). However, this reactivation of the Xp chromosome in embryonic cells has not been observed in other species.

At around the time of epiblast and hypoblast specification , the second wave of XCI is initiated in the mouse, coinciding with downregulation of pluripotency genes such as Nanog, Oct4/Pou5f1 and Sox2 (Escamilla-Del-Arenal *et al.*, 2011).

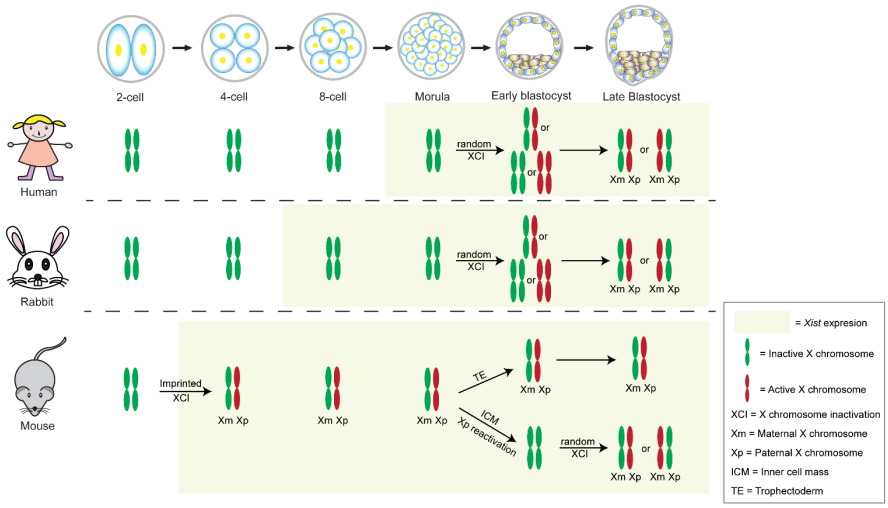

Figure 3. Initiation of X chromosome inactivation in human, rabbit and mouse embryos during embryonic development.

In other species, however, the establishment of XCI appears to be lineage dependent, without observation of a second wave of XCI during preimplantation development (Okamoto *et al.*, 2011). Eventually, both X chromosomes have an equal probability of being inactivated and this inactive status is maintained in adult mammalian cells (Escamilla-Del-Arenal *et al.*, 2011).

Regulation of transcription factors

Transcription factors are proteins that bind specific DNA sequences to regulate expression of genes. Transcription factors bind to either the promoter regions of DNA, and are involved in the initiation of transcription, or the regulatory sequences of DNA (enhancers and silencers) to activate or repress transcription. During embryonic development, cell fate is controlled and maintained by specific transcription factors (Iwafuchi-Doi and Zaret, 2016).

The segregation between TE and ICM starts at the morula stage and triggers the transition to the blastocyst. The caudal-type homeodomain protein CDX2 and the zinc finger transcription factor GATA3 are expressed in the outer cells of the embryo, and direct TE lineage determination (Strumpf *et al.* , 2005). Expression of CDX2 and GATA3 is weak and stochastic at the morula stage, but their expression increases gradually and becomes limited to the outer cells by the

blastocyst stage (Sasaki, 2017). Meanwhile, the fate of the ICM is governed by the Sox family protein, SOX2, and POU family protein, OCT3/4 (encoded by Pou5f1). The expression of SOX2 is restricted exclusively to the inner cells at the 16-cell stage and, subsequently, the cells of the ICM (Goissis and Cibelli, 2014, Guo *et al.* , 2010, Liu *et al.* , 2015). While the expression of OCT3/4 is not exclusively restricted to the ICM cells at the early blastocyst stage, it becomes ICM restricted by the late blastocyst stage (Dietrich and Hiiragi, 2007, Szczepańska *et al.* , 2011). During the second cell fate determination, the homeodomain protein NANOG is a key regulator of epiblast formation while GATA6 is essential for endoderm differentiation. Like the expression of OCT3/4, the expression of NANOG and GATA6 becomes restricted to the epiblast and endoderm, respectively, only by the late blastocyst stage (Wicklow *et al.* , 2014).

These transcription factors also play an important role in maintaining both blastocyst viability and cell fate (Sasaki, 2017). In the mouse, Cdx2-null embryos can give rise to blastocysts, but lose the epithelial integrity of their TE by the late blastocyst stage and die between 3.5- and 5.5-days post coitum (dpc) (Chawengsaksophak *et al.* , 2004, Huang *et al.* , 2017, Marikawa and Alarcón, 2009). In addition, Cdx2-null embryos fail to repress OCT3/4 expression in the TE. Moreover, it has been shown that CDX2 promotes expression of TE genes in the TE, such as Eomes (Strumpf *et al.*, 2005). Similarly, Oct4-null embryos can initially develop into normal blastocysts, but the ICM cells of Oct4-null blastocysts cannot maintain pluripotency (Nichols *et al.* , 1998).

Studies have revealed that the Hippo signaling pathway establishes the expression patterns of transcription factors that play an essential role in segregation of ICM and TE during mouse embryonic development (Frum and Ralston, 2015, Sasaki, 2017). The Hippo signaling pathway was initially identified as a regulator of organ size and tissue growth during development and regeneration, and is highly conserved from nematodes to man (Kim *et al.* , 2019c, Meng *et al.* , 2016). The core cascade components of the Hippo signaling pathway are LATS1/2 protein kinase, YAP1, TAZ and TEAD (Cairns *et al.* , 2017, Lorthongpanich *et al.* , 2013, Yu and Guan, 2013). When the Hippo pathway is active, LATS1/2 phosphorylates YAP1 and its co-activator TAZ. Phosphorylated YAP1 and TAZ localize in the cytoplasm and then become ubiquitinated in preparation for degradation (Kim and Jho, 2018, Yu and Guan, 2013). When the Hippo pathway is inactive, YAP1/TAZ are unphosphorylated and migrate to the nucleus (Yu and Guan, 2013). In the nucleus, unphosphorylated YAP1/TAZ bind to TEAD family members, which promote expression of TE genes (Wu and Guan,

2021). During the first cell fate determination, YAP1/TAZ are unphosphorylated and localize in the cytoplasm in the outer cells of the morula, indicating that the Hippo pathway is repressed. By binding to TEAD proteins, the expression of CDX2 and GATA3 is promoted and expression of SOX2 is inhibited, leading to a TE fate (Chen *et al.* , 2019, Karasek *et al.* , 2020, Wicklow *et al.*, 2014). By contrast, the Hippo pathway is active in the inside cells of the morula, where phosphorylated YAP cannot bind to TEAD4 to activate CDX2 expression in the nucleus, driving the cell towards an ICM fate (Frum and Ralston, 2015, Wicklow *et al.*, 2014). It has been shown that CDX2 expression is greatly downregulated at the morula stage and completely absent at later stages in Tead4 mutant embryos (Nishioka *et al.* , 2008). These Tead4 mutant embryos cannot establish trophoblast giant cells, leading to embryonic lethality at preimplantation stages (Nishioka *et al.*, 2008, Yagi *et al.* , 2007). However, a recent study has shown that YAP overexpression elevates expression of OCT4 (an ICM marker) in both human embryonic stem cells and induced pluripotent stem cells (Qin *et al.* , 2016). Overall, the Hippo signaling pathway plays an essential role during determination of the first cell fates but its function in cell segregation may differ among mammalian species.

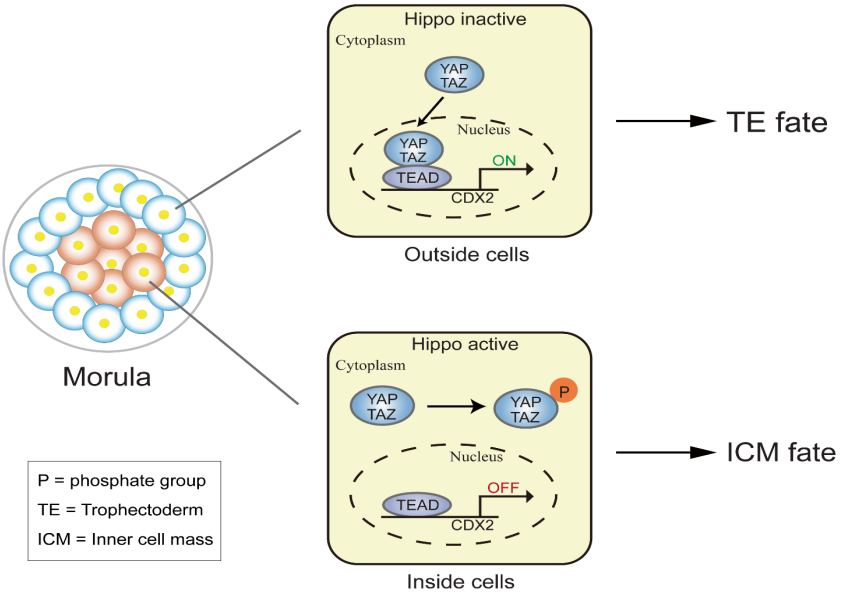

Figure 4. The Hippo pathways in mouse morula stage embryos.

The second cell fate determination during embryonic development is the segregation of epiblast (EPI) and primitive endoderm (PE). Similar to the segregation of ICM and TE, determination of EPI and PE is achieved by differential expression of transcription factors. Within the ICM, the homeobox transcription factors NANOG and the GATA6 promote the formation of EPI and PE, respectively. It has been demonstrated that Nanog-deficient embryos fail to form recognizable EPI tissues and die after implantation (Mitsui *et al.* , 2003). Similarly, Gata6-null embryos fail to establish the PE lineage and die at the early blastocyst stage (Koutsourakis *et al.* , 1999).

The fibroblast growth factor (FGF) / mitogen-activated protein kinase (MAPK) signaling pathway appears to be critical for PE and EPI cell fate determination. FGF4/MAPK signaling promotes Gata6 expression and suppresses the expression of Nanog and Sox2 in the presumptive PE cells within the ICM (Frum and Ralston, 2015). Homozygous mutants for *Fgf4*, *Fgfr2* and *Grb2* all lead to peri-implantation embryo death without formation of PE (Yamanaka *et al.* , 2010). Moreover, all cells in the ICM develop an EPI fate, with a lack of PE formation, in mouse Grb2 -mutant blastocysts (Chazaud *et al.* , 2006). By contrast, all ICM cells in mouse and bovine preimplantation embryos express GATA6 when FGF signaling is stimulated (Kuijk *et al.* , 2012a, Yamanaka *et al.*, 2010). Interestingly, in human embryos, the percentage of GATA6 positive cells in the ICM does not change after inhibition of MAPK, indicating fundamental differences in lineage segregation between mammalian species (Kuijk *et al.*, 2012a).

Embryo quality evaluation

In vitro fertilization (IVF) is a technique for fertilizing an oocyte in a laboratory setting and is the archetypal assisted reproductive technology (ART). Since the first IVF baby was born in 1978, this technique has helped millions of sub-fertile couples to conceive their own children and has helped to produce even more progeny from valuable livestock. The number of in vitro produced (IVP) embryos has increased over the years, but the clinical pregnancy rate after human IVF-embryo transfer is still far from optimal, at around 30–40%. The pregnancy rate is, however, better when embryos graded as being of ‘high quality’ are transferred. It is therefore important to be able to accurately predict the developmental competence of embryos prior to embryo transfer.

Morphological assessment of embryos is routinely used to evaluate embryo quality. The primary goal of morphological assessment is to select the embryo

with the highest developmental potential and likelihood of successful implantation. One of the important parameters of morphological assessment is the presence of extruded cells or cellular fragments in the perivitelline space, which is considered as a sign of reduced embryo quality (Van Soom *et al.* , 2003). The presence of cellular fragments is a fairly common finding in human IVP embryos and the extent of fragmentation is regarded as one of the most important morphological factors for embryo selection (Hardarson *et al.* , 2002). The extent of cellular fragmentation is often expressed as a percentage of the cleavage cavity occupied by nuclear cytoplasmic fragments (Alikani *et al.* , 1999, Johansson *et al.* , 2003), and has been classified into different distinct patterns (Alikani *et al.*, 1999, Hardy *et al.* , 2003). Overall, a large number of fragments in the perivitelline space predicts a poor blastocyst formation potential and lower blastocyst cell number (Hardy *et al.*, 2003). Increased fragmentation is also associated with reduced implantation and pregnancy rates (Racowsky *et al.* , 2000). For example, embryos with a fragmentation volume exceeding 35% generate a clinical pregnancy rate of only 14.8% of in human IVF (Alikani *et al.*, 1999). On the other hand, the presence of minor amounts of fragmentation does not have a negative impact on blastocyst formation (Hardy *et al.*, 2003), nor does it appear to lead to lower pregnancy rates (Alikani *et al.*, 1999).

Another commonly used indicator of embryo quality is the developmental stage with respect to time. It has been confirmed that fast-cleaving embryos have more potential to reach later developmental stages and result in higher birth rates after transfer (Luna *et al.* , 2008, van Soom *et al.* , 1997). Moreover, embryos that achieve morula compaction or blastocyst formation more quickly generate higher pregnancy rates after embryo transfer (Harada *et al.* , 2020). Other morphological parameters, such as embryo size, embryo shape, embryo color, compaction and integrity of the zona pellucida, are also commonly used for embryo quality evaluation and can be easily performed by regular stereomicroscopy. However, embryo quality determination based on morphological observation is considered to be a subjective assessment with significant variation between clinicians (Baxter Bendus *et al.* , 2006, Kim *et al.* , 2019b).

In practice, embryos are taken out of the incubator once a day to assess morphological parameters. The disadvantages of regular morphology assessment are obvious. Firstly, the embryos are exposed to undesirable culture conditions due to sudden changes in humidity, temperature and pH during every examination (Zhang *et al.* , 2010). Secondly, a few snapshots at different time points during embryonic development can only provide limited and incomplete information for

embryo quality prediction (Kovacs, 2014). More importantly, embryo morphology can change within short time intervals, resulting in different scores for the same embryos within a few hours (Montag *et al.* , 2011). To overcome these limitations, embryos can be continuously observed inside the incubator by time-lapse monitoring (Kirkegaard *et al.* , 2012). Digital images can be evaluated using computer algorithms to indicate the best quality embryos (Liao *et al.* , 2021). Besides time-lapse monitoring, preimplantation genetic testing (PGT) is also used to collect more in-depth information about embryo quality. The main purpose of PGT is to select embryos free from genetic diseases or chromosomal abnormalities. However, in most countries, PGT is not a routine procedure in IVF but is performed preferentially for couples carrying genetically inherited disorders that could lead to devastating disease (Krones *et al.* , 2005).

Until recently, human embryos were most often transferred into the uterus on the third day after IVF, when the embryo was at the 4- to 8-cell stage. However, more than 50% of these 4- to 8–cell embryos stop growing and fail to reach the blastocyst stage if cultured in vitro. To exclude embryos with poor developmental potential, there is a growing trend to transfer embryos at the blastocyst stage in human IVF. Indeed, studies have shown that implantation and clinical pregnancy rates are significantly higher after blastocyst transfer, compared to when embryos are transferred at cleavage-stages (Gardner *et al.* , 2000, Milki *et al.* , 2000, Papanikolaou *et al.* , 2005). In cattle and most domestic animal species, it is a common to transfer morula-blastocyst stage embryos in clinical programs (Van Soom *et al.* , 2001).

Besides the timing of blastocyst formation, other parameters are used for blastocyst quality assessment, such as: degree of blastocoele expansion, hatching status and size of the ICM (Du *et al.* , 2016, Lagalla *et al.* , 2015). However, one of the most important parameters for morphological assessment is the presence of cellular fragments in the perivitelline space, which can be difficult to identify after blastocyst expansion because the perivitelline space becomes very small (Van Soom *et al.*, 2001). As a result, there is a little information about whether cellular fragments are a reliable predictor of blastocyst quality after expansion.

Thesis outline

In this thesis, various aspects of gene expression regulation during oocyte maturation and early embryo development were investigated. Bovine oocytes and embryos were used to investigate this subject because the cow shares important reproductive characteristics with man. For example, both man and the cow are

mono-ovulatory species, with very similar time courses of oocyte maturation and preimplantation development. In addition, large quantities of bovine oocytes can be collected from slaughterhouse ovaries that are not wanted for food production. In this respect, bovine embryos can be cultured to the blastocyst stage efficiently from oocytes, without having to resort to the use of experimental animals.

Since regulation of gene expression is mainly achieved by regulation of maternal mRNAs in oocytes and embryos before zygotic genome activation, **Chapter 2** describes dynamic gene expression and changes to the poly(A) tail of maternal mRNAs in oocytes and early embryos. In fact, we discovered that because of this poly(A) tail regulation in oocytes and early embryos, the choice of reverse transcription priming method affects the validity of choices for gene expression normalisation. Gene expression in oocytes and very early embryos is affected by epigenetic alterations that either silence or activate genes. **Chapter 3** investigated the initiation of X chrosome inactivation during female bovine embryo development. X-linked gene regulation after XCI initiation was also analysed in this chapter in part to determine if there were consistent differences within different cell lineages (ICM versus trophectoderm). **Chapter 4** further focused on the role of Hippo-YAP signaling in the activation of transcription factor CDX2 expression in bovine embryos, and therefore in cell lineage determination.

Finally, because identification of high-quality embryos is important for clinicians if they are to select the best embryo to transfer, and for researchers to validate the relevance of experimental interventions. **Chapter 5** describes whether the presence or absence of cellular fragments in the perivitelline space is a readily observable and non-invasive predictor of blastocyst quality.

References

Alikani M, Cohen J, Tomkin G, Garrisi GJ, Mack C, Scott RT. Human embryo fragmentation in vitro and its implications for pregnancy and implantation. *Fertility and sterility* 1999;**71**:836-842.

Balaton BP, Brown CJ. Escape Artists of the X Chromosome. *Trends in genetics : TIG* 2016;**32**:348-359.

Bannister AJ, Kouzarides T. Regulation of chromatin by histone modifications. *Cell research* 2011;**21**:381-395.

Barragán-Iglesias P, Lou TF, Bhat VD, Megat S, Burton MD, Price TJ, Campbell ZT. Inhibition of Poly(A)-binding protein with a synthetic RNA mimic reduces pain sensitization in mice. *Nature communications* 2018;**9**:10.

Baxter Bendus AE, Mayer JF, Shipley SK, Catherino WH. Interobserver and intraobserver variation in day 3 embryo grading. *Fertility and sterility* 2006;**86**:1608-1615.

Bergsmedh A, Donohoe ME, Hughes RA, Hadjantonakis AK. Understanding the molecular circuitry of cell lineage specification in the early mouse embryo. *Genes (Basel)* 2011;**2**:420-448.

Berletch JB, Ma W, Yang F, Shendure J, Noble WS, Disteche CM, Deng X. Escape from X inactivation varies in mouse tissues. *PLoS genetics* 2015;**11**:e1005079.

Bernstein BE, Kamal M, Lindblad-Toh K, Bekiranov S, Bailey DK, Huebert DJ, McMahon S, Karlsson EK, Kulbokas EJ, 3rd, Gingeras TR *et al.* Genomic maps and comparative analysis of histone modifications in human and mouse. *Cell* 2005;**120**:169-181.

Brockdorff N. Polycomb complexes in X chromosome inactivation. *Philosophical transactions of the Royal Society of London Series B, Biological sciences* 2017;**372**.

Cairns L, Tran T, Kavran JM. Structural Insights into the Regulation of Hippo Signaling. *ACS chemical biology* 2017;**12**:601-610.

Calabrese JM, Sun W, Song L, Mugford JW, Williams L, Yee D, Starmer J, Mieczkowski P, Crawford GE, Magnuson T. Site-specific silencing of regulatory elements as a mechanism of X inactivation. *Cell* 2012;**151**:951-963.

Canovas S, Ross PJ. Epigenetics in preimplantation mammalian development. *Theriogenology* 2016;**86**:69-79.

Cao Q, Richter JD. Dissolution of the maskin-eIF4E complex by cytoplasmic polyadenylation and poly(A)-binding protein controls cyclin B1 mRNA translation and oocyte maturation. *The EMBO journal* 2002;**21**:3852-3862.

Charlesworth A, Meijer HA, de Moor CH. Specificity factors in cytoplasmic polyadenylation. *Wiley interdisciplinary reviews RNA* 2013;**4**:437-461.

Chawengsaksophak K, de Graaff W, Rossant J, Deschamps J, Beck F. Cdx2 is essential for axial elongation in mouse development. *Proceedings of the National Academy of Sciences of*

the United States of America 2004;**101**:7641-7645.

Chazaud C, Yamanaka Y, Pawson T, Rossant J. Early lineage segregation between epiblast and primitive endoderm in mouse blastocysts through the Grb2-MAPK pathway. *Developmental cell* 2006;**10**:615-624.

Chen YA, Lu CY, Cheng TY, Pan SH, Chen HF, Chang NS. WW Domain-Containing Proteins YAP and TAZ in the Hippo Pathway as Key Regulators in Stemness Maintenance, Tissue Homeostasis, and Tumorigenesis. *Frontiers in oncology* 2019;**9**:60.

Combes AN, Whitelaw E. Epigenetic reprogramming: enforcer or enabler of developmental fate? *Development, growth & differentiation* 2010;**52**:483-491.

Cooley L, Theurkauf WE. Cytoskeletal functions during *Drosophila* oogenesis. *Science (New York, NY)* 1994;**266**:590-596.

Dahl JA, Reiner AH, Klungland A, Wakayama T, Collas P. Histone H3 lysine 27 methylation asymmetry on developmentally-regulated promoters distinguish the first two lineages in mouse preimplantation embryos. *PloS one* 2010;**5**:e9150.

de Napoles M, Mermoud JE, Wakao R, Tang YA, Endoh M, Appanah R, Nesterova TB, Silva J, Otte AP, Vidal M *et al.* Polycomb group proteins Ring1A/B link ubiquitylation of histone H2A to heritable gene silencing and X inactivation. *Developmental cell* 2004;**7**:663-676.

Despic V, Neugebauer KM. RNA tales - how embryos read and discard messages from mom. *Journal of cell science* 2018;**131**.

Dickson KS, Thompson SR, Gray NK, Wickens M. Poly(A) polymerase and the regulation of cytoplasmic polyadenylation. *The Journal of biological chemistry* 2001;**276**:41810-41816.

Dietrich JE, Hiiragi T. Stochastic patterning in the mouse pre-implantation embryo. *Development (Cambridge, England)* 2007;**134**:4219-4231.

Du QY, Wang EY, Huang Y, Guo XY, Xiong YJ, Yu YP, Yao GD, Shi SL, Sun YP. Blastocoele expansion degree predicts live birth after single blastocyst transfer for fresh and vitrified/warmed single blastocyst transfer cycles. *Fertility and sterility* 2016;**105**:910-919.e911.

Escamilla-Del-Arenal M, da Rocha ST, Heard E. Evolutionary diversity and developmental regulation of X-chromosome inactivation. *Human genetics* 2011;**130**:307-327.

Esencan E, Kallen A, Zhang M, Seli E. Translational activation of maternally derived mRNAs in oocytes and early embryos and the role of embryonic poly(A) binding protein (EPAB). *Biology of reproduction* 2019;**100**:1147-1157.

Frum T, Ralston A. Cell signaling and transcription factors regulating cell fate during formation of the mouse blastocyst. *Trends in genetics : TIG* 2015;**31**:402-410.

Gao Y, Hyttel P, Hall VJ. Regulation of H3K27me3 and H3K4me3 during early porcine embryonic development. *Molecular reproduction and development* 2010;**77**:540-549.

Gardner DK, Lane M, Stevens J, Schlenker T, Schoolcraft WB. Blastocyst score affects

implantation and pregnancy outcome: towards a single blastocyst transfer. *Fertility and sterility* 2000;**73**:1155-1158.

Goissis MD, Cibelli JB. Functional characterization of SOX2 in bovine preimplantation embryos. *Biology of reproduction* 2014;**90**:30.

Guo G, Huss M, Tong GQ, Wang C, Li Sun L, Clarke ND, Robson P. Resolution of cell fate decisions revealed by single-cell gene expression analysis from zygote to blastocyst. *Developmental cell* 2010;**18**:675-685.

Hamm DC, Bondra ER, Harrison MM. Transcriptional activation is a conserved feature of the early embryonic factor Zelda that requires a cluster of four zinc fingers for DNA binding and a low-complexity activation domain. *The Journal of biological chemistry* 2015;**290**:3508-3518.

Harada Y, Maeda T, Fukunaga E, Shiba R, Okano S, Kinutani M, Horiuchi T. Selection of high-quality and viable blastocysts based on timing of morula compaction and blastocyst formation. *Reproductive medicine and biology* 2020;**19**:58-64.

Hardarson T, Löfman C, Coull G, Sjögren A, Hamberger L, Edwards RG. Internalization of cellular fragments in a human embryo: time-lapse recordings. *Reproductive biomedicine online* 2002;**5**:36-38.

Hardy K, Stark J, Winston RM. Maintenance of the inner cell mass in human blastocysts from fragmented embryos. *Biology of reproduction* 2003;**68**:1165-1169.

Huang D, Guo G, Yuan P, Ralston A, Sun L, Huss M, Mistri T, Pinello L, Ng HH, Yuan G *et al.* The role of Cdx2 as a lineage specific transcriptional repressor for pluripotent network during the first developmental cell lineage segregation. *Scientific reports* 2017;**7**:17156.

Iwafuchi-Doi M, Zaret KS. Cell fate control by pioneer transcription factors. *Development (Cambridge, England)* 2016;**143**:1833-1837.

Jackson RJ, Hellen CU, Pestova TV. Termination and post-termination events in eukaryotic translation. *Advances in protein chemistry and structural biology* 2012;**86**:45-93.

Johansson M, Hardarson T, Lundin K. There is a cutoff limit in diameter between a blastomere and a small anucleate fragment. *Journal of assisted reproduction and genetics* 2003;**20**:309-313.

Jones KT. Turning it on and off: M-phase promoting factor during meiotic maturation and fertilization. *Molecular human reproduction* 2004;**10**:1-5.

Karasek C, Ashry M, Driscoll CS, Knott JG. A tale of two cell-fates: role of the Hippo signaling pathway and transcription factors in early lineage formation in mouse preimplantation embryos. *Molecular human reproduction* 2020;**26**:653-664.

Kim JH, Richter JD. RINGO/cdk1 and CPEB mediate poly(A) tail stabilization and translational regulation by ePAB. *Genes & development* 2007;**21**:2571-2579.

Kim MK, Park JK, Jeon Y, Choe SA, Lee HJ, Kim J, Chang EM, Kim JW, Lyu SW, Kim JY *et al.* Correlation between Morphologic Grading and Euploidy Rates of Blastocysts, and Clinical Outcomes in In Vitro Fertilization Preimplantation Genetic Screening. *Journal of Korean*

medical science 2019a;**34**:e27.

Kim W, Cho YS, Wang X, Park O, Ma X, Kim H, Gan W, Jho EH, Cha B, Jeung YJ *et al.* Hippo signaling is intrinsically regulated during cell cycle progression by APC/C(Cdh1). *Proceedings of the National Academy of Sciences of the United States of America* 2019b;**116**:9423-9432.

Kim Y, Jho E-H. Regulation of the Hippo signaling pathway by ubiquitin modification. *BMB Rep* 2018;**51**:143-150.

Kirkegaard K, Agerholm IE, Ingerslev HJ. Time-lapse monitoring as a tool for clinical embryo assessment. *Human reproduction (Oxford, England)* 2012;**27**:1277-1285.

Kotani T, Yasuda K, Ota R, Yamashita M. Cyclin B1 mRNA translation is temporally controlled through formation and disassembly of RNA granules. *The Journal of cell biology* 2013;**202**:1041-1055.

Koutsourakis M, Langeveld A, Patient R, Beddington R, Grosveld F. The transcription factor GATA6 is essential for early extraembryonic development. *Development (Cambridge, England)* 1999;**126**:723-732.

Kovacs P. Embryo selection: the role of time-lapse monitoring. *Reproductive biology and endocrinology : RB&E* 2014;**12**:124.

Krones T, Schlüter E, Manolopoulos K, Bock K, Tinneberg HR, Koch MC, Lindner M, Hoffmann GF, Mayatepek E, Huels G *et al.* Public, expert and patients' opinions on preimplantation genetic diagnosis (PGD) in Germany. *Reproductive biomedicine online* 2005;**10**:116-123.

Kuijk EW, van Tol LT, Van de Velde H, Wubbolts R, Welling M, Geijsen N, Roelen BA. The roles of FGF and MAP kinase signaling in the segregation of the epiblast and hypoblast cell lineages in bovine and human embryos. *Development (Cambridge, England)* 2012;**139**:871-882.

Lagalla C, Barberi M, Orlando G, Sciajno R, Bonu MA, Borini A. A quantitative approach to blastocyst quality evaluation: morphometric analysis and related IVF outcomes. *Journal of assisted reproduction and genetics* 2015;**32**:705-712.

Lee MT, Bonneau AR, Giraldez AJ. Zygotic genome activation during the maternal-to-zygotic transition. *Annual review of cell and developmental biology* 2014;**30**:581-613.

Liao Q, Zhang Q, Feng X, Huang H, Xu H, Tian B, Liu J, Yu Q, Guo N, Liu Q *et al.* Development of deep learning algorithms for predicting blastocyst formation and quality by time-lapse monitoring. *Communications biology* 2021;**4**:415.

Lim J, Lee M, Son A, Chang H, Kim VN. mTAIL-seq reveals dynamic poly(A) tail regulation in oocyte-to-embryo development. *Genes & development* 2016;**30**:1671-1682.

Liu S, Bou G, Sun R, Guo S, Xue B, Wei R, Cooney AJ, Liu Z. Sox2 is the faithful marker for pluripotency in pig: evidence from embryonic studies. *Developmental dynamics : an official publication of the American Association of Anatomists* 2015;**244**:619-627.

Lorthongpanich C, Messerschmidt DM, Chan SW, Hong W, Knowles BB, Solter D. Temporal reduction of LATS kinases in the early preimplantation embryo prevents ICM lineage differentiation. *Genes & development* 2013;**27**:1441-1446.

Luna M, Copperman AB, Duke M, Ezcurra D, Sandler B, Barritt J. Human blastocyst morphological quality is significantly improved in embryos classified as fast on day 3 (>or=10 cells), bringing into question current embryological dogma. *Fertility and sterility* 2008;**89**:358-363.

Luong XG, Daldello EM, Rajkovic G, Yang CR, Conti M. Genome-wide analysis reveals a switch in the translational program upon oocyte meiotic resumption. *Nucleic acids research* 2020;**48**:3257-3276.

Marcho C, Cui W, Mager J. Epigenetic dynamics during preimplantation development. *Reproduction (Cambridge, England)* 2015;**150**:R109-120.

Marikawa Y, Alarcón VB. Establishment of trophectoderm and inner cell mass lineages in the mouse embryo. *Molecular reproduction and development* 2009;**76**:1019-1032.

Medvedev S, Yang J, Hecht NB, Schultz RM. CDC2A (CDK1)-mediated phosphorylation of MSY2 triggers maternal mRNA degradation during mouse oocyte maturation. *Developmental biology* 2008;**321**:205-215.

Meng Z, Moroishi T, Guan K-L. Mechanisms of Hippo pathway regulation. *Genes & development* 2016;**30**:1-17.

Messerschmidt DM, Knowles BB, Solter D. DNA methylation dynamics during epigenetic reprogramming in the germline and preimplantation embryos. *Genes & development* 2014;**28**:812-828.

Milki AA, Hinckley MD, Fisch JD, Dasig D, Behr B. Comparison of blastocyst transfer with day 3 embryo transfer in similar patient populations. *Fertility and sterility* 2000;**73**:126-129.

Mitsui K, Tokuzawa Y, Itoh H, Segawa K, Murakami M, Takahashi K, Maruyama M, Maeda M, Yamanaka S. The homeoprotein Nanog is required for maintenance of pluripotency in mouse epiblast and ES cells. *Cell* 2003;**113**:631-642.

Montag M, Liebenthron J, Köster M. Which morphological scoring system is relevant in human embryo development? *Placenta* 2011;**32 Suppl 3**:S252-256.

Monti M. Oocytes - Maternal Information and Functions. *European journal of histochemistry : EJH* 2017;**61**:2849.

Moore LD, Le T, Fan G. DNA methylation and its basic function. *Neuropsychopharmacology : official publication of the American College of Neuropsychopharmacology* 2013;**38**:23-38.

Nichols J, Zevnik B, Anastassiadis K, Niwa H, Klewe-Nebenius D, Chambers I, Schöler H, Smith A. Formation of pluripotent stem cells in the mammalian embryo depends on the POU transcription factor Oct4. *Cell* 1998;**95**:379-391.

Nishioka N, Yamamoto S, Kiyonari H, Sato H, Sawada A, Ota M, Nakao K, Sasaki H. Tead4 is required for specification of trophectoderm in pre-implantation mouse embryos.

Mechanisms of development 2008;**125**:270-283.

O'Neill C. The epigenetics of embryo development. *Animal Frontiers* 2015;**5**:42-49.

Okamoto I, Patrat C, Thépot D, Peynot N, Fauque P, Daniel N, Diabangouaya P, Wolf JP, Renard JP, Duranthon V *et al.* Eutherian mammals use diverse strategies to initiate X-chromosome inactivation during development. *Nature* 2011;**472**:370-374.

Papanikolaou EG, D'Haeseleer E, Verheyen G, Van de Velde H, Camus M, Van Steirteghem A, Devroey P, Tournaye H. Live birth rate is significantly higher after blastocyst transfer than after cleavage-stage embryo transfer when at least four embryos are available on day 3 of embryo culture. A randomized prospective study. *Human reproduction (Oxford, England)* 2005;**20**:3198-3203.

Plath K, Fang J, Mlynarczyk-Evans SK, Cao R, Worringer KA, Wang H, de la Cruz CC, Otte AP, Panning B, Zhang Y. Role of histone H3 lysine 27 methylation in X inactivation. *Science (New York, NY)* 2003;**300**:131-135.

Pokrywka NJ, Stephenson EC. Microtubules are a general component of mRNA localization systems in *Drosophila* oocytes. *Developmental biology* 1995;**167**:363-370.

Qin H, Hejna M, Liu Y, Percharde M, Wossidlo M, Blouin L, Durruthy-Durruthy J, Wong P, Qi Z, Yu J *et al.* YAP Induces Human Naive Pluripotency. *Cell reports* 2016;**14**:2301-2312.

Racowsky C, Jackson KV, Cekleniak NA, Fox JH, Hornstein MD, Ginsburg ES. The number of eight-cell embryos is a key determinant for selecting day 3 or day 5 transfer. *Fertility and sterility* 2000;**73**:558-564.

Rivera RM, Ross JW. Epigenetics in fertilization and preimplantation embryo development. *Progress in biophysics and molecular biology* 2013;**113**:423-432.

Santos-Rosa H, Schneider R, Bannister AJ, Sherriff J, Bernstein BE, Emre NC, Schreiber SL, Mellor J, Kouzarides T. Active genes are tri-methylated at K4 of histone H3. *Nature* 2002;**419**:407-411.

Sasaki H. Roles and regulations of Hippo signaling during preimplantation mouse development. *Development, growth & differentiation* 2017;**59**:12-20.

Seisenberger S, Peat JR, Hore TA, Santos F, Dean W, Reik W. Reprogramming DNA methylation in the mammalian life cycle: building and breaking epigenetic barriers. *Philosophical transactions of the Royal Society of London Series B, Biological sciences* 2013;**368**:20110330.

Strumpf D, Mao CA, Yamanaka Y, Ralston A, Chawengsaksophak K, Beck F, Rossant J. Cdx2 is required for correct cell fate specification and differentiation of trophectoderm in the mouse blastocyst. *Development (Cambridge, England)* 2005;**132**:2093-2102.

Subtelny AO, Eichhorn SW, Chen GR, Sive H, Bartel DP. Poly(A)-tail profiling reveals an embryonic switch in translational control. *Nature* 2014;**508**:66-71.

Szczepańska K, Stańczuk L, Maleszewski M. Oct4 protein remains in trophectoderm until late stages of mouse blastocyst development. *Reproductive biology* 2011;**11**:145-156.

van den Berg IM, Galjaard RJ, Laven JS, van Doorninck JH. XCI in preimplantation mouse and human embryos: first there is remodelling…. *Human genetics* 2011;**130**:203-215.

Van Soom A, Mateusen B, Leroy J, De Kruif A. Assessment of mammalian embryo quality: what can we learn from embryo morphology? *Reproductive biomedicine online* 2003;**7**:664-670.

Van Soom A, Vanroose G, de Kruif A. Blastocyst evaluation by means of differential staining: a practical approach. *Reproduction in domestic animals = Zuchthygiene* 2001;**36**:29-35.

van Soom A, Ysebaert MT, de Kruif A. Relationship between timing of development, morula morphology, and cell allocation to inner cell mass and trophectoderm in in vitro-produced bovine embryos. *Molecular reproduction and development* 1997;**47**:47-56.

Vastenhouw NL, Cao WX, Lipshitz HD. The maternal-to-zygotic transition revisited. *Development (Cambridge, England)* 2019;**146**.

Wicklow E, Blij S, Frum T, Hirate Y, Lang RA, Sasaki H, Ralston A. HIPPO pathway members restrict SOX2 to the inner cell mass where it promotes ICM fates in the mouse blastocyst. *PLoS genetics* 2014;**10**:e1004618.

Winata CL, Korzh V. The translational regulation of maternal mRNAs in time and space. *FEBS letters* 2018;**592**:3007-3023.

Wu Z, Guan KL. Hippo Signaling in Embryogenesis and Development. *Trends in biochemical sciences* 2021;**46**:51-63.

Yagi R, Kohn MJ, Karavanova I, Kaneko KJ, Vullhorst D, DePamphilis ML, Buonanno A. Transcription factor TEAD4 specifies the trophectoderm lineage at the beginning of mammalian development. *Development (Cambridge, England)* 2007;**134**:3827-3836.

Yamanaka Y, Lanner F, Rossant J. FGF signal-dependent segregation of primitive endoderm and epiblast in the mouse blastocyst. *Development (Cambridge, England)* 2010;**137**:715-724.

Yang F, Wang W, Cetinbas M, Sadreyev RI, Blower MD. Genome-wide analysis identifies cis-acting elements regulating mRNA polyadenylation and translation during vertebrate oocyte maturation. *RNA (New York, NY)* 2020;**26**:324-344.

Yu F-X, Guan K-L. The Hippo pathway: regulators and regulations. *Genes & development* 2013;**27**:355-371.

Zeng Y, Chen T. DNA Methylation Reprogramming during Mammalian Development. *Genes (Basel)* 2019a;**10**:257.

Zeng Y, Chen T. DNA Methylation Reprogramming during Mammalian Development. *Genes (Basel)* 2019b;**10**.

Zhang JQ, Li XL, Peng Y, Guo X, Heng BC, Tong GQ. Reduction in exposure of human embryos outside the incubator enhances embryo quality and blastulation rate. *Reproductive biomedicine online* 2010;**20**:510-515

Chapter 2

Reverse transcription priming methods affect normalization choices for gene expression levels in oocytes and early embryos

Bo Yu[1], Helena T. A. van Tol[1], Tom A.E. Stout[2] and Bernard A. J. Roelen[3]*

[1]Farm Animal Health; Department of Population Health Sciences, Faculty of Veterinary Medicine, Utrecht University, Utrecht, The Netherlands.

[2]Equine Sciences; Department Clinical Sciences, Faculty of Veterinary Medicine, Utrecht University, Utrecht, The Netherlands.

[3]Embryology, Anatomy and Physiology; Department Clinical Sciences, Faculty of Veterinary Medicine, Utrecht University, Utrecht, The Netherlands.

Adapted from *Molecular Human Reproduction, 2021 Jul 1;27(7):gaab040*
Doi:10.1093/molehr/gaab040.

Abstract

Mammalian oocytes and embryos rely exclusively on maternal mRNAs to accomplish early developmental processes. Since oocytes and early embryos are transcriptionally silent after meiotic resumption, most of the synthesized maternal mRNA does not undergo immediate translation but is instead stored in the oocyte. Quantitative RT-PCR is commonly used to quantify mRNA levels, and correct quantification relies on reverse transcription and the choice of reference genes. Different methods for reverse transcription may affect gene expression determination in oocytes. In this study, we examined the suitability of either random or oligo(dT) primers for reverse transcription to be used for quantitative RT-PCR. We further looked for changes in poly(A) length of the maternal mRNAs during oocyte maturation. Our data indicated that depending on the method of reverse transcription, the optimal combination of reference genes for normalization differed. Surprisingly, we observed a shortening of the poly(A) tail lengths of maternal mRNA as oocytes progressed from GV to MII. Overall, our findings suggest dynamic maternal regulation of mRNA structure and gene expression during oocyte maturation and early embryo development.

Introduction

Early embryonic development is primarily controlled by maternal mRNAs, which are produced by the oocyte during oogenesis (Vastenhouw *et al.*, 2019). Unlike in somatic cells, most mRNA synthesized in an oocyte is not immediately translated but is stored for future events (Hamatani *et al.* , 2004). After breakdown of the germinal vesicle (GV), the chromatin in an oocyte becomes condensed, resulting in transcriptional silencing of meiotic oocytes (Dumdie *et al.* , 2018, Tan *et al.* , 2009). This period of reduced transcription lasts until the maternal to zygotic transition (MZT), when the zygotic genome is activated and maternal mRNA is largely degraded. Before the MZT, oocytes and embryos therefore rely on maternal mRNA to accomplish dynamic events accompanying final oocyte maturation, fertilization and early embryo development (Winata and Korzh, 2018). In short, precise regulation of maternal mRNA dynamics plays an essential role during maturation of the oocyte and early embryo development. Precise regulation of maternal mRNA expression ensures that dynamic events required for successful oocyte maturation and early embryo development can be accomplished; quantitative reverse transcription PCR (qRT-PCR) is a useful method for monitoring the regulation of (maternal) mRNA abundance or

expression. It is routinely used in life science research because of its sensitivity and cost effectiveness. It has proven to be a useful method to quantify gene expression levels in sparse or limited RNA samples such as from oocytes and embryos.

One of the key steps in qRT-PCR is the synthesis of complementary DNA (cDNA) by reverse transcription, which should result in a cDNA pool that quantitatively reflects the original mRNA copy number (Stangegaard *et al.* , 2006). There are two major priming strategies for reverse transcription used in qRT-PCR, namely random primers and oligo(dT) primers. Random primers with randomly ordered base sequences can potentially anneal to any RNA species, at any position (from 5' to 3'). Reverse transcription based on oligo(dT) primers can only anneal to the 3' poly(A) tail of RNA. Maternal mRNA is, however, usually stored in a short poly(A) tail state (Mendez and Richter, 2001, Stangegaard *et al.*, 2006). It is therefore possible that, depending on the method of synthesis, cDNA may not quantitatively reflect the population of maternal mRNA available for translation.

Normalization is an essential step when analyzing gene expression to account for factors such as the total amount of mRNA recovered from different samples (Evans *et al.* , 2018). Even though selection of reference genes for normalization in preimplantation embryos has been documented in various mammalian species (Goossens *et al.* , 2005a, Kuijk *et al.* , 2007, Mamo *et al.* , 2007), the possible effect of different reverse transcription priming strategies has not been analyzed in detail.

Translational control of maternal mRNA is achieved mainly by polyadenylation and deadenylation, and in particular by regulating the length of the poly(A) tail (Eichhorn *et al.* , 2016, Winata and Korzh, 2018). The regulation of maternal mRNA availability has been investigated primarily in *Drosophila*, *Xenopus*, and the mouse (Mendez and Richter, 2001, Morgan *et al.* , 2017, Richter, 2007, Sallés *et al.* , 1994). It has been reported that, in immature oocytes, maternal mRNA is kept in a relatively short poly(A) tail state, stored in cytoplasmic granules (Anderson and Kedersha, 2009, Winata and Korzh, 2018). Since the oocyte is transcriptionally silent during and after its nuclear maturation, it has been hypothesized that stored maternal mRNA is released from RNA granules when translation is required (Anderson and Kedersha, 2009, Kotani *et al.*, 2013, Winata and Korzh, 2018).

Oocyte progression through meiosis is highly dependent on the activity of maturation-promoting factor (MPF), a complex of the regulatory subunit cyclin

B, coded for by the CCNB gene, and the catalytic subunit cyclin dependent kinase 1 (CDK1). An increase in MPF activity from germinal vesicle breakdown (GVBD) to the metaphase I (MI) and metaphase II (MII) stages is achieved by temporally-controlled synthesis of cyclin B from stored maternal mRNA (Ihara *et al.* , 1998, Mendez and Richter, 2001, Nagahama and Yamashita, 2008, Nakahata *et al.* , 2003). Recently, it has been reported that a high *CCNB* mRNA translation rate is associated with elongation of the CCNB poly(A) tail in mouse oocytes (Daldello *et al.* , 2019, Kotani *et al.*, 2013). Cyclin A (coded by CCNA) can also bind to CDK1 and regulate the activity of MPF during oocyte maturation (Li *et al.* , 2019). Moreover, a recent study demonstrated that cyclin A1 expression prevents segregation of chromosomes and anaphase entry (Radonova *et al.* , 2020).

We hypothesized that different priming strategies for reverse transcription may result in different fidelities of cDNA generation when using samples from oocytes or embryos. We chose cyclin genes to study, because they are highly regulated during oocyte maturation which might lead to different gene expression patterns if different reverse transcription strategies were performed. We also focused on CDK2 and EIF4A3, since they play important role during oocyte maturation and early embryo development. We therefore extracted mRNA from bovine oocytes and embryos, and synthesized cDNA using random primers and oligo(dT) primers. We used qRT-PCR to examine the gene expression patterns of cyclin genes and examined poly(A) tail length of various genes in oocytes from the GV to the MII stage. Our data uncovered differences in poly(A) tail length of mRNA during oocyte maturation and early embryo development. It is concluded that one should be critical in deciding which primer-type to use for reverse transcription when gene expression levels are examined in oocytes and pre-MZT embryos.

Material and Methods

Bovine in vitro embryo culture and sample collection

Bovine ovaries were collected from a local slaughterhouse rinsed with water and kept in 0.9% NaCl (B. Braun, Melsungen, Germany) supplemented with penicillin/streptomycin (PS) (100 µg/mL) (Gibco, Paisley, UK) at 30 °C during processing. Cumulus-oocyte complexes (COCs) were aspirated from follicles with a diameter of 2-8 mm and identified using a stereomicroscope. The COCs were matured *in vitro* as described previously (Brinkhof *et al.* , 2015b) and for subsequent analysis, GV oocytes were collected immediately after COC recovery

and GVBD, MI and MII stage oocytes were collected at 6, 12 and 23 h of in vitro maturation, respectively; in all cases, cumulus cells were removed by vortexing. In vitro fertilization was done as described (Brinkhof et al., 2015). In short, after 23 h maturation, COCs were transferred to fertilization medium. Motile sperm cells were introduced into the fertilization medium at a final concentration of 1×10^6 per mL, and this was considered as day 0. After incubation with sperm for 20-22 h, presumptive zygotes were denuded of their cumulus cells by vortexing for 3 min, and then cultured further in synthetic oviductal fluid (SOF) (Brinkhof *et al.* , 2017) in a humidified atmosphere containing 5% CO_2 and 7% O_2 at 39 °C. At day 5 after fertilization, developing embryos were transferred to fresh SOF for further culture until day 8.

RNA Extraction and cDNA Generation

Oocytes or embryos in pools of 50 were rinsed in PBS and stored in 200 µL RLT lysis buffer (Qiagen, Valencia, CA, USA) at -80 °C until RNA extraction. Total RNA isolation was performed using the RNeasy Micro Kit (Qiagen) according to the manufacturer's instruction Reverse transcription was carried out directly after RNA isolation, using two different priming strategies. Two reverse transcription (RT) mixtures were prepared from 10 µL of the RNA sample, 4 µL of 5 × RT buffer (Invitrogen, Breda, the Netherlands), 10 mM DTT (Invitrogen), 0.5 mM dNTP (Promega, Leiden, the Netherlands), 8 units RNAsin/ RNAse inhibitor (Promega) and 150 units Superscript III reverse transcriptase (Invitrogen) in a total volume of 20 µL, supplemented with 1.8 units per mL random primers (Invitrogen) or 2.5 µM oligo(dT) primers (Invitrogen) respectively. Minus-RT controls were made up of the same reagents as above, using primers but without the reverse transcriptase. The mixtures were incubated at 70 °C for 5 min, followed by 1 h at 50 °C, and 5 min at 80 °C. Samples were subsequently stored at -20 °C until further analysis.

Quantitative PCR

All amplification reactions were performed on three independent cDNA samples or -RT blanks in duplicate, following the manufacturer's protocol of the CFX detection system (Bio-Rad, Hercules, CA, USA). The reaction mixture contained 1 µL cDNA, 9 µL RNAse- and DNAse-free water (Invitrogen) and 10 µL iQ SYBR Green supermix (Biorad) with a final primer concentration of 500 nM. Initial denaturation took place for 3 min at 95 °C, followed by 40 cycles of 95 °C for 20 sec, the primer specific annealing temperature (supplemental Table S1) for 20 sec, and elongation at 72 °C for 20 sec. To determine quantitative

amplification efficiency, standard curves for each primer pair were made by four-fold dilution series of cDNA from 400 oocytes or 100 blastocysts.

Poly(A) tail assay

Poly(A) tail assays were performed as described (Rassa *et al.* , 2000) with a few modifications. Total RNA was extracted from 50 GV or MII oocytes as described above. After denaturation at 70 °C, the mRNA was ligated with 50 pmol of primer GB-135 (5′-P-GGTCACCTTGATCTGAAGC-NH_2-3′) (Eurogentec) at 37 °C for 1 h in a total volume of 20 µL using T4 RNA ligase (New England Biolabs, Ipswich, MA, USA). GB-135 contained a 3′ amino modification to block ligation at this end. To inactivate RNA ligase, samples were boiled at 100 °C for 5 min and cooled on ice. Reverse transcription was performed as described above using 50 pmol of primer GB-136 (5′-GCTTCAGATCAAGGTGACCTTTTT-3′) (Eurogentec), and the anchored cDNA was used for amplification. First round amplification was performed using gene specific primer (P1) and GB-136. The product of the first round amplification was used as template for the second round amplification, using a gene specific primer starting after the 3' site of P1 (P2) and GB-136. The PCR was performed as described above with 40 cycles for first round amplification and 20 cycles for second round amplification. Samples were electrophoresed on 1.0% agarose (Eurogentec) gels and visualized with ethidium bromide (Invitrogen).

Transformation and DNA sequencing

The PCR products resulting from the second round amplification as described above were inserted into the pGEM-T Easy vector (Promega) using T4 DNA ligase (New England Biolabs) and transformed into E. coli JM109 competent cells (Promega) by heat-shock transformation according to the manufacturer's instructions. Transformants were selected on LB/Ampicillin/IPTG/X-Gal plates according to the manufacturer's instructions. At least 12 clones from each reaction were examined by digestion with Eco52I (Thermo Fisher Scientific, Eindhoven, the Netherlands) restriction followed by sequencing in case of correct insert size.

DNA sequencing reactions were conducted using T7 primer (5′-TAATACGACTCACTATAGGG-3′) (Eurogentec) according to the manufacturer's instructions for the BigDye™ Terminator v3.1 Cycle Sequencing Kit (Applied Biosystems, Beverly, MA, USA), and determined using a 3500XL Genetic Analyzer (Applied Biosystems). DNA sequencing results were analyzed using Sequencing Analysis Software v6.0 (Thermo Fisher Scientific) and aligned

by cluster W method using DNASTAR Lasergene 14 (DNASTAR, Madison, WI, USA).

Statistical analysis

Stability analysis for the reference genes was performed using geNorm (Vandesompele *et al.* , 2002). Data from the PCRs were tabulated in Microsoft Excel and statistical differences were examined using GraphPad Prism 7 (https://www. graphpad.com/scientific-software/prism/). Pools of embryos from three biological replicates were analyzed for gene expression. Normal distributions of data sets were determined by the Shapiro-Wilk tests. Differences between two groups were analyzed by the Mann Whitney test or, in the case of multiple groups, by one-way ANOVA followed by a post-hoc Tukey test. In bar graphs, differences between groups are indicated with different letters above the bars, with statistical significance set as $P < 0.05$. Asterisks indicate levels of significance (*$P < 0.05$, **$P < 0.005$, ***$P < 0.0005$ and ****$P < 0.0001$). Error bars indicate standard deviation.

Results

Stability of potential reference genes during oocyte maturation

As different priming strategies for reverse transcription in oocytes may result in different pools of cDNA, we hypothesized that suitable reference genes for normalization are different between cDNA synthesized using random primers and cDNA generated using oligo(dT) primers. To determine whether the optimal set of stably expressed reference genes differs in differently generated cDNA samples from GV, GVBD, MI and MII oocytes, expression of six commonly-used reference genes (*ACTB*, *GAPDH*, *HPRT1*, *RPL15*, *SDHA* and *YWHAZ*) was analyzed using qRT-PCR and the software packages of geNorm (Vandesompele *et al.*, 2002).

Using geNorm, gene expression stability can be evaluated by the average expression stability (M value), with a low M value indicating high stability of expression. In cDNA samples synthesized using random primers, *RPL15* and *SDHA* were the most stably expressed, followed by *ACTB*, *HPRT1*, *GAPDH* and *YWHAZ* (Fig. 1A). The highest stability of gene expression in cDNA samples synthesized using oligo(dT) primers was recorded for *HRPT1* and *YWHAZ*, followed by *ACTB*, *SDHA*, *RPL15* and *GAPDH* (Fig. 1C). To determine the optimal number of reference genes for accurate normalization, the pairwise variation (V) was calculated between two sequential normalization factors. In

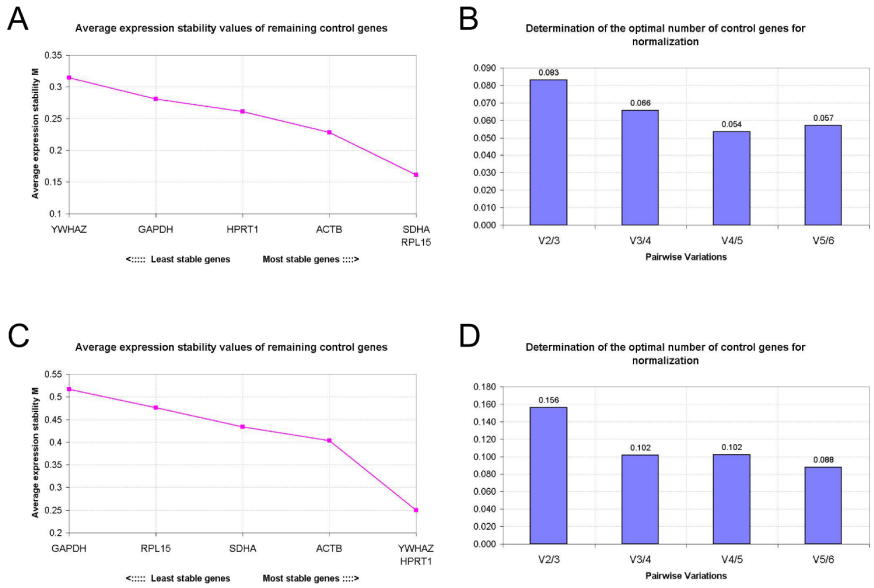

Figure 1. Stability of potential reference genes during oocyte maturation. The calculation of the average expression stability (M value) of candidate reference genes as determined by quantitative RT-PCR. The y-axis presents the M value and the x-axis presents the ranking of reference genes in order of increasing stability (from left to right); cDNA samples synthesized with random primers (A) or oligo(dT) primers (C). The optimal number of reference genes for normalization was determined by Pairwise variation (V) between the normalization factors (Vn and Vn+1). The optimal number of reference genes for cDNA samples synthesized with random primers (B) or oligo(dT) primers (D). Samples were derived from pools of 50 oocytes with three biological replicates.

both cDNA samples synthesized with random primers and oligo(dT) primers, the inclusion of a 3rd gene improved normalization (high $V_{2/3}$ value), but the inclusion of a 4th gene had little effect (low $V_{3/4}$ value) (Fig. 1B and D). Overall, the optimal combination of reference genes for normalization in cDNA samples differed between cDNA synthesized using random primers and oligo(dT) primers. With random primers, the combination of *RPL15*, *SDHA* and *ACTB* was favoured, whereas in cDNA samples synthesized using oligo(dT) primers it was *HPRT1*, *YWHAZ* and *ACTB*.

Gene expression patterns during oocyte maturation

We next focused on the expression patterns of *CCNA1*, *CCNB1*, *CCNB2*, *CDK2* and *EIF4A3* in oocyte cDNA samples synthesized using random primers and oligo(dT) primers, since these genes play important roles during oocyte and early

embryo development (Jansova *et al.* , 2018, Mendez and Richter, 2001). In cDNA samples synthesized with random primers, the expression of *CCNA1*, *CCNB1*, *CCNB2*, *CDK*2 and *EIF4A3* was relatively stable throughout maturation from GV to MII (Fig. 2A-E). Even though expression of *CCNA1* increased significantly from the GV to the MI stage, the GV/MI ratio of *CCNA1* expression was only 1.32 (Fig. 2A). In cDNA samples synthesized using oligo(dT) primers, the expression level patterns for *CCNA1*, *CCNB1*, *CDK*2 and *EIF4A3* were similar to those for cDNA synthesized using random primers (Fig. 2A, B, C and E).

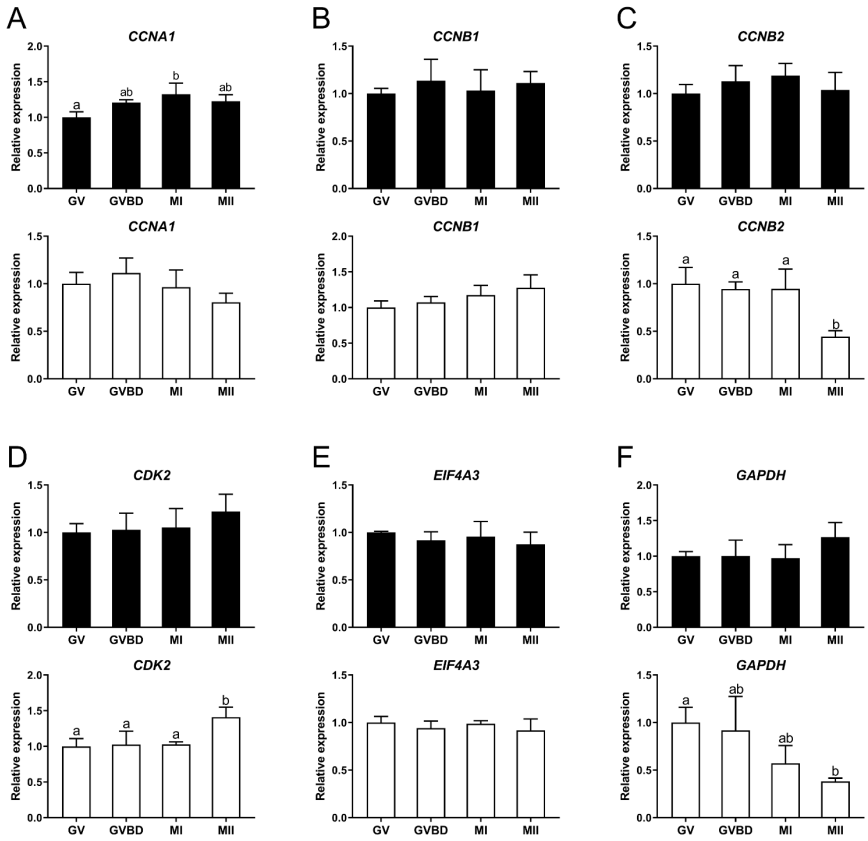

Figure 2. Gene expression patterns during oocyte maturation. The relative expression of genes in cDNA samples synthesized using random (black bars) or oligo(dT) primers (white bars) from bovine GV to MII oocytes**.** (A) *CCNA1*, (B) *CCNB1*, (C) *CCNB2*, (D) *CDK2*, (E) *EIF4A3*, (F) *GAPDH*. GV, GVBD, MI and MII respectively refer to germinal vesicle, germinal vesicle breakdown, metaphase I and metaphase II stages. Relative expression in GV oocytes was set as 1. Significant differences between groups are indicated by different letters above the bars ($p < 0.05$). *ACTB*, *RPL15* and *SDHA* were used for normalization in cDNA samples synthesized using random primers; *ACTB, HPRT1,* and *YWHAZ* were used for normalization in cDNA samples synthesized using oligo(dT) primers. Samples were collected from pools of 50 oocytes with three biological replicates.

By contrast, the expression of *CCNB2* decreased significantly from the MI to the MII stage (Fig. 2C).

We then examined the relative expression of *GAPDH* in oocytes from GV to MII, since *GAPDH* expression was not used for normalization. The patterns of apparent oocyte *GAPDH* expression were similar from GV to MII in cDNA samples synthesized with random primers (Fig. 2F). To our surprise, *GAPDH* expression levels decreased stepwise from the GV to MII stage in cDNA samples synthesized using oligo(dT) primers (Fig. 2F).

We therefore examined whether the expression levels of other potential reference genes also varied from GV to MII in cDNA samples synthesized using oligo(dT) primers. Because RNA was extracted from groups of 50 oocytes, the relative expression levels were first compared without normalization. Unexpectedly, the expression levels of both the reference and other (target) genes examined decreased as oocytes matured from the GV to the MII stage (Fig. 3A to K). Due to a high standard deviation among the three biological replicates, these differences were not statistically significant, expect *RLP15* ($p<0.05$), but the pattern was consistent for all genes examined. For comparison, the expression levels of reference and target genes, from GV to MII in cDNA samples synthesised using oligo(dT) primers, are shown in (Fig. S5).

Poly(A) tail length regulation during oocyte maturation

Because oocytes rely for a relatively long time on maternal mRNA during and after oocyte maturation, it is not unlikely that the poly(A) tail length is regulated during oocyte maturation. We therefore conducted poly(A) tail length assays (Rassa *et al.*, 2000) to investigate differences in the length of the poly(A) tails of *GAPDH*, *CCNB1*, *CCNB2* and *HPRT1* mRNA at different stages of oocyte maturation. For the poly(A) tail length assays, a nested PCR was performed using gene-specific forward primers with the addition of GB136 to increase the specificity of the PCR products (Fig. 4A). Second round PCR products were then size-separated by agarose gel electrophoresis. The PCR increase the specificity of the PCR products (Fig. 4A). Second round PCR products were then size-separated by agarose gel electrophoresis. The PCR products from GV oocytes showed slightly slower mobility than products from the MII oocytes in all of the genes we examined (Fig. 4B), indicating that mRNA in GV oocytes contained longer poly(A) tails than in MII oocytes.

To further confirm the decrease in poly(A) tail length during oocyte maturation, we performed DNA sequencing of amplicons (Fig. 4A). We

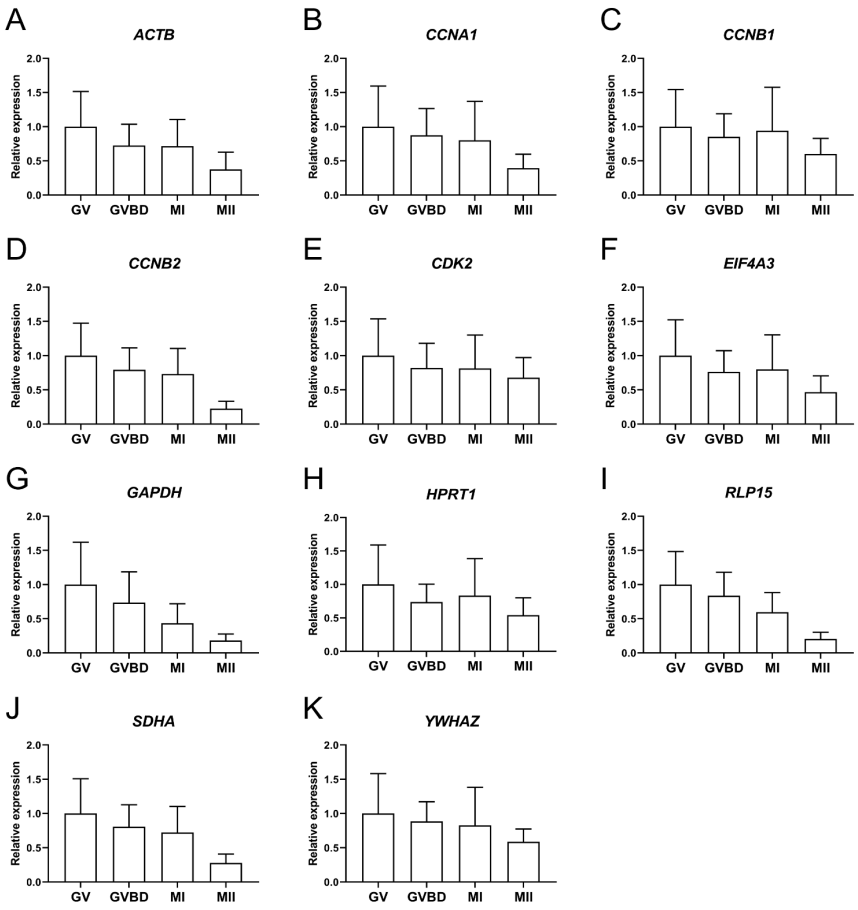

Figure 3. Gene expression patterns during oocyte maturation using oligo(dT) primers. Relative expression in cDNA samples synthesized using oligo(dT) primers in maturing bovine oocytes, as determined by quantitative RT-PCR without normalization. (A) *ACTB*, (B) *CCNA1*, (C) *CCNB1*, (D) *CCNB2*, (E) *CDK2*, (F) *EIF4A3*, (G) *GAPDH*, (H) *HRRT1*, (I) *RLP15*, (J) *SDHA*, (K) *YWHAZ*. GV, GVBD, MI, MII respectively refer to germinal vesicle, germinal vesicle breakdown, metaphase I and metaphase II stages. Absolute expression in GV oocytes is set at 1. Samples were collected from pools of 50 oocytes with three biological replicates.

determined that the length of the poly(A) tails ranged from 0-29 nucleotides (Fig. 4D, E). We further compared the poly(A) tail length of *GAPDH*, *CCNB1*, *CCNB2* and *HPRT1* mRNA in oocytes at the GV and MII stages. Consistent with the agarose gel electrophoresis results, significantly longer poly(A) tails were detected for *GAPDH*, *CCNB1* and *CCNB2* mRNA in GV oocytes, compared with MII oocytes (Fig. 4E). compared to GV oocytes but this difference was not statistically significant (Fig. 4E).

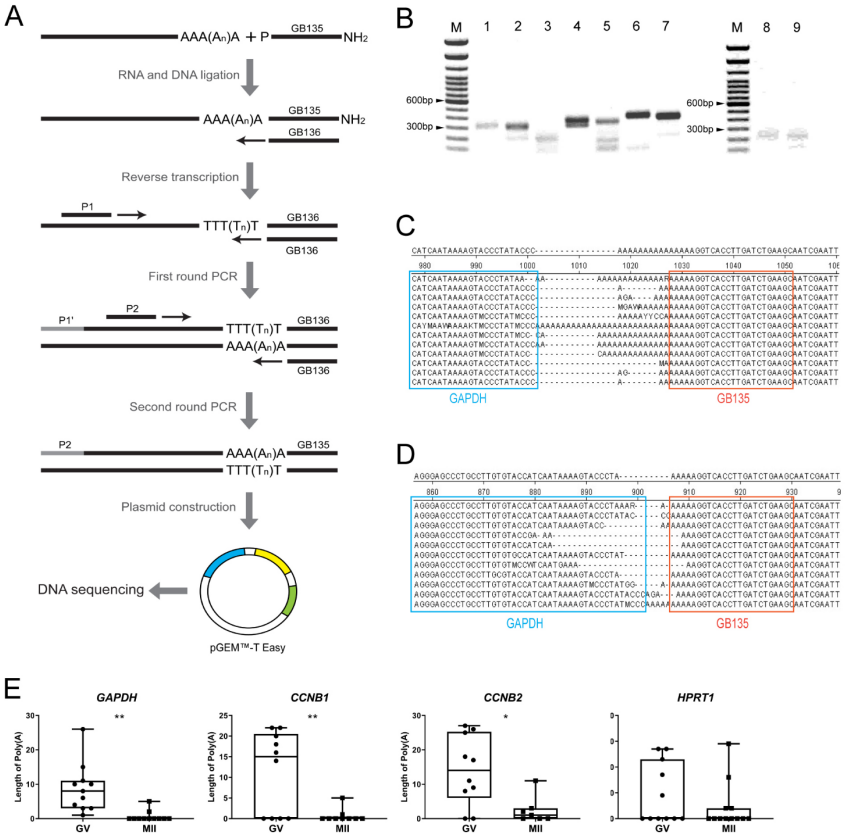

Figure 4. Poly(A) tail length regulation during oocyte maturation. (A) Schematic representation of the polyadenylation assay and poly (A) sequencing. mRNAs were ligated to a synthetic primer containing a 3' amino blocking group (GB135). The ligation products are then used as templates for a reverse transcription reaction using GB136 primers complementary to GB135. To amplify cDNA and increase the specificity of the amplicons, first round amplification was performed using a gene specific primer (P1) and GB136, and second round amplification was performed using a gene specific primer which started after the 3' site of P1 (P2) and GB136. The second round amplified product was then ligated with pGEM™-T Easy plasmid, followed by transformation with JM109 cells before DNA sequencing. (B) Agarose gel electrophoresis of second round amplified products. Lane M: 100 bp ladder; Lane 1: positive control; Lanes 2-3: *CCNB1* at germinal vesicle (GV) and metaphase II (MII) stage; Lanes 4-5: *CCNB2* at GV and MII stage; Lanes 6-7: *GAPDH* at GV and MII stage; Lanes 8-9: *HPRT1* at GV and MII stage. DNA sequencing result for GAPDH at GV stage (C) and MII stage (D) aligned by cluster W method. The end sequence of GAPDH is outlined with the cyan box and sequence of GB135 is included in the orange box. (E) Length of poly(A) tail of *GAPDH*, *CCNB1*, *CCNB2* and *HPRT1* at the GV and MII stages. Samples were collected from pools of 50 oocytes with three biological replicates.

Reference gene selection and gene expression patterns in morulae and blastocysts

Our next aim was to identify the most suitable reference genes for normalization, and to examine expression patterns for specific target genes in morulae and blastocysts. Maternal mRNA is largely degraded soon after major zygotic genome activation, which occurs at around the 8-cell stage in cattle embryos, similar to that in human embryos(Niakan *et al.* , 2012). *SDHA* and *YWHAZ* were the most stably expressed genes when cDNA was synthesized using random primers, while *RPL15* and *YWHAZ* were most stably expressed in cDNA synthesized using oligo(dT) primers (Fig. 5A, C). However, the three most stably expressed candidate reference genes were the same for cDNA synthesized using random primers or oligo(dT) primers, namely *RPL15*, *SDHA* and *YWHAZ* (Fig. 5A to D). We therefore used a combination of *RPL15*, *SDHA* and *YWHAZ* to normalize gene expression in embryos. The expression patterns of *CCNA1*, *CCNB1*, *CCNB2*, *CDK2* and *EIF4A3* in morulae and blastocysts were very similar between cDNA samples synthesized using random primers and oligo(dT)

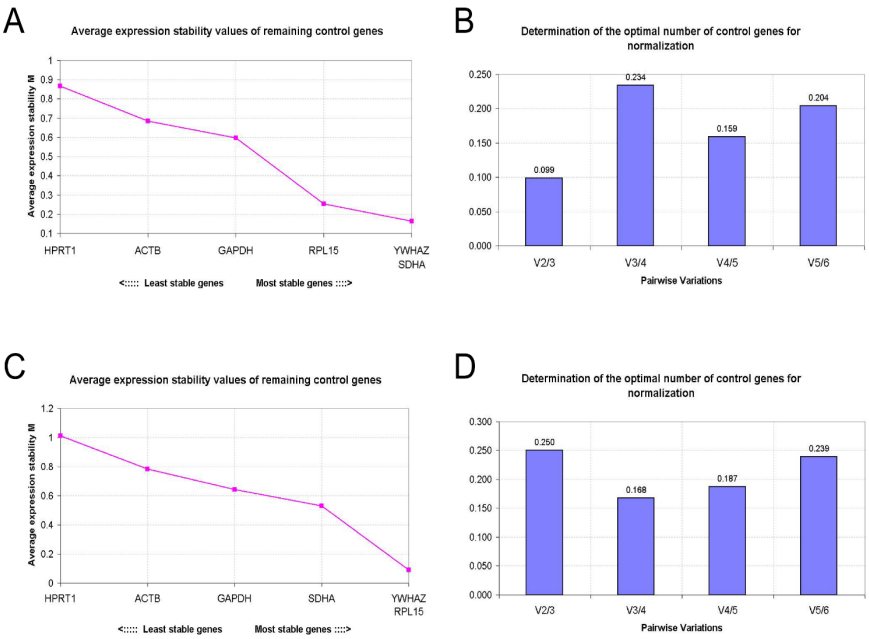

Figure 5. Reference gene selection in morulae and blastocysts. The geNorm analysis of the average expression stability (M value) of all candidate reference genes determined by quantitative RT-PCR, cDNA samples synthesized using random primers (A) or oligo(dT) primers (C). More stable reference genes are positioned on the right side of the diagram, less stable on the left side. The optimal number of reference genes for normalization determined by Pairwise variation (V) between the normalization factors (Vn and Vn+1). The optimal number of reference genes for cDNA samples synthesized with random primers (B) or oligo(dT) primers(D). Samples were collected from pools of 50 embryos with three biological replicates.

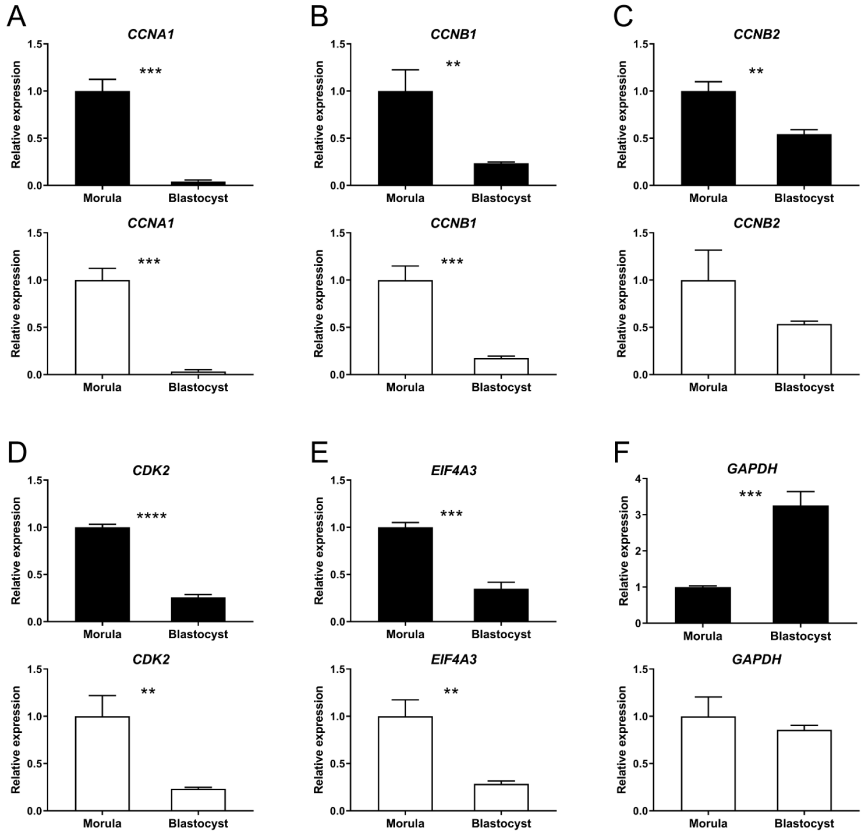

Figure 6. Gene expression patterns in morulae and blastocysts. The relative expressions of genes in cDNA samples synthesized using random primers (black bars) or oligo(dT) primers (white bars) in bovine morulae and blastocysts. (A) *CCNA1*, (B) *CCNB1*, (C) *CCNB2*, (D) *CDK2*, (E) *EIF4A3*, (F) *GAPDH*. Relative expression in morulae set at 1; * ($p < 0.05$), ** ($p < 0.005$), *** ($p < 0.0005$) and **** ($p < 0.0001$) indicate significant differences between morulae and blastocysts. *RPL15*, *SDHA* and *YWHAZ* were used for normalization for cDNA samples synthesized with both random primers and oligo(dT) primers. Samples were collected from pools of 50 embryos with three biological replicates.

primers (Fig. 6A to E). Surprisingly, the expression of GAPDH increased markedly from morula to blastocyst in cDNA samples synthesized using random primers but did not differ in cDNA samples synthesized using oligo(dT) primers (Fig. 6F). We also included 8-cell embryos to identify the best reference genes for normalization and expression patterns from 8-cell embryos to blastocysts. The three most stably expressed reference genes were still *RPL15*, *SDHA* and *YWHAZ* in cDNA samples synthesized with random primers while *GAPDH*, *SDHA* and *YWHAZ* were the most suitable reference genes for normalization in cDNA samples synthesized with oligo(dT) primers (Fig. S3). Expression patterns of

CCNB1, *CCNB2* and *CDK2* were similar from 8-cell embryos to blastocysts between cDNA samples synthesized using random primers and oligo(dT) primers (Fig. S4B to D). On the hand, the expression of *CCNA1* and *EIF4A3* was down-regulated from the 8-cell embryo to the blastocyst stage in cDNA samples synthesized using random primers, whereas expression of *CCNA1* and *EIF4A3* was significantly elevated at the morula stage in cDNA samples synthesized using oligo(dT) primers (Fig. S4A, E).

Discussion

Proper quantification of mRNA expression levels with qRT-PCR relies on the use of stably expressed reference genes (Goossens *et al.*, 2005a, Kuijk *et al.*, 2007, Mamo *et al.*, 2007). A critical step in the process, in particular reverse transcription, has however been less well studied. The RNA concentration, quality and the type of reverse transcriptase can influence reverse transcription, but when samples received the same experimental handling and relative levels are determined, quantification can be reliable (Cholet *et al.* , 2020). Here, we demonstrate that the combination of genes optimal for normalization is dependent on the priming strategy, i.e. random hexamers or oligo(dT), used for reverse transcription in oocytes. Bovine oocytes were used, since these can be collected in fairly large quantities from leftover slaughterhouse ovaries. In addition the oocytes can be efficiently fertilized in vitro and embryos cultured to the blastocyst stage. No laboratory animals were therefore required, in accordance with the 3Rs of animal experimentation. Above all, the timing of bovine oocyte maturation and preimplantation development is very similar to that of human oocytes and embryos.

Selection of reference genes for normalization is an essential step for accurate gene expression analysis. The software program geNorm was used to determine stability of gene expression. Comparisons with other programs such as BestKeeper and NormFinder, revealed that they gave very similar results. (De Spiegelaere *et al.* , 2015, Spinsanti *et al.* , 2006). More importantly, geNorm is the most commonly used normalization algorithm, because geNorm does not need large data sets and the raw data for this program do not need to be normally distributed (Mehdi Khanlou and Van Bockstaele, 2012). Even though the selection of reference genes for normalization in bovine oocytes has been documented (Caetano *et al.* , 2019, Goossens *et al.*, 2005a, Khan *et al.* , 2016), the effect of different reverse transcription priming strategies to the choice of reference genes has not been addressed in detail. It has been reported that the

combination of suitable reference genes includes *HPRT1* and *B2M* in bovine oocyte cDNA samples synthesized using random primers (Caetano *et al.*, 2019), while the ideal reference genes were *ACTB* and *GAPDH* in bovine oocyte cDNA samples synthesized using oligo(dT)s (Khan *et al.*, 2016). Consistently, in our study, even though the same original mRNA and system were applied, suitable reference genes for normalization were different if reverse transcription priming strategies were different.

In morulae and blastocysts, the combination of suitable reference genes seems to be less dependent on the priming strategy. This may be due to the large numbers of maternal mRNA transcripts present in oocytes and very early embryos, and the degradation of these maternal transcripts following the onset of zygotic gene expression at around the 8-cell stage in bovine embryos. To demonstrate that this difference is dependent on the method used for reverse transcription but not the efficiency of RNA extraction, we split RNA samples into two equal parts for the different reverse transcription strategies after extraction. Interestingly, it has been reported that *GAPDH*, *PPIA*, *ACTB*, *RPL15*, *GUSB*, and *H2A.2* are not suitable reference genes for normalization, because of their inconstant levels throughout preimplantation development (Ross *et al.* , 2010). In our study, suitable reference genes for normalization in oocytes are different from those in morulae and blastocysts even when reverse transcription is performed using the same priming strategy. We suggest using different combinations of reference genes for normalization before and after zygotic genome activation, due to the switch from maternal to zygotic mRNA content.

In this study, we show that gene expression levels as determined by qRT-PCR change during oocyte maturation and can differ depending on the priming strategy used for reverse transcription. This is in agreement with previous studies in which relative gene expression was directly compared when reverse transcription was performed using random primers and oligo(dT) primers (Gohin *et al.* , 2014, Thélie *et al.* , 2007). In cDNA samples synthesized using random primers, the expression was stable from the GV to MII stage in oocytes for every gene we examined, indicating that maternal mRNAs were not degraded after resumption of meiosis. Indeed, it has been documented that, at least in bovine oocytes, there is no decrease in total RNA content during meiosis (Lequarre *et al.* , 2004). We also detected a surge in absolute gene expression in oocytes between the GV and GVBD stages when no normalization was applied, suggesting that large amounts of maternal RNA are synthesized within the 6 hours prior to GVBD. Therefore, when gene expression levels are examined using qRT-

PCR, reverse transcription using random primers is preferable.

In the mouse, high levels of cyclin B protein in MI and MII oocytes are achieved by control of maternal mRNA translation, which coincides with an elongation of the *CCNB1* mRNA (Kotani *et al.*, 2013). High levels of cyclin B have been observed in MI and MII oocytes (Heikinheimo and Gibbons, 1998, Quetglas *et al.* , 2010, Wu *et al.* , 1997). We detected consistent levels of *CCNB1* expression throughout oocyte maturation, while detected *CCNB2* levels were significantly reduced from GV to MII oocytes when cDNA was synthesized with oligo(dT) primers. To address how cyclin B gene expression was regulated in oocytes, we analyzed our qRT-PCR data without normalization, since numbers of oocytes were equal in all groups. Both *CCNB1* and *CCNB2* expression, as well as reference gene expression levels could be seen to be down-regulated from the GV to the MII stage.

Associated to our qRT-PCR without normalization data, the poly(A) tail lengths for *CCNB1*, *CCNB2* and *HPRT1* also decreased from the GV to the MII stage. In contrast, it has been reported that the poly(A) tail of CCNB1 is elongated during oocyte maturation in the mouse, *Xenopus* and zebrafish (Kotani *et al.*, 2013, Mendez and Richter, 2001). A decrease in poly(A) tail length and a down-regulation of gene expression when normalization was not applied was also observed for other genes, indicating a general deadenylation of maternal mRNA during bovine oocyte maturation. In agreement with our findings, it has been reported that the amount of poly(A) RNA is reduced by half, but that the total RNA content does not change during bovine oocyte maturation (Lequarre *et al.*, 2004). It is therefore possible that maternal mRNAs have long poly(A) tails to increase their stability during long time storage before meiosis resumption. Interestingly, other studies have shown that mRNAs have much longer poly(A) tails, up to 250 nucleotides (Lim *et al.*, 2016, Vaur *et al.* , 2002), than the poly(A) lengths we detected.

In conclusion, we observed that the genes used for normalization of expression levels may differ in terms of apparent stability of expression in oocytes depending on the priming strategy used to synthesize the cDNA, and the priming strategy should therefore be tailored to the question addressed. In embryos at a stage beyond zygotic genome activation such as morulae and blastocysts, the method of cDNA generation appears to be less critical to obtaining reliable qRT-PCR results. In general, the poly(A) tail of mRNA species synthesized before GVBD in oocytes seems to shorten during meiotic maturation to the MII stage in bovine oocytes.

Acknowledgements

We thank Arend Rijneveld and Christine Oei for assistance with oocyte recovery.

Authors' roles

B.Y., H.T., and B.R. conceived and designed the experiments. B.Y. and H.T. performed the experiments. B.Y. collected and analysed the data. B.R. contributed the reagents, materials and analysis tools. B.Y., T.S. and B.R. wrote the manuscript. All authors read and approved the manuscript.

Supplementals

Supplemental figures and tables in this chapter are available at *Molecular Human Reproduction* (https://academic.oup.com/molehr/article/27/7/gaab040/6307270) online.

References

Anderson P, Kedersha N. RNA granules: post-transcriptional and epigenetic modulators of gene expression. *Nature reviews Molecular cell biology* 2009;**10**:430-436.

Brinkhof B, van Tol HT, Groot Koerkamp MJ, Riemers FM, SG IJ, Mashayekhi K, Haagsman HP, Roelen BA. A mRNA landscape of bovine embryos after standard and MAPK-inhibited culture conditions: a comparative analysis. *BMC genomics* 2015;**16**:277.

Brinkhof B, van Tol HT, Groot Koerkamp MJ, Wubbolts RW, Haagsman HP, Roelen BA. Characterization of bovine embryos cultured under conditions appropriate for sustaining human naïve pluripotency. *PloS one* 2017;**12**:e0172920.

Caetano LC, Miranda-Furtado CL, Batista LA, Pitangui-Molina CP, Higa TT, Padovan CC, Rosa ESA. Validation of reference genes for gene expression studies in bovine oocytes and cumulus cells derived from in vitro maturation. *Animal reproduction* 2019;**16**:290-296.

Cholet F, Ijaz UZ, Smith CJ. Reverse transcriptase enzyme and priming strategy affect quantification and diversity of environmental transcripts. *Environmental microbiology* 2020;**22**:2383-2402.

Daldello EM, Luong XG, Yang CR, Kuhn J, Conti M. Cyclin B2 is required for progression through meiosis in mouse oocytes. *Development (Cambridge, England)* 2019;**146**.

De Spiegelaere W, Dern-Wieloch J, Weigel R, Schumacher V, Schorle H, Nettersheim D, Bergmann M, Brehm R, Kliesch S, Vandekerckhove L *et al.* Reference gene validation for RT-qPCR, a note on different available software packages. *PloS one* 2015;**10**:e0122515.

Dumdie JN, Cho K, Ramaiah M, Skarbrevik D, Mora-Castilla S, Stumpo DJ, Lykke-Andersen J, Laurent LC, Blackshear PJ, Wilkinson MF *et al.* Chromatin Modification and Global Transcriptional Silencing in the Oocyte Mediated by the mRNA Decay Activator ZFP36L2. *Developmental cell* 2018;**44**:392-402.e397.

Eichhorn SW, Subtelny AO, Kronja I, Kwasnieski JC, Orr-Weaver TL, Bartel DP. mRNA poly(A)-tail changes specified by deadenylation broadly reshape translation in *Drosophila* oocytes and early embryos. *eLife* 2016;**5**.

Evans C, Hardin J, Stoebel DM. Selecting between-sample RNA-Seq normalization methods from the perspective of their assumptions. *Briefings in bioinformatics* 2018;**19**:776-792.

Gohin M, Fournier E, Dufort I, Sirard MA. Discovery, identification and sequence analysis of RNAs selected for very short or long poly A tail in immature bovine oocytes. *Molecular human reproduction* 2014;**20**:127-138.

Goossens K, Van Poucke M, Van Soom A, Vandesompele J, Van Zeveren A, Peelman LJ. Selection of reference genes for quantitative real-time PCR in bovine preimplantation embryos. *BMC developmental biology* 2005;**5**:27.

Hamatani T, Carter MG, Sharov AA, Ko MS. Dynamics of global gene expression changes during mouse preimplantation development. *Developmental cell* 2004;**6**:117-131.

Heikinheimo O, Gibbons WE. The molecular mechanisms of oocyte maturation and early embryonic development are unveiling new insights into reproductive medicine. *Molecular human reproduction* 1998;**4**:745-756.

Ihara J, Yoshida N, Tanaka T, Mita K, Yamashita M. Either cyclin B1 or B2 is necessary and sufficient for inducing germinal vesicle breakdown during frog (Rana japonica) oocyte maturation. *Molecular reproduction and development* 1998;**50**:499-509.

Jansova D, Tetkova A, Koncicka M, Kubelka M, Susor A. Localization of RNA and translation in the mammalian oocyte and embryo. *PloS one* 2018;**13**:e0192544.

Khan DR, Landry DA, Fournier É, Vigneault C, Blondin P, Sirard MA. Transcriptome meta-analysis of three follicular compartments and its correlation with ovarian follicle maturity and oocyte developmental competence in cows. *Physiological genomics* 2016;**48**:633-643.

Kotani T, Yasuda K, Ota R, Yamashita M. Cyclin B1 mRNA translation is temporally controlled through formation and disassembly of RNA granules. *The Journal of cell biology* 2013;**202**:1041-1055.

Kuijk EW, du Puy L, van Tol HT, Haagsman HP, Colenbrander B, Roelen BA. Validation of reference genes for quantitative RT-PCR studies in porcine oocytes and preimplantation embryos. *BMC developmental biology* 2007;**7**:58.

Lequarre AS, Traverso JM, Marchandise J, Donnay I. Poly(A) RNA is reduced by half during bovine oocyte maturation but increases when meiotic arrest is maintained with CDK inhibitors. *Biology of reproduction* 2004;**71**:425-431.

Li J, Qian WP, Sun QY. Cyclins regulating oocyte meiotic cell cycle progression†. *Biology of reproduction* 2019;**101**:878-881.

Lim J, Lee M, Son A, Chang H, Kim VN. mTAIL-seq reveals dynamic poly(A) tail regulation in oocyte-to-embryo development. *Genes & development* 2016;**30**:1671-1682.

Mamo S, Gal AB, Bodo S, Dinnyes A. Quantitative evaluation and selection of reference genes in mouse oocytes and embryos cultured in vivo and in vitro. *BMC developmental biology* 2007;**7**:14.

Mehdi Khanlou K, Van Bockstaele E. A critique of widely used normalization software tools and an alternative method to identify reliable reference genes in red clover (Trifolium pratense L.). *Planta* 2012;**236**:1381-1393.

Mendez R, Richter JD. Translational control by CPEB: a means to the end. *Nature reviews Molecular cell biology* 2001;**2**:521-529.

Morgan M, Much C, DiGiacomo M, Azzi C, Ivanova I, Vitsios DM, Pistolic J, Collier P, Moreira PN, Benes V *et al.* mRNA 3' uridylation and poly(A) tail length sculpt the mammalian maternal transcriptome. *Nature* 2017;**548**:347-351.

Nagahama Y, Yamashita M. Regulation of oocyte maturation in fish. *Development, growth & differentiation* 2008;**50 Suppl 1**:S195-219.

Nakahata S, Kotani T, Mita K, Kawasaki T, Katsu Y, Nagahama Y, Yamashita M. Involvement

of *Xenopus* Pumilio in the translational regulation that is specific to cyclin B1 mRNA during oocyte maturation. *Mechanisms of development* 2003;**120**:865-880.

Niakan KK, Han J, Pedersen RA, Simon C, Pera RA. Human pre-implantation embryo development. *Development (Cambridge, England)* 2012;**139**:829-841.

Quetglas MD, Adona PR, de Bem TH, Pires PR, Leal CL. Effect of cyclin-dependent kinase (CDK) inhibition on expression, localization and activity of maturation promoting factor (MPF) and mitogen activated protein kinase (MAPK) in bovine oocytes. *Reproduction in domestic animals = Zuchthygiene* 2010;**45**:1074-1081.

Radonova L, Pauerova T, Jansova D, Danadova J, Skultety M, Kubelka M, Anger M. Cyclin A1 in Oocytes Prevents Chromosome Segregation And Anaphase Entry. *Scientific reports* 2020;**10**:7455.

Rassa JC, Wilson GM, Brewer GA, Parks GD. Spacing constraints on reinitiation of paramyxovirus transcription: the gene end U tract acts as a spacer to separate gene end from gene start sites. *Virology* 2000;**274**:438-449.

Richter JD. CPEB: a life in translation. *Trends in biochemical sciences* 2007;**32**:279-285.

Ross PJ, Wang K, Kocabas A, Cibelli JB. Housekeeping gene transcript abundance in bovine fertilized and cloned embryos. *Cellular reprogramming* 2010;**12**:709-717.

Sallés FJ, Lieberfarb ME, Wreden C, Gergen JP, Strickland S. Coordinate initiation of *Drosophila* development by regulated polyadenylation of maternal messenger RNAs. *Science (New York, NY)* 1994;**266**:1996-1999.

Spinsanti G, Panti C, Lazzeri E, Marsili L, Casini S, Frati F, Fossi CM. Selection of reference genes for quantitative RT-PCR studies in striped dolphin (Stenella coeruleoalba) skin biopsies. *BMC molecular biology* 2006;**7**:32.

Stangegaard M, Dufva IH, Dufva M. Reverse transcription using random pentadecamer primers increases yield and quality of resulting cDNA. *BioTechniques* 2006;**40**:649-657.

Tan JH, Wang HL, Sun XS, Liu Y, Sui HS, Zhang J. Chromatin configurations in the germinal vesicle of mammalian oocytes. *Molecular human reproduction* 2009;**15**:1-9.

Thélie A, Papillier P, Pennetier S, Perreau C, Traverso JM, Uzbekova S, Mermillod P, Joly C, Humblot P, Dalbiès-Tran R. Differential regulation of abundance and deadenylation of maternal transcripts during bovine oocyte maturation in vitro and in vivo. *BMC developmental biology* 2007;**7**:125.

Vandesompele J, De Preter K, Pattyn F, Poppe B, Van Roy N, De Paepe A, Speleman F. Accurate normalization of real-time quantitative RT-PCR data by geometric averaging of multiple internal control genes. *Genome biology* 2002;**3**:Research0034.

Vastenhouw NL, Cao WX, Lipshitz HD. The maternal-to-zygotic transition revisited. *Development (Cambridge, England)* 2019;**146**.

Vaur S, Montreau N, Dautry F, Andéol Y. Differential post-transcriptional regulations of wnt mRNAs upon axolotl meiotic maturation. *The International journal of developmental biology*

2002;**46**:731-739.

Winata CL, Korzh V. The translational regulation of maternal mRNAs in time and space. *FEBS letters* 2018;**592**:3007-3023.

Wu B, Ignotz G, Currie WB, Yang X. Dynamics of maturation-promoting factor and its constituent proteins during in vitro maturation of bovine oocytes. *Biology of reproduction* 1997;**56**:253-259.

Chapter 3

Initiation of X chromosome inactivation during bovine embryo development

Bo Yu[1], Helena T. A. van Tol[1], Tom A.E. Stout[2] and Bernard A. J. Roelen[3]*

[1]Farm Animal Health; Department of Population Health Sciences, Faculty of Veterinary Medicine, Utrecht University, Utrecht, The Netherlands.

[2]Equine Sciences; Department Clinical Sciences, Faculty of Veterinary Medicine, Utrecht University, Utrecht, The Netherlands.

[3]Embryology, Anatomy and Physiology; Department Clinical Sciences, Faculty of Veterinary Medicine, Utrecht University, Utrecht, The Netherlands.

Adapted from *Cells. 2020 Apr; 9(4): 1016*
Doi: 10.3390/cells9041016.

Abstract

X chromosome inactivation (XCI) is a developmental process that aims to equalize dosage of X-linked gene products between XY males and XX females in eutherian mammals. In female mouse embryos, paternal XCI is initiated at the 4-cell stage; however, the X chromosome is reactivated in the inner cell mass cells of blastocysts, and random XCI is subsequently initiated in epiblast cells. However, recent findings show that the patterns of XCI are not conserved among mammals. In this study, we used quantitative RT-PCR and RNA in situ hybridization combined with immunofluorescence to investigate the pattern of XCI during bovine embryo development. Expression of *XIST* (X-inactive specific transcript) RNA was significantly upregulated at the morula stage. For the first time, we demonstrate that *XIST* accumulation in bovine embryos starts in nuclei of female morulae, but its colocalization with histone H3 lysine 27 trimethylation was first detected in day 7 blastocysts. Both in the inner cell mass and in putative epiblast precursors, we observed a proportion of cells with XIST RNA and H3K27me3 colocalization. Surprisingly, the onset of XCI did not lead to a global downregulation of X-linked genes even in day 9 blastocysts. Together our findings confirm that diverse different patterns of XCI initiation exist among developing mammalian embryos.

Introduction

In placental mammals, dosage compensation for X-encoded genes between female (XX) and male (XY) cells is achieved by inactivation of one of the two X chromosomes in female cells. This so-called X-chromosome inactivation (XCI) leads to stochastic transcriptional silencing of one of the two female X chromosomes, and is effected by the long non-coding RNA *XIST* (Heard *et al.* , 1997, Lyon, 1961). *XIST* accumulates in 'clouds' along the future inactive X-chromosome (Xi), which can be visualized using RNA fluorescence in situ hybridization (FISH). To silence the chromatin and repress the X-linked genes from that chromosome, *XIST* recruits epigenetic modifiers (Sado and Brockdorff, 2013). Histone H3 lysine 27 trimethylation (H3K27me3) is a representative epigenetic hallmark associated with gene silencing and reported to be enriched on the Xi, and indeed colocalizes with *XIST* RNA (Yue *et al.* , 2014).

X-chromosome inactivation is established during early embryonic development and maintained thereafter (Deng *et al.* , 2014). In the mouse, imprinted XCI is initiated at the 4-cell stage embryo stage with exclusive

inactivation of the paternal X chromosome (Xp). Indeed, the paternal X-chromosome remains inactive in trophectoderm (TE) cells during and after formation of the mouse blastocyst (Patrat *et al.* , 2009, Takagi and Sasaki, 1975). In the inner cell mass (ICM) of female embryos, however, the inactive Xp is reactivated, resulting in two active X chromosomes (XaXa). At around the time of implantation when the epiblast is being established, XCI is re-established with either maternal or paternal X-chromosomes inactivated randomly in different cells, a process known as random X chromosome inactivation (Mak *et al.* , 2004). Although the initiation of XCI has been extensively explored in mouse embryos, the pattern of XCI in other mammalian species is less clear. In rabbits and humans for example, XCI starts later at the morula and blastocyst stages, respectively, and is not subject to imprinting (Okamoto *et al.*, 2011). Furthermore, large *XIST* clouds have been detected around both X chromosomes in cells of rabbit and human embryos, even in the ICM (Okamoto *et al.*, 2011, Petropoulos *et al.* , 2016). It appears therefore that XCI does not follow a uniform pattern in mammals.

In female mice, one of the defining characteristics of the naïve pluripotent state is the presence of two active X chromosomes, i.e. XaXa (Prudhomme *et al.* , 2015). Similar to the ICM, the absence of *XIST* expression from both X chromosomes has been observed in female mouse embryonic stem (ES) cells and induced pluripotent stem cells (Bruck and Benvenisty, 2011). Moreover, the pluripotency factors OCT4, SOX2, and NANOG have been implicated in suppression of *XIST* expression, by binding to its first intron (Navarro *et al.* , 2008). Upon pluripotent cell differentiation, the pluripotency factors are transcriptionally down-regulated and *XIST* expression increases, leading to random XCI (Minkovsky *et al.* , 2012). In human cells, however, the correlation between pluripotency state and XCI is less clear (Minkovsky *et al.*, 2012). Even though the XaXa state has been reported in female human ES cells, these cell lines were shown to be very unstable during passages (Geens and Chuva De Sousa Lopes, 2017). Meanwhile, inactive X chromosomes (Xi) were detected in other human ES and induced pluripotent stem cells, with *XIST* coating and accumulation of heterochromatin markers on the Xi (Barakat and Gribnau, 2010). Interestingly, female mouse epiblast stem cells, considered to be at a primed pluripotency state, also exhibit random XCI and share several morphological and molecular similarities with human ES cells. It has been hypothesized that human ES cells are at a primed pluripotent state and that the presence of XaXa in female cells may still be a hallmark of naïve pluripotency in human cells (Barakat and Gribnau, 2010, Huang *et al.* , 2014, Lovell-Badge, 2007). So far, however, the

connection between pluripotency and XCI state in other mammals has not been investigated in depth. Interestingly, stable primed pluripotent embryonic stem cell lines have recently been established from bovine embryos; however, their X chromosome activation states have not yet been reported (Bogliotti *et al.* , 2018).

One of the major consequences of XCI is the downregulation expression of X-linked genes on the inactivated X chromosome. During mouse development, silencing of X-linked genes follows the *XIST* coating (Mak *et al.*, 2004, Okamoto *et al.* , 2004). Despite the *XIST* coating of the inactivated X-chromosome, several X-linked genes escape silencing and are still expressed, as has been demonstrated in human and rabbit embryos (Okamoto *et al.*, 2011). In bovine blastocysts, X-linked genes were expressed at higher levels in female compared with male suggesting that X-chromosome inactivation was not yet operational (Min *et al.* , 2017). These data suggest that downregulation of X-linked genes after XCI initiation is not uniformly conserved among species.

Here, we examined the timing of XCI, its initiation in different lineage segregation and regulation of X-linked gene expression during bovine embryo development. By performing quantitative RT-PCR, immunofluorescence and RNA in situ hybridization, we established that *XIST* expression is initiated at around the morula stage and can be detected in both the ICM and TE, but does not lead to chromosome-wide downregulation of gene expression.

Materials and Methods

In vitro embryo production and collection of samples

Bovine ovaries collected from a local slaughterhouse were transported to the laboratory in a thermos flask and rinsed with water at 30 °C. After rinsing, the ovaries were immersed in 0.9% NaCl supplemented with penicillin/streptomycin (PS) (100 µg/mL) at 30 °C. Cumulus-oocyte complexes (COCs) were aspirated from follicles with a diameter of 2-8mm using a winged infusion set (18G) connected to a vacuum aspiration system. Aspirated follicular fluid was collected in 50 mL centrifuge tubes. To isolate the COCs, sediment from the fluid was transferred to Petri dishes and COCs were identified using a stereomicroscope. The COCs were then matured by 23h incubation at 39 °C in a humidified atmosphere of 5% CO_2 in air as described previously (Brinkhof *et al.* , 2015a). Next, the matured oocytes were fertilized with $1*10^6$/mL sperm cells. Presumptive female or male embryos were generated by using X-sorted or Y-sorted sperm (CRV, Arnhem, the Netherlands). Prior to introduction, sperm

motility was checked under a stereomicroscope, and the moment that COCs were co-incubated with sperm was considered day 0. After incubation with sperm for 20-22h, COCs were denuded by vortexing for 3 min. The presumptive zygotes were then placed in synthetic oviductal fluid (SOF) (Brinkhof *et al.*, 2017) for further development in a humidified atmosphere containing 5% CO_2 and 7% O_2 at 39 °C. At day 5, developing embryos were transferred to fresh SOF and further cultured until day 9.

For subsequent analysis, germinal vesicle (GV) oocytes and Metaphase II (MII) oocytes were collected immediately after COC recovery and after 23h in vitro maturation culture, respectively. Zygotes, 2, 4 and 8 cell embryos were collected at 20, 32, 38 and 56 h after the start of fertilization respectively, and morulae and blastocysts were collected after 5 and 8 days, respectively of in vitro culture.

Inner cell mass (ICM) and trophectoderm (TE) cells were separated and collected from day 9 blastocysts using tungsten needles as described previously (Brinkhof *et al.*, 2015a). Isolated ICMs and TE cells were immediately placed in groups (range 43-59) in RNase free tubes on ice containing100 µL RLT buffer (Qiagen, Venlo, The Netherlands) and then stored at -80 °C until RNA isolation.

Isolation of oviduct cells and cell culture

Oviducts were collected from a local slaughterhouse and transported to the laboratory on ice. After removal of surrounding tissue, the oviducts were washed three times in PBS supplemented with penicillin (10 µg/mL) and streptomycin (10 µg/mL) (Gibco). Oviduct luminal epithelial cells were collected from the ampullary end of the oviducts by squeezing. The cells were washed twice in HEPES-buffered Medium 199 (Gibco) supplemented with penicillin (100 µg/mL), streptomycin (100 µg/mL) and gentamicin (50 µg/mL, Sigma, G1272) and centrifuged at 500×g for 5 min at 25 °C. The cells were then cultured for 24 h at 37 °C with 5% CO_2 in HEPES-buffered Medium 199 supplemented with penicillin (100 µg/mL), streptomycin (100 µg/mL), gentamicin (50 µg/mL) and 10% fetal calf serum (FCS; Bovogen Biologicals, Melbourne, Australia).

HEK293 (human embryonic kidney) cells were grown in DMEM/F12 supplemented with penicillin (100 µg/mL), streptomycin (100 µg/mL), gentamicin (50 µg/mL) and 10% FCS at 37 °C with 5% CO_2.

RNA extraction and cDNA generation

Oocytes and embryos in pools of 20 were washed in PBS and stored in RLT

buffer at -80 °C until RNA extraction. Total RNA isolation was performed using the RNeasy Micro Kit (Qiagen, Valencia, CA, USA) according to the manufacturer's instruction. Complementary DNA (cDNA) synthesis was carried out directly after RNA isolation. The reverse transcription (RT) mixture was prepared from 10 µL of the RNA sample, 4 µL of 5 × RT buffer (Invitrogen, Breda, The Netherlands), 10 mM DTT (Invitrogen), 0.5 mM dNTP (Promega), 8 units RNAsin/ RNAse inhibitor (Promega) and 150 units Superscript III reverse transcriptase (Invitrogen) in a total volume of 20 µL. Minus-RT controls were made up of the same reagents as above, except the reverse transcriptase. The mixtures were incubated at 70 °C for 5 min, followed by 1 h at 50 °C, and 5 min at 80 °C. Samples were subsequently stored at -20 °C.

Quantitative reverse transcription-PCR

Primer pairs (Eurogentec) were designed on Primer-Blast (http://www.ncbi.nlm.nih.gov/tools/primer-blast) using *Bos taurus* mRNA (Genbank; http://www.ncbi.nlm.nih.gov/nucleotide) as the template. Amplification took place in 10 µL iQ SYBR Green supermix (Biorad), 9 µL RNAse- and DNAse-free water (Invitrogen) and 1 µL cDNA with a final primer concentration of 500 nM. Reactions were performed in a CFX detection system (Biorad) following the manufacturer's protocol. The mixture was kept at 95 °C for 3 min, followed by 40 cycles of 95 °C for 20 sec, the primer specific annealing temperature (Table S1) for 20 sec and extension at 72 °C for 20 sec. To verify the purity of the PCR products, melting curves were generated with temperature increments of 0.5 °C from 65 °C to 95 °C for 5 sec each step. All the reactions were performed on three independent cDNA samples in duplicate. To determine quantitative (q)RT-PCR amplification efficiency, standard curves for primers were made by 4 folds dilutions of cDNA from 400 oocytes. *YWHAZ*, *GAPDH* and *SDHA* were used for normalization (Goossens *et al.* , 2005b).

Combined RNA FISH and immunofluorescence

Bovine *XIST* oligo probes (Table S2) were designed using the Stellaris online probe designer (https://www.biosearchtech.com/support/tools/design-software/stellaris-probe-designer) and *Bos taurus XIST* transcript variants X1, X2 and X3 (Genbank; http://www.ncbi.nlm.nih.gov/nucleotide) as the templates. Embryos and cells were fixed with 4% paraformaldehyde for 10 min. After washing twice in PBST (1x PBS, 0.01% Triton X-100), samples were permeabilized using Cytoskeletal Buffer (10 mM PIPES, pH 6.8; 100 mM NaCl; 300 mM sucrose; 3 mM $MgCl_2$) containing 0.5% Triton X-100 on ice for 5 min.

After three further washes in PBST, samples were kept in 70% ethanol at 4 °C for at least 2 h until further use.

After fixation and permeabilization, embryos and cells were washed twice in PBST and then incubated in dilution buffer (1x PBS, 0.3% Triton X-100, 0.4 units/mL RNAsin/ RNAse inhibitor) with the primary antibodies at 37 °C for at least 2 h. The primary antibodies were rabbit monoclonal antibody against H3K27me3 (Cell Signaling Technologies; #9733; 1:500), mouse monoclonal antibody against CDX2 (Biogenex; CDX2-88; 1:200) and mouse monoclonal antibody against NANOG (eBiosciences; 14-5768-82;1:250). Following three washes in PBST, samples were incubated with the secondary antibodies; goat anti mouse Alexa488 or goat anti rabbit Alexa568 (Invitrogen, Venlo, The Netherlands) at 37°C for 1 h.

The RNA FISH protocol was based on the Stellaris protocol for adherent cells (https://biosearchassets.blob.core.windows.net/assets/bti_stellaris_protocol_adherent_cell.pdf) with a few modifications. Embryos or cells were incubated in Stellaris RNA FISH Buffer A (SMF-WA1-60, Biosearch Technologies) at 37 °C for 1 h and then in 250 nM Stellaris Probe (https://www.biosearchtech.com/products/rna-fish/custom-stellaris-probe-sets) diluted in Stellaris RNA FISH Hybridization Buffer (SMF-HB1-10, Bio-search Technologies) at 37 °C overnight. After hybridization, samples were incubated in Stellaris RNA FISH Buffer A at 37 °C for 30 min, followed by nuclear staining using DAPI (Sigma Aldrich) diluted in Buffer A. After three washes in RNA FISH Wash Buffer B (SMF-WB1-20, Bio-search Technologies), samples were mounted with Vectashield (Brunschwig Chemie, Amsterdam, The Netherlands) on Cavity slides with epoxy coating (VWR, 631-0457) and stored at 4 °C before imaging. Images were obtained using a confocal laser scanning microscope (SPE-II-DMI4000; Leica, Son, The Netherlands) and were further analyzed using Fiji (http://fiji.sc/Fiji) and IMARIS software (Bitplane, Zürich, Switzerland).

Gender determination of single embryos

Individual embryos were collected from Cavity slides after imaging. To extract genomic DNA (gDNA) from single embryos, the prepGem kit (ZyGem, Hamilton, New Zealand) was used according to the manufacturer's instructions. A 20 µL PCR mixture was made up of 10 µL iQ SYBR Green supermix (Biorad), 5 µL RNAse- and DNAse-free water (Invitrogen) and 5 µL gDNA with final primer concentrations of 500 nM. The reaction steps were as described above for qRT-PCR. Presence of gDNA was confirmed using primers for Gremlin that were

not separated by an intron (forward; 5'- CATCAACCGCTTCTGCTACG-3', reverse; 5'- TGGCTGGAGTTCAGGACAGT-3') and identification of embryos as male was determined using SRY (forward; 5'- ACAGTCATAGCGCAAAT GATCAGTG-3', reverse; 5'-GGGTTGCATAGTATTGAAGAGTCTGC-3'). Cycle threshold (Ct) values lower than 33 with appropriate melting curves were regarded as valid for gender determination.

Statistical analysis

All calculations were carried out in Excel and statistical differences were examined using GraphPad Prism 7 (https://www. graphpad.com/scientific-software/prism/). Differences between two groups were determined by two-tailed unpaired Students *t*-tests and differences between multiple groups were analyzed by one-way ANOVA, followed by a post-hoc Tukey test. Statistical significance was set at $p < 0.05$.

Results

Expression of genes related to X-chromosome inactivation

X-chromosome inactivation is a dynamic process and the timing of its initiation during preimplantation development varies among mammalian species (Okamoto *et al.*, 2011). Here we performed qRT-PCR to examine the relative expression of XCI related genes from bovine GV and MII stage oocytes and embryo stages up to day 8 blastocysts. The expression level of *XIST* was relatively low and stable at developmental stages ranging from the GV oocyte to the 4-cell embryo. Expression at the 8-cell embryo stage was below the detectable level, presumably due to degradation of maternal mRNA after embryonic genome activation. Expression of *XIST* increased significantly at the morula and blastocyst stages (Figure 1A). *HPRT1* is an X-linked gene known to be inactivated after XCI; its down-regulation has been proposed as a marker for XCI (Jeon *et al.* , 2012, Ji *et al.* , 2015). Expression of *HPRT1* was detected in oocytes and embryo stages up to the blastocyst, but was significantly down-regulated between the morula and the blastocyst stages (Figure 1B). Together, these data suggest that XCI expression starts around the morula stage in bovine embryos.

We also investigated gene expression for two members of the polycomb repressive complex 2 (PRC2), namely EED and EZH2. PRC2 has been reported to accumulate on the inactive X chromosome and to be required for establishing histone methylation (Cao and Zhang, 2004, Silva *et al.* , 2003). Expression of *EED* was relatively constant throughout embryonic development but was

significantly elevated at the morula stage (Figure 1C). *EZH2* expression was stable until the 8-cell stage, after which expression decreased gradually (Figure 1D).

HNRNPK can bind to *XIST* to recruit polycomb repressive complex 1 (PRC1) (Jansz *et al.* , 2018). HNRNPU, another *XIST* RNA binding protein, was previously reported to be essential for *XIST* recruitment to the inactive X-chromosome (Xi) (Wang *et al.* , 2016b). *HNRNPK* (Figure 1E) exhibited a similar expression pattern to *EED*. The expression of *HNRNPU* was relatively constant throughout embryo development (Figure 1F).

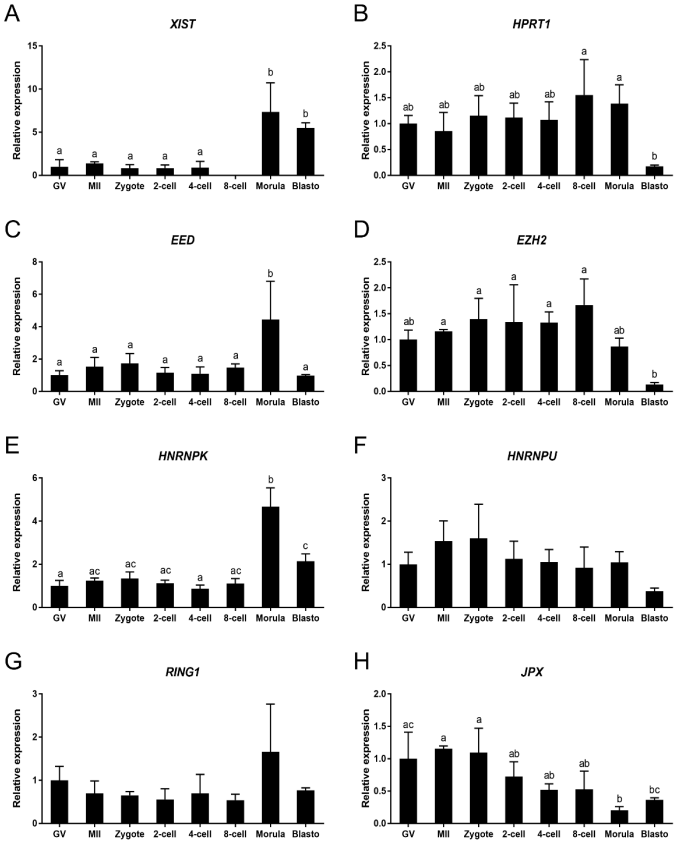

Figure 1. The relative expression of XCI related genes during *in vitro* bovine embryo development as determined by quantitative RT-PCR. (A) *XIST*, (B) *HPRT1*, (C) *EED*, (D) *EZH2*, (E) *HNRNPK*, (F) *HNRNPU*, (G) *RING1*, (H) *JPX*. GV, MII, PN, 2C, 4C, 8C, MO and BL refer to germinal vesicle, metaphase II, pronuclear, 2-cell, 4-cell, 8-cell, morula and blastocyst stages, respectively. Embryos were derived by fertilization with non-sexed sperm. Relative expression in GV oocytes set at 1. Significant differences are indicated by different letters above bars ($p<0.05$). Error bars indicate standard deviation of three independent biological replicates.

We also examined *RING1* and *JPX* expression during embryo development. RING1, a polycomb repressive complex 1 factor, is involved in Ubiquitination of Histone H2A of Xi (de Napoles *et al.* , 2004b). The expression of *RING1* was relatively stable in all oocyte and embryo groups (Figure 1G). *JPX*, a long noncoding X-linked RNA, has been reported to act as a molecular switch for XCI (Tian *et al.* , 2010). Surprisingly, we found expression of *JPX* to decrease at the morula stage (Figure 1H), the opposite to the expression of *XIST*, suggesting that its function is not conserved between mouse and cow. We also examined expression of another major *XIST* activator, RNF12 (Gontan *et al.* , 2012). Expression of *RNF12* was below the detectable level throughout embryo development.

Gene expression differences between male and female embryos

To determine the difference in expression of XCI related genes in female and male embryos, we used sex-sorted sperm to fertilize oocytes. To check the accuracy of sperm selection, the sex of single blastocysts made using X-sorted or Y-sorted sperm was determined by the PCR for *DDX3Y, USP9Y* and *ZRSR2Y* on genomic DNA from blastocysts. Control experiments indicated that sorted sperm was indeed suitable for generation of sex-specific embryos (Table S3) (Hamilton *et al.* , 2012). Here we focused on the period between the 8-cell stage and the blastocyst, since we found most changes in XCI related gene expression to arise after the 8-cell stage (Figure 1). Expression of all the selected XCI-related genes was detected in both female and male embryos, with the exception of *XIST* at the 8-cell stage (Figure 2A). The expression of *HPRT1* was significantly higher in female than male embryos (Figure 2B). As expected, significantly higher expression of *XIST* and *HPRT1* was detected in female than male morulae (Figure 2A and Figure 2B). At the blastocyst stage, only *XIST* was expressed at higher levels in female than male embryos (Figure 2C), while expression of the other XCI related genes showed no significant sex-related differences from the 8-cell stage embryo to the blastocyst (Figure 2C to Figure 2H).

XIST RNA detection in female morulae

One of the hallmarks of XCI is *XIST* RNA accumulation on the Xi and colocalization with an area of extensive histone H3 lysine 27 trimethylation. The presence of *XIST* RNA can be detected by Fluorescence In Situ Hybridization (FISH), while H3K27me3 can be detected by immunostaining. In both cases the Xi can be observed as a spot within the nucleus. To establish *XIST* RNA FISH

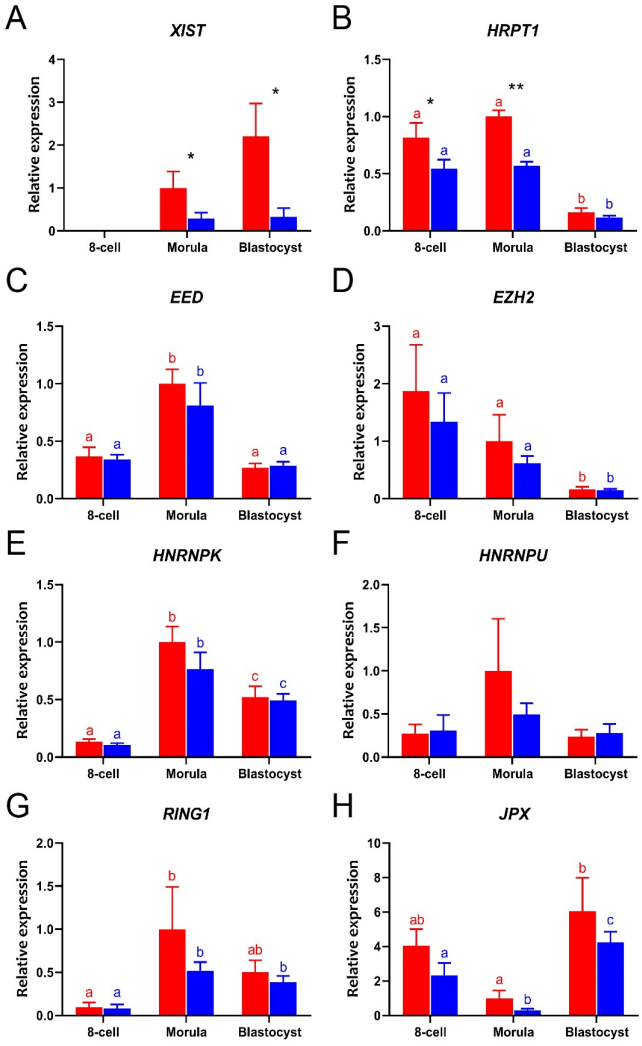

Figure 2. The relative expression of XCI related genes in female (red bars) and male (blue bars) bovine embryos from 8-cell stage to day 8 blastocyst as determined by quantitative RT-PCR. (A) *XIST*, (B) *HPRT1*, (C) *EED*, (D) *EZH2*, (E) *HNRNPK*, (F) *HNRNPU*, (G) *RING1*, (H) *JPX.* Relative expression from femalemorulae set at 1; * ($p<0.05$) and **($p<0.005$) indicate significant differences between female and male. Significant differences among embryos with same gender are indicated by different letters with same color ($p<0.05$). Error bars indicate standard deviation of three independent biological replicates.

combined with H3K27me3 immunofluorescence, we first optimized human *XIST* RNA FISH on HEK293 cells. These female cells are known for their abnormal

chromosome numbers, including supernumerary X-chromosomes. Indeed, using the RNA FISH method we detected multiple *XIST* spots in the nuclei of HEK293 cells (Figure S1A) (Xiao *et al.* , 2007). Next, we tested the newly designed bovine *XIST* probe on bovine oviduct epithelial cells, and then combined staining with immunofluorescence for H3K27me3. As expected, one spot of *XIST* RNA was detected within the nuclei of most cells and colocalized with a H3K27me3 positive spot (Figure 3A).

We then addressed localization of *XIST* RNA and H3K27me3 in embryos from the 8-cell stage up to day 9 blastocysts. The sex of individual embryos was determined by PCR, with the exception of 8-cell stage embryos for which insufficient genomic DNA was available. In agreement to what we found by qRT-PCR (Figure 1A and Figure 2A), there was no expression of *XIST* in any 8-cell stage embryo we examined by RNA FISH; instead, spots of *XIST* were first detected in female embryos at the morula stage (Figure 3A, Figure S1B).

In fact, we observed three different patterns of *XIST* staining (no spot, one spot or two spots) in embryonic nuclei. Nuclei without any *XIST* spots were found at all stages from the 8-cell stage embryo up to the day 9 female blastocyst. However, the percentage of nuclei without a *XIST* spot decreased markedly from 100% at the 8-cell stage to 60% in the morulae, and 36% in day 7 blastocysts (Figure 3B). Conversely, the percentage of nuclei with one *XIST* spot increased significantly from 0% at the 8-cell stage to 32% at the morula stage and 50% in day 7 blastocysts (Figure 3C). Nuclei with two *XIST* spots represented only a small proportion of the total nuclei, namely 9% at the morula stage and 15% in day 7 blastocysts (Figure 3D). Interestingly, the percentages of nuclei displaying the three different numbers of *XIST* spots were relatively stable across day 7 to day 9 blastocysts, indicating that the accumulation of *XIST* RNA was already established at day 7.

We then focused on the colocalization H3K27me3 spots with *XIST* RNA spots during embryo development. Very weak H3K27me3 staining was first detected at the morula stage; however, convincing H3K27me3 spots were absent at this stage. Clear H3K27me3 spots started to form in day 7 blastocysts, i.e. later than *XIST* RNA accumulation began, but they did consistently colocalize with the *XIST* RNA spots (Figure 3A). The percentage of *XIST* RNA and H3K27me3 spot colocalization increased from 0% in morulae, to 49% in day 7 blastocysts, 62% in day 8 blastocysts, and 76% in day 9 blastocysts (Figure 3E). In short, H3K27me3 on the X chromosome started after *XIST* accumulation. In contrast, we did not find any *XIST* RNA or H3K27me3 spots in male embryos (Figure

S1B). Based on these data, we conclude that XCI is initiated at the morula stage of bovine female embryo development.

Fewer XIST RNA spots were present in the inner cell mass than the trophectoderm

In female mouse blastocysts, *XIST* expression was low and no clear *XIST* spots were found in ICM cells (Mak *et al.*, 2004). In bovine embryos, however, we observed several ICM cells with distinct *XIST* RNA spots (Figure 3A). This suggests that XCI was already initiated in ICM cells during preimplantation development in bovine embryos.

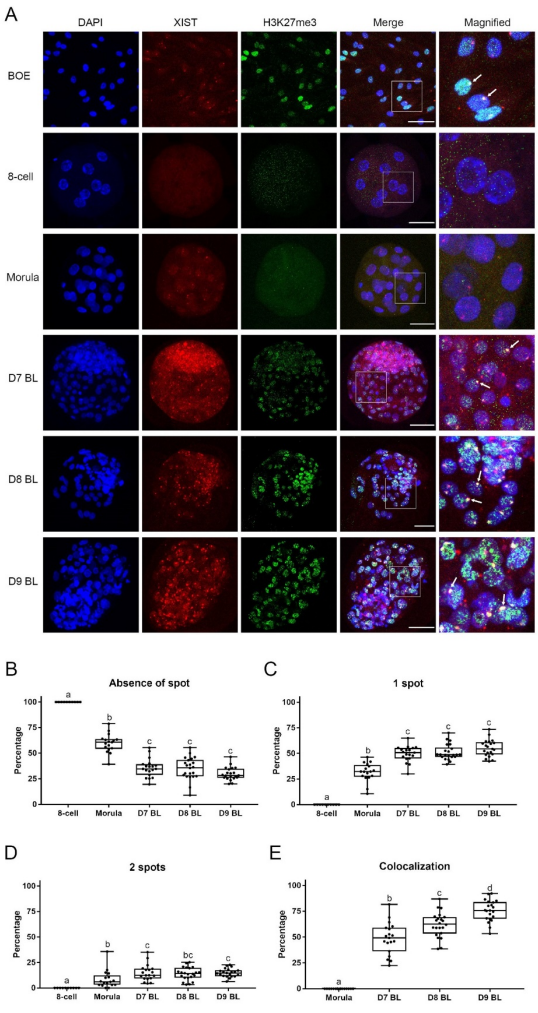

Figure 3. Combined *XIST* RNA FISH and H3K27me3 immunofluorescence in bovine oviduct epithelial cells and female embryos. *XIST* RNA FISH combined with H3K27me3 immunofluorescence in oviduct cells and the 8-cell embryo up to day (D) 9 blastocysts (A), *XIST* and H3K27me3 colocalization are indicated (arrow), Scale bar = 50µm. White boxes indicate areas presented in the right column at higher magnification. Percentage of cells lacking a *XIST* spot (B), 1 *XIST* spot (C), 2 *XIST* spots (D) from 8-cell embryos up to D9 blastocysts. Percentage of *XIST* and H3K27me3 colocalization from morula to day 9 blastocyst (E). Significant differences are indicated by different letters ($p<0.05$). BL=blastocyst.

To confirm *XIST* expression in ICM cells of the ICM, we examined ICM and TE cells separated mechanically. This was performed on embryos produced with unsorted sperm since X and Y sorted sperm yields many fewer embryos, whereas we needed large numbers of blastocysts to obtain sufficient RNA from embryo fragments. The specificity of isolated ICM and TE fragments was determined by relative expression of *OCT4*, *SOX2* and *CDX2*, with similar results to those reported previously (Brinkhof *et al.*, 2015a) (Figure 4A). Interestingly, expression of *XIST* in ICM cells was at a higher level in TE cells but this difference did not reach statistical significance (P>0.361). In addition, other XCI related genes were expressed at similar levels in the ICM and TE (Figure 4A).

We then examined *XIST* RNA spots and their colocalization with H3K27me3 in ICM cells. TE cells were identified by CDX2 expression, and CDX2-negative cells were regarded as ICM. While putative epiblast precursors were stained with a NANOG antibody, NANOG negative cells were regarded as a combination of TE and hypoblast. Again, we detected nuclei with clear *XIST* spots in both CDX2 negative cells and NANOG positive cells; this included cells with colocalized *XIST* and H3K27me3 spots (Figure 4B, 4C). These data indicate that XCI in the blastocyst was already initiated in some ICM cells, including potential epiblast precursors.

In order to understand the relationship between XCI and pluripotency in bovine embryos, we determined the percentages of nuclei with different numbers of *XIST* spots (no spot, one spot and two spots) and their colocalization with H3K27me3. In day 7 blastocysts, the percentage of nuclei without a *XIST* spot was similar in CDX2 negative and NANOG positive cells. The percentages of nuclei with no *XIST* spot in CDX2 positive and NANOG negative cells were also similar and were less abundant than among the CDX2 negative cells and NANOG positive cells (Figure 5A). More nuclei with a single *XIST* spot were detected in CDX2 positive and NANOG negative cells, compared to the potentially pluripotent CDX2 negative and NANOG positive cells (Figure 5B). Nuclei with two *XIST* spots were less common (less than 19%) and there was no significant difference between CDX2 positive, CDX2 negative, NANOG positive and NANOG negative cells (Figure 5C). Day 8 and day 9 blastocysts showed similar patterns of *XIST* spot numbers to day 7 blastocysts, although a higher proportion of nuclei with two spots was found in NANOG positive cells of day 8 blastocysts (23%) (Figure 5E to Figure 5G and Figure 5I to Figure 5K). We also analyzed the frequency of *XIST* and H3K27me3 co-localization. More cells with colocalized *XIST* and H3K27me3 staining were observed in CDX2 positive than CDX2

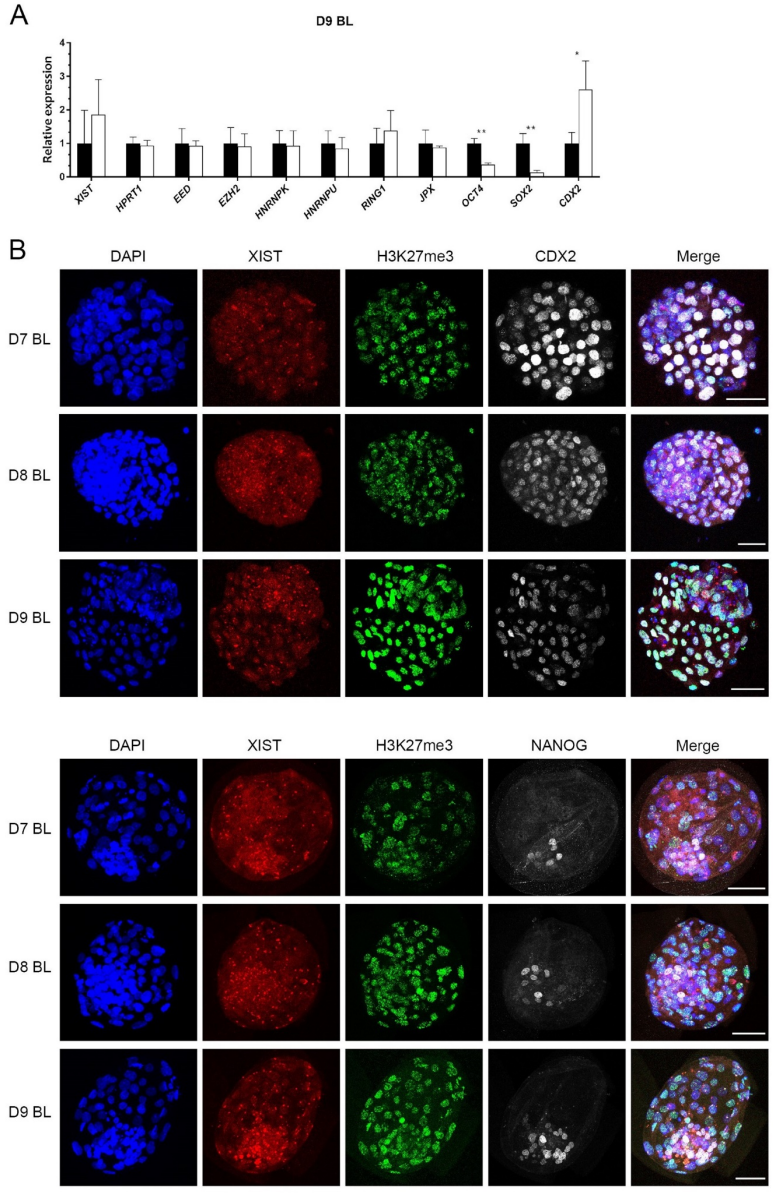

Figure 4. The relative expression of XCI related genes in inner cell mass (ICM) cells (black bars) and trophectoderm (TE) cells (white bars), and *XIST* RNA FISH combined with immunofluorescence in female embryos. The relative expression of XCI related genes (A), relative expression in ICM set at 1; * ($p<0.05$) and **($p<0.05$) indicate significant differences. Error bars indicate standard deviation of three biological replicates. *XIST* RNA FISH combined with double staining of H3K27me3 and CDX2 (B) or NANOG (C) from day 7 (D7) to day 9 (D9) blastocysts, Scale bar = 50µm. BL=blastocyst.

negative cells, in blastocysts at all stages (day 7 to 9: Figure 5D, H, L). However, the frequency of co-localization was similar in NANOG positive and NANOG negative cells at all stages of blastocyst development, albeit that there was considerable variability between samples (Figure 5D, H, L). Combined, these data suggest that cells with a higher degree of pluripotency have a lower tendency to initiate XCI during embryo development.

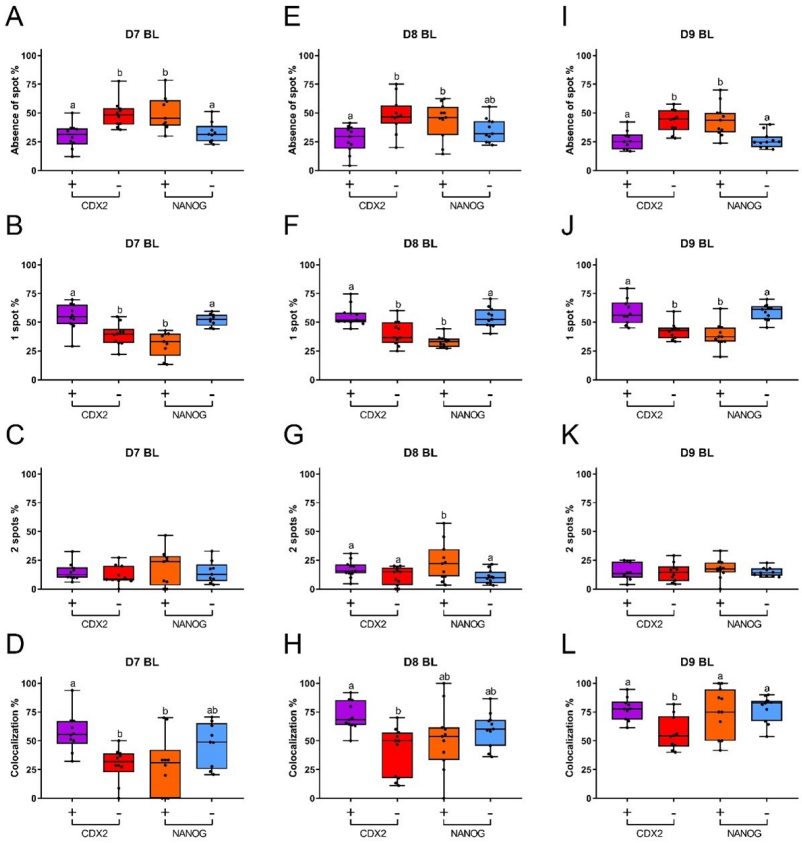

Figure 5. Percentage of nuclei with different number of *XIST* spots in CDX2 and NANOG positive or negative cells, and percentage of colocalization of *XIST* and H3K27me3 from day 7 to day 9 female blastocysts. Absence of an *XIST* spot (A), 1 *XIST* spot (B), 2 *XIST* spots (C) and colocalization of *XIST* and H3K27me3 (D) in day 7 (D7) blastocysts; Absence of an *XIST* spot (E), 1 *XIST* spot (F), 2 *XIST* spots (G) and colocalization of *XIST* and H3K27me3 (H) in day 8 (D8) blastocysts; Absence of an *XIST* spot (I), 1 *XIST* spot (J), 2 *XIST* spots (K) and colocalization of *XIST* and H3K27me3 (L) in day 9 (D9) blastocysts. Presence (purple box) and absence (red box) of CDX2 are indicated by + and -, respectively. Presence (orange box) and absence (blue box) of NANOG are indicated by + and -, respectively. Significant differences are indicated by different letters ($p<0.05$). BL=blastocyst.

X-linked gene regulation after XCI initiation

To assess whether the initiation of XCI triggered downregulation of X-linked gene expression during development, we analyzed previously generated microarray data in which we had compared gene expression levels between morulae and blastocysts (Brinkhof *et al.*, 2015a). In total, expression of 930 genes located on the X chromosome was evaluated, with differential expression determined using cut-offs of 1.5-fold and $p<0.05$ (Table S4, S5). The observation of a higher percentage of cells with *XIST* spots in blastocysts than morulae (Figure 3C, D), indicated that more cells start to undergo XCI during this transition. Despite an increase in *XIST* coating as observed as *XIST* spots, the increase was apparently not abundant enough in all cells to cause a significant change in X-linked gene expression. Indeed, most (693) X-linked genes showed no difference in expression and the number of down regulated genes in blastocysts compared to morulae (127) was similar to the number of genes that was up-regulated (110) (Figure 6A). Nevertheless, a higher expression of *XIST* and lower expression of *HPRT1* in blastocysts was found in the microarray data (Figure 6B). We then compared the expression of X-linked genes in ICM cells and TE cells of day 9 blastocysts. Only a small number of X-linked genes was differentially expressed, of which 37 genes were up-regulated and 22 genes were down-regulated in ICM cells compared to TE cells (Figure 6C). Moreover, there was no significant difference in expression of *XIST* and *HPRT1* between ICM and TE cells (Figure 6D), which was consistent with our qRT-PCR findings

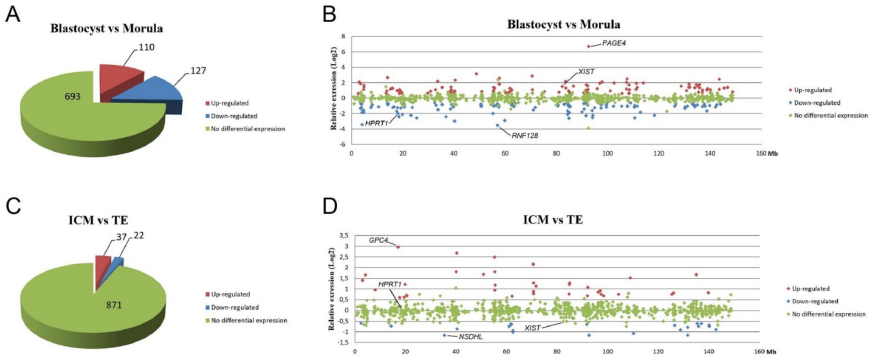

Figure 6. Proportional distribution of X-linked gene expression in blastocysts versus morulae and inner cell mass cells versus trophectoderm cells. Proportional distribution of up-regulated (red), down-regulated (blue) and equally expressed (green) X-linked genes in blastocysts versus morulae (A) and inner cell mass cells versus trophectoderm cells (C). The relative expression (Log2) of X-linked genes in blastocysts versus morulae (B) and inner cell mass cells versus trophectoderm cells (D) are plotted according to their location on the X chromosome.

(Figure 4A). Overall, the data suggest that in bovine embryos, XCI initiation does not lead to the downregulation of most X-linked genes.

Discussion

X chromosome dosage compensation between XX female and XY male cells is achieved by XCI during early female embryonic development. Although this process has been intensively studied in the mouse, recent studies showed different patterns of XCI in other mammals (Okamoto *et al.*, 2011, Ramos-Ibeas *et al.* , 2019, van den Berg *et al.* , 2011b). However, little is known about the timing of XCI initiation and its relationship with lineage segregation in non-rodent species. Therefore, we studied XCI in early bovine embryos.

XIST, one of the major effectors of XCI, accumulates on the future Xi and initiates silencing in *cis* (Boumil and Lee, 2001). In bovine sperm cells the *XIST* gene does not appear methylated, suggesting that *XIST* could be expressed in these cells (Mendonca *et al.* , 2019). The absence of *XIST* transcripts at the 2 cell stage indicates that possible *XIST* expression in sperm cells is no longer detectable after fertilization.

XIST expression is first detected at the 4-cell stage in mouse embryos and the 8-cell stage in human and rabbit embryos (Augui *et al.* , 2011, Briggs *et al.* , 2015a, Okamoto *et al.*, 2011, van den Berg *et al.*, 2011b). In this study we show that in bovine embryos expression of *XIST* is up-regulated after the 8-cell stage and that expression is predominantly observed in female embryos. This is in agreement with previous studies in which the expression of *XIST* was detected after the 16–32-cell stage and was higher in female than male embryos at both the morula and the blastocyst stage (Ruddock *et al.* , 2004, Wrenzycki *et al.* , 2002). Recently, presence of *XIST* transcripts had been reported as early as the two cell stage in bovine embryos (Mendonca *et al.*, 2019). The levels of expression were not quantified however and may have been very low. Indeed *XIST* transcripts were detected in all examined embryos and cells at the 2-cell stage (Mendonca *et al.*, 2019) where one would not expect functional *XIST* levels in male embryos, suggesting that if expressed the *XIST* levels would be very low at these stages. Notably, the embryonic genome is activated at around the 2-4-cell stage in mouse, the 4-8-cell stage in human and the 8-16-cell stage in rabbit and cattle embryos (Morgan *et al.* , 2005, Telford *et al.* , 1990), suggesting that mammalian XCI initiation closely follows activation of the embryonic genome.

The expression of other factors involved in XCI was also examined in this

study. Higher expression of *HPRT1* was detected at the 8-cell and the morula stage in female than in male embryos, but no difference in *HPRT1* expression was found between female and male blastocysts, indicating the normalization of *HPRT1* expression between female and male embryos is accomplished soon after the initiation of XCI. However, the expression of genes coding for polycomb complex components and other XCI activators was not significantly different between female and male embryos during early development. More recently, it has been reported that in mouse embryos SPEN is recruited to the X chromosome immediately upon *Xist* upregulation (Dossin *et al.* , 2020). Nevertheless, we did not detect significant upregulation of *SPEN* expression from morulae to blastocysts in our microarray data, while *XIST* expression was significantly upregulated. This may be due to their multiple functions during development or because of alternative functions that are not conserved between mouse and cattle.

The combination of RNA FISH with immunofluorescence enabled simultaneous localization of *XIST* RNA and H3K27me3 at the single cell level. This is technically challenging because the reaction conditions of the two procedures conflict in several ways (Yoon *et al.* , 2016). Here we found cytoskeletal buffer supplemented with Triton X-100 to be optimal for permeabilization. In mouse and human preimplantation embryos, “pinpoint” signals of *XIST* were observed in both female and male cells, and regarded to indicate an early stage of XCI (Matsui *et al.* , 2001, van den Berg *et al.* , 2009). We did not observe pinpoint-like *XIST* accumulation in any of the female or male embryos examined. Even though we observed that the *XIST* cloud was smaller in female morulae than female blastocysts, it was still larger than the pinpoints described, which were around 100 times smaller than a full *XIST* cloud (van den Berg *et al.*, 2009). We therefore hypothesize that the accumulation of *XIST* on the future inactive X is faster during bovine embryo development than in the mouse and human.

Another interesting observation obtained by RNA FISH was the accumulation of *XIST* on both X chromosomes during embryo development. This phenomenon has also been observed in human and rabbit embryos (Okamoto *et al.*, 2011, van den Berg *et al.*, 2009), but it is still poorly understood. In our study, the existence of two *XIST* spots was detected in the majority of female embryos we examined, but in a relatively small percentage of cells. Possibly, cell with two *XIST* spots were mixoploid and contained more than two X-chromosomes. In particular diploid-triploid mixoploidy is common in bovine blastocysts, with mixoploidy presented in around 10% of the cells (Viuff *et al.* , 1999a). Indeed,

two *XIST* spots were also detected in HEK293 cells that contain supernumerary X-chromosomes, and we never observed cells with two *XIST* spots in differentiated oviduct epithelial cells.

Alternatively, two *XIST* spots in female cells represent a transient inactive X-chromosome state when the cells exit from naïve pluripotency (Sousa *et al.* , 2018). However, we did not observe any difference in the percentages of cells with two spots in CDX2-positive trophectoderm and CDX2-negative presumed pluripotent cells. Only in day 8 blastocysts, but not in day 7 or day 9 blastocysts, did we observe a slightly higher percentage of cells with two XIST spots in NANOG positive compared to NANOG negative cells.

In mice, the two active X chromosome state is regarded as a hallmark of naïve pluripotency in female ES cells and embryonic cells (De Los Angeles *et al.* , 2012, Nichols and Smith, 2009). However, two active X chromosomes are considered unstable in human ES cells, and *XIST* accumulation on X chromosomes was detected in ICM cells of human and rabbit embryos (Geens and Chuva De Sousa Lopes, 2017, Okamoto *et al.*, 2011), indicating that this hallmark may not be conserved across mammals. Here, we also detected *XIST* expression in bovine ICM cells using both qRT-PCR and RNA FISH combined with immunofluorescence. Overall, fewer *XIST* spots were observed in ICM cells than trophectoderm cells. The patterns of *XIST* spot numbers we observed were very similar between CDX negative (presumed epiblast and hypoblast) and NANOG positive (presumed epiblast) cells, which suggests the levels of XCI in epiblast and hypoblast cells are similar in bovine embryos. Indeed, we have previously observed that ICM cells can switch from NANOG-positive epiblast precursors to GATA6-positive hypoblast cells, and vice-versa, even in day 8 blastocysts, indicating a large degree of fate flexibility (Kuijk *et al.* , 2012b). Besides, like human ES cells, ES cells derived from bovine ICM cells display epigenetic features of the primed rather than the naïve pluripotent state (Bogliotti *et al.*, 2018). Taking all together, we suggest the reason why XCI was also initiated in ICM cells in cattle is that those cells are already in primed rather than naïve pluripotent state.

In mouse embryos, reduced expression of X-linked genes was observed after *XIST* accumulation on the X chromosome during preimplantation development (Wang *et al.* , 2016a). However, in bovine embryos, we found *XIST* accumulation did not lead to globally reduced expression of X-linked genes, similar to what has been reported for human embryos (Okamoto *et al.*, 2011). In agreement with our findings, microarray and RNA seq analyses in bovine blastocysts demonstrated

enhanced expression of X chromosome linked genes in intact female compared with male blastocysts which indicates that dosage compensation had not initiated at this stage (Bermejo-Alvarez *et al.* , 2010, Min *et al.*, 2017). Interestingly, we did observe a significant increase of intense H3K27me3 spots within nuclei from the morula to the blastocyst stage, indicating that this histone modification also did not lead to global downregulation of X-linked genes. Chromatin immunoprecipitation could help to identify the genes on the X chromosome that are specifically linked with H3K27me3.

Conclusions

We observed the onset of XCI at around the morula stage of bovine embryo development. At the blastocyst stage, ICM cells demonstrate a lower incidence of XCI than TE cells. Moreover, *XIST* accumulation does not lead to global downregulation of X-linked genes. Our data confirmed diverse patterns of XCI initiation exist in different mammalian species during early development.

Author Contributions

Conceptualization, B.Y., H.T., T.S. and B.R.; methodology, B.Y., H.T., and B.R.; funding acquisition, B.R.; investigation, B.Y., H.T., and B.R.; resources, B.R.; data curation, B.Y.; writing—original draft preparation, B.Y.; writing—review and editing, T.S., and B.R.; visualization, B.Y.; supervision, T.S. and B.R..; project administration, B.R. All authors have read and agreed to the submitted version of the manuscript.

Acknowledgments

We are very grateful to Richard Wubbolts (Center for Cellular Imaging, Faculty of Veterinary Medicine, Utrecht University) for assistance with imaging. We also thank Arend Rijneveld and Christine Oei for assistance with oocyte recovery.

Supplementals

Supplemental figures and tables in this chapter are available online at *cells* (https://www.mdpi.com/2073-4409/9/4/1016)

References

Augui S, Nora EP, Heard E. Regulation of X-chromosome inactivation by the X-inactivation centre. *Nature Reviews Genetics* 2011;**12**:429-442.

Barakat TS, Gribnau J. X chromosome inactivation and embryonic stem cells. *Adv Exp Med Biol* 2010;**695**:132-154.

Bermejo-Alvarez P, Rizos D, Rath D, Lonergan P, Gutierrez-Adan A. Sex determines the expression level of one third of the actively expressed genes in bovine blastocysts. *Proceedings of the National Academy of Sciences of the United States of America* 2010;**107**:3394-3399.

Bogliotti YS, Wu J, Vilarino M, Okamura D, Soto DA, Zhong C, Sakurai M, Sampaio RV, Suzuki K, Izpisua Belmonte JC *et al.* Efficient derivation of stable primed pluripotent embryonic stem cells from bovine blastocysts. *Proc Natl Acad Sci U S A* 2018;**115**:2090-2095.

Boumil RM, Lee JT. Forty years of decoding the silence in X-chromosome inactivation. *Human Molecular Genetics* 2001;**10**:2225-2232.

Briggs SF, Dominguez AA, Chavez SL, Pera RAR. Single-Cell XIST Expression in Human Preimplantation Embryos and Newly Reprogrammed Female Induced Pluripotent Stem Cells. *Stem Cells* 2015;**33**:1771-1781.

Brinkhof B, van Tol HT, Groot Koerkamp MJ, Riemers FM, SG IJ, Mashayekhi K, Haagsman HP, Roelen BA. A mRNA landscape of bovine embryos after standard and MAPK-inhibited culture conditions: a comparative analysis. *BMC Genomics* 2015;**16**:277.

Brinkhof B, van Tol HT, Groot Koerkamp MJ, Wubbolts RW, Haagsman HP, Roelen BA. Characterization of bovine embryos cultured under conditions appropriate for sustaining human naive pluripotency. *PLoS One* 2017;**12**:e0172920.

Bruck T, Benvenisty N. Meta-analysis of the heterogeneity of X chromosome inactivation in human pluripotent stem cells. *Stem Cell Res* 2011;**6**:187-193.

Cao R, Zhang Y. SUZ12 is required for both the histone methyltransferase activity and the silencing function of the EED-EZH2 complex. *Molecular Cell* 2004;**15**:57-67.

De Los Angeles A, Loh YH, Tesar PJ, Daley GQ. Accessing naive human pluripotency. *Current Opinion in Genetics & Development* 2012;**22**:272-282.

de Napoles M, Mermoud JE, Wakao R, Tang YA, Endoh M, Appanah R, Nesterova TB, Silva J, Otte AP, Vidal M *et al.* Polycomb group proteins Ring1A/B link ubiquitylation of histone H2A to heritable gene silencing and X inactivation. *Developmental Cell* 2004;**7**:663-676.

Deng X, Berletch JB, Nguyen DK, Disteche CM. X chromosome regulation: diverse patterns in development, tissues and disease. *Nat Rev Genet* 2014;**15**:367-378.

Dossin F, Pinheiro I, Zylicz JJ, Roensch J, Collombet S, Le Saux A, Chelmicki T, Attia M, Kapoor V, Zhan Y *et al.* SPEN integrates transcriptional and epigenetic control of X-inactivation. *Nature* 2020.

Geens M, Chuva De Sousa Lopes SM. X chromosome inactivation in human pluripotent stem

cells as a model for human development: back to the drawing board? *Hum Reprod Update* 2017;**23**:520-532.

Gontan C, Achame EM, Demmers J, Barakat TS, Rentmeester E, van IJcken W, Grootegoed JA, Gribnau J. RNF12 initiates X-chromosome inactivation by targeting REX1 for degradation. *Nature* 2012;**485**:386-U138.

Goossens K, Van Poucke M, Van Soom A, Vandesompele J, Van Zeveren A, Peelman LJ. Selection of reference genes for quantitative real-time PCR in bovine preimplantation embryos. *Bmc Developmental Biology* 2005;**5**.

Hamilton CK, Combe A, Caudle J, Ashkar FA, Macaulay AD, Blondin P, King WA. A novel approach to sexing bovine blastocysts using male-specific: gene expression. *Theriogenology* 2012;**77**:1587-1596.

Heard E, Clerc P, Avner P. X-chromosome inactivation in mammals. *Annu Rev Genet* 1997;**31**:571-610.

Huang K, Maruyama T, Fan G. The naive state of human pluripotent stem cells: a synthesis of stem cell and preimplantation embryo transcriptome analyses. *Cell Stem Cell* 2014;**15**:410-415.

Jansz N, Nesterova T, Keniry A, Iminitoff M, Hickey PF, Pintacuda G, Masui O, Kobelke S, Geoghegan N, Breslin KA *et al.* Smchd1 Targeting to the Inactive X Is Dependent on the Xist-HnrnpK-PRC1 Pathway. *Cell Reports* 2018;**25**:1912-+.

Jeon BG, Rho GJ, Betts DH, Petrik JJ, Favetta LA, King WA. Low Levels of X-Inactive Specific Transcript in Somatic Cell Nuclear Transfer Embryos Derived from Female Bovine Freemartin Donor Cells. *Sexual Development* 2012;**6**:151-159.

Ji BH, Higa KK, Kelsoe JR, Zhou XJ. Over-expression of XIST, the Master Gene for X Chromosome Inactivation, in Females With Major Affective Disorders. *Ebiomedicine* 2015;**2**:909-918.

Kuijk EW, van Tol LTA, Van de Velde H, Wubbolts R, Welling M, Geijsen N, Roelen BAJ. The roles of FGF and MAP kinase signaling in the segregation of the epiblast and hypoblast cell lineages in bovine and human embryos. *Development* 2012;**139**:871-882.

Lovell-Badge R. Many ways to pluripotency. *Nat Biotechnol* 2007;**25**:1114-1116.

Lyon MF. Gene action in the X-chromosome of the mouse (Mus musculus L.). *Nature* 1961;**190**:372-373.

Mak W, Nesterova TB, de Napoles M, Appanah R, Yamanaka S, Otte AP, Brockdorff N. Reactivation of the paternal X chromosome in early mouse embryos. *Science* 2004;**303**:666-669.

Matsui J, Goto Y, Takagi N. Control of Xist expression for imprinted and random X chromosome inactivation in mice. *Human Molecular Genetics* 2001;**10**:1393-1401.

Mendonca ADS, Silveira MM, Rios AFL, Mangiavacchi PM, Caetano AR, Dode MAN, Franco MM. DNA methylation and functional characterization of the XIST gene during in vitro early embryo development in cattle. *Epigenetics* 2019;**14**:568-588.

Min B, Park JS, Jeon K, Kang YK. Characterization of X-Chromosome Gene Expression in Bovine Blastocysts Derived by In vitro Fertilization and Somatic Cell Nuclear Transfer. *Frontiers in Genetics* 2017;**8**.

Minkovsky A, Patel S, Plath K. Concise review: Pluripotency and the transcriptional inactivation of the female Mammalian X chromosome. *Stem Cells* 2012;**30**:48-54.

Morgan HD, Santos F, Green K, Dean W, Reik W. Epigenetic reprogramming in mammals. *Human Molecular Genetics* 2005;**14**:R47-R58.

Navarro P, Chambers I, Karwacki-Neisius V, Chureau C, Morey C, Rougeulle C, Avner P. Molecular coupling of Xist regulation and pluripotency. *Science* 2008;**321**:1693-1695.

Nichols J, Smith A. Naive and Primed Pluripotent States. *Cell Stem Cell* 2009;**4**:487-492.

Okamoto I, Otte AP, Allis CD, Reinberg D, Heard E. Epigenetic dynamics of imprinted X inactivation during early mouse development. *Science* 2004;**303**:644-649.

Okamoto I, Patrat C, Thepot D, Peynot N, Fauque P, Daniel N, Diabangouaya P, Wolf JP, Renard JP, Duranthon V *et al.* Eutherian mammals use diverse strategies to initiate X-chromosome inactivation during development. *Nature* 2011;**472**:370-374.

Patrat C, Okamoto I, Diabangouaya P, Vialon V, Le Baccon P, Chow J, Heard E. Dynamic changes in paternal X-chromosome activity during imprinted X-chromosome inactivation in mice. *Proc Natl Acad Sci U S A* 2009;**106**:5198-5203.

Petropoulos S, Edsgard D, Reinius B, Deng Q, Panula SP, Codeluppi S, Reyes AP, Linnarsson S, Sandberg R, Lanner F. Single-Cell RNA-Seq Reveals Lineage and X Chromosome Dynamics in Human Preimplantation Embryos. *Cell* 2016;**167**:285.

Prudhomme J, Dubois A, Navarro P, Arnaud D, Avner P, Morey C. A rapid passage through a two-active-X-chromosome state accompanies the switch of imprinted X-inactivation patterns in mouse trophoblast stem cells. *Epigenetics Chromatin* 2015;**8**:52.

Ramos-Ibeas P, Sang F, Zhu QF, Tang WWC, Withey S, Klisch D, Wood L, Loose M, Surani MA, Alberio R. Pluripotency and X chromosome dynamics revealed in pig pre-gastrulating embryos by single cell analysis. *Nature Communications* 2019;**10**.

Ruddock NT, Wilson KJ, Cooney MA, Korfiatis NA, Tecirlioglu RT, French AJ. Analysis of imprinted messenger RNA expression during bovine preimplantation development. *Biology of Reproduction* 2004;**70**:1131-1135.

Sado T, Brockdorff N. Advances in understanding chromosome silencing by the long non-coding RNA Xist. *Philosophical Transactions of the Royal Society B-Biological Sciences* 2013;**368**.

Silva J, Mak W, Zvetkova I, Appanah R, Nesterova TB, Webster Z, Peters AH, Jenuwein T, Otte AP, Brockdorff N. Establishment of histone h3 methylation on the inactive X chromosome requires transient recruitment of Eed-Enx1 polycomb group complexes. *Dev Cell* 2003;**4**:481-495.

Sousa EJ, Stuart HT, Bates LE, Ghorbani M, Nichols J, Dietmann S, Silva JCR. Exit from

Naive Pluripotency Induces a Transient X Chromosome Inactivation-like State in Males. *Cell Stem Cell* 2018;**22**:919-+.

Takagi N, Sasaki M. Preferential inactivation of the paternally derived X chromosome in the extraembryonic membranes of the mouse. *Nature* 1975;**256**:640-642.

Telford NA, Watson AJ, Schultz GA. Transition from Maternal to Embryonic Control in Early Mammalian Development - a Comparison of Several Species. *Molecular Reproduction and Development* 1990;**26**:90-100.

Tian D, Sun S, Lee JT. The Long Noncoding RNA, Jpx, Is a Molecular Switch for X Chromosome Inactivation. *Cell* 2010;**143**:390-403.

van den Berg IM, Galjaard RJ, Laven JSE, van Doorninck JH. XCI in preimplantation mouse and human embryos: first there is remodelling ... *Human Genetics* 2011;**130**:203-215.

van den Berg IM, Laven JSE, Stevens M, Jonkers I, Galjaard RJ, Gribnau J, van Doorninck JH. X Chromosome Inactivation Is Initiated in Human Preimplantation Embryos. *American Journal of Human Genetics* 2009;**84**:771-779.

Viuff D, Rickords L, Offenberg H, Hyttel P, Avery B, Greve T, Olsaker I, Williams JL, Callesen H, Thomsen PD. A high proportion of bovine blastocysts produced in vitro are mixoploid. *Biology of Reproduction* 1999;**60**:1273-1278.

Wang F, Shin JD, Shea JM, Yu J, Boskovic A, Byron M, Zhu X, Shalek AK, Regev A, Lawrence JB *et al.* Regulation of X-linked gene expression during early mouse development by Rlim. *Elife* 2016a;**5**.

Wang JL, Syrett CM, Kramer MC, Basu A, Atchison ML, Anguera MC. Unusual maintenance of X chromosome inactivation predisposes female lymphocytes for increased expression from the inactive X. *Proceedings of the National Academy of Sciences of the United States of America* 2016b;**113**:E2029-E2038.

Wrenzycki C, Lucas-Hahn A, Herrmann D, Lemme E, Korsawe K, Niemann H. In vitro production and nuclear transfer affect dosage compensation of the X-linked gene transcripts G6PD, PGK, and Xist in preimplantation bovine embryos. *Biology of Reproduction* 2002;**66**:127-134.

Xiao CY, Sharp JA, Kawahara M, Davalos AR, Difilippantonio MJ, Hu Y, Li WM, Cao L, Buetow K, Ried T *et al.* The XIST noncoding RNA functions independently of BRCA1 in X inactivation. *Cell* 2007;**128**:977-989.

Yoon DS, Pendergrass DL, Lee MH. A simple and rapid method for combining fluorescent in situ RNA hybridization (FISH) and immunofluorescence in the C. elegans germline. *Methodsx* 2016;**3**:378-385.

Yue MH, Richard JLC, Yamada N, Ogawa A, Ogawa Y. Quick Fluorescent In Situ Hybridization Protocol for Xist RNA Combined with Immunofluorescence of Histone Modification in X-chromosome Inactivation. *Jove-Journal of Visualized Experiments* 2014.

Chapter 4

Lysophosphatidic acid accelerates blastocyst formation through the Hippo/YAP pathway

Bo Yu[1], Helena T. A. van Tol[1], Christine H. Y. Oei[1], Tom A.E. Stout[2] and Bernard A. J. Roelen[3]*

[1]Farm Animal Health; Department of Population Health Sciences, Faculty of Veterinary Medicine, Utrecht University, Utrecht, The Netherlands.

[2]Equine Sciences; Department Clinical Sciences, Faculty of Veterinary Medicine, Utrecht University, Utrecht, The Netherlands.

[3]Embryology, Anatomy and Physiology; Department Clinical Sciences, Faculty of Veterinary Medicine, Utrecht University, Utrecht, The Netherlands.

Adapted from *International Journal of Molecular Sciences. 2021, 22(11), 5915* Doi: 10.3390/ijms22115915.

Abstract

The segregation of trophectoderm (TE) and inner cell mass in early embryos is driven primarily by the transcription factor CDX2. The signals that trigger CDX2 activation are, however, less clear. In mouse embryos, the Hippo-YAP signaling pathway is important for the activation of CDX2 expression; it is less clear whether this relationship is conserved in other mammals. Lysophosphatidic acid (LPA) has been reported to increase YAP levels by inhibiting its degradation. In this study, we cultured bovine embryos in the presence of LPA and examined changes in gene and protein expression. LPA was found to accelerate the onset of blastocyst formation on days 5 and 6, without changing the TE/inner cell mass ratio. We further observed that the expression of *TAZ* and *TEAD4* was up-regulated, and YAP was overexpressed, in LPA-treated day 6 embryos. However, LPA induced up-regulation of CDX2 expression was only evident in day 8 embryos. Overall, our data suggest that the Hippo signaling pathway is involved in the initiation of bovine blastocyst formation, but does not affect the cell lineage constitution of blastocysts.

Introduction

During mammalian development, the first cell lineage specification is initiated at the compact morula stage, resulting in the formation of a blastocyst with an outer trophectoderm (TE) and an inner cell mass (ICM). During lineage segregation, the transcription factor CDX2 is crucial for proper TE specification (Huang *et al.*, 2017), whereas OCT4, NANOG, and SOX2 are core regulators of ICM formation (Boyer *et al.* , 2005). However, the mechanisms that control the expression of these transcription factors is not well understood.

The Hippo signaling pathway is highly conserved in mammals, and was initially described as a pathway involved in specifying organ size by controlling cell proliferation and apoptosis (Chen *et al.* , 2020, Watt *et al.* , 2017, Zhao *et al.* , 2011, Zheng and Pan, 2019). Emerging evidence has indicated that the Hippo-YAP signaling pathway also plays an essential role in controlling the expression of the key transcription factors in first-lineage segregation (ICM and TE differentiation) during mouse preimplantation development (Bergsmedh *et al.*, 2011, Frum *et al.* , 2018, Karasek *et al.*, 2020, Nishioka *et al.* , 2009). In the cells on the outside of the morula, where the Hippo pathway is inactive, YAP/TAZ remain unphosphorylated and migrate to the nucleus to bind the transcriptional coactivator TEAD4 facilitating *Cdx2* expression, and subsequently driving them

to a TE fate (Karasek *et al.*, 2020, Nishioka *et al.*, 2009, Yao *et al.* , 2019). Moreover, it has been reported that both maternal and zygotic derived YAP promote CDX2 expression, and that *Tead4*-deleted mouse embryos fail to develop TE (Frum *et al.*, 2018, Nishioka *et al.*, 2008). When the Hippo pathway is active, YAP/TAZ are phosphorylated, remain cytoplasmic and become ubiquitinated. As a result, there is no *Cdx2* expression in these cells, driving them towards an ICM fate (Chen *et al.*, 2019, Lorthongpanich and Issaragrisil, 2015).

Interestingly, unlike in the mouse, YAP is localized to the nucleus of both the ICM and TE cells of human blastocysts. In addition, YAP overexpression has been reported to promote naïve pluripotency in human embryonic, and induced pluripotent, stem cells (Qin *et al.*, 2016). These data indicate that role of the Hippo/YAP pathway in first-lineage determination differs among mammalian species.

Lysophosphatidic acid (LPA) is a bioactive phospholipid that regulates a broad range of cellular effects by activating specific G protein-coupled receptors (Frisca *et al.* , 2012, Lin *et al.* , 2010, Sheng *et al.* , 2015). It has been demonstrated that LPA-mediated signaling plays a crucial role in embryo spacing and the timing of implantation in mice (Hama *et al.* , 2007, Ye *et al.* , 2005). Recent studies have demonstrated that LPA inhibits the Hippo pathway kinases LATS1 and LATS2 via Ga12/13-coupled receptors (Felley-Bosco and Stahel, 2014, Qin *et al.*, 2016, Yu *et al.* , 2012). Phosphorylation of YAP/TAZ via LATS1/2 leads to ubiquitination-dependent degradation (Liu *et al.* , 2018, Yu *et al.*, 2012), a process that is inhibited by LPA.

To understand the role of the Hippo signaling pathway in bovine preimplantation embryo development, we cultured bovine *in vitro* produced embryos in the presence of 10μM LPA from the timing of fertilization. The results suggest that in the presence of LPA, blastocyst formation starts earlier, YAP expression is up-regulated and CDX2 expression is subsequently increased. Combined, the data suggest that in bovine embryos the Hippo/YAP signaling pathway plays an important role in blastocoel formation and the first cell lineage segregation event.

Results

LPA accelerates blastocyst formation

To examine how the Hippo pathway is involved in embryo development, bovine oocytes were fertilized in vitro and then cultured to the day 8 blastocyst stage in

the presence of 10^{-5} M LPA. Blastocyst formation was first detected on day 6 in the control group. In the presence of LPA, however, blastocysts were already formed at day 5 (Figure 1A). In addition, the blastocyst percentage on day 6 was 14.1% in the control group, whereas in the LPA group it had increased to 26.6% ($p<0.01$). A consistently higher ($p<0.05$) expanded blastocyst percentage was detected on day 6 for embryos cultured with LPA (5.4%), compared to control embryos (1.3%) (Figure 1B). However, the percentages of both blastocysts and expanded blastocysts on days 7 and 8 of culture were similar between embryos cultured with and without LPA (Figure 1A, B). Similar to our observation on days 7 and 8 of embryo culture, no significant differences were found in the percentages of uncleaved zygotes, 2-8-cell embryos and >8-cell embryos at day 5 of culture (Figure 1C).

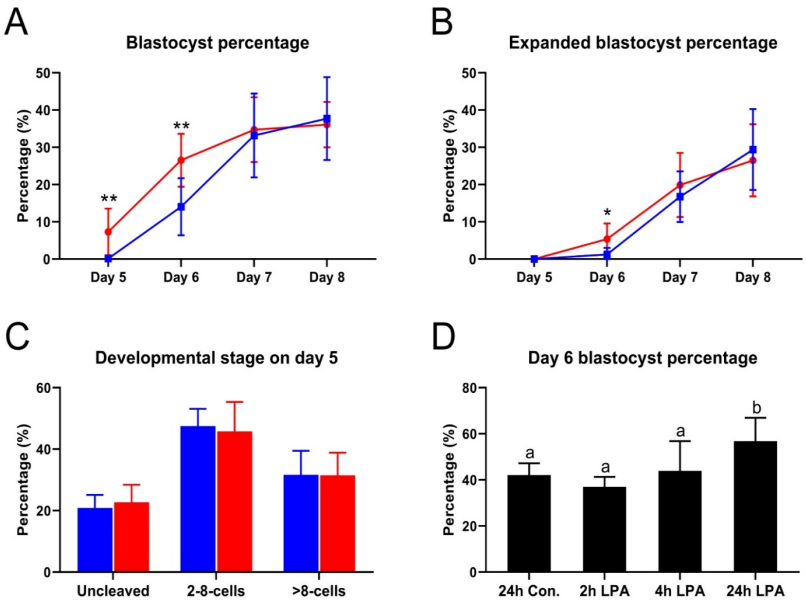

Figure 1. Effect of lysophosphatidic acid (LPA) on bovine embryo development. Blastocyst percentage (A) and expanded blastocyst percentage (B) after *in vitro* culture in the absence (blue) or presence (red) of 10^{-5} M LPA. Significant differences are individual timepoints are indicated by * ($p<0.05$) and **($p<0.01$). (C) Embryo development at day 5 after culture without (blue) and with (red) LPA. (D) Blastocyst percentage on day 6. Embryos with >8 cells were collected on day 5 and cultured without LPA (control) and with LPA for different time periods as indicated, and further cultured without LPA to complete the 24 hours. Significant differences among columns are indicated by different letters above the bars. Data are depicted as mean ± standard deviation of more than three independent biological replicates. Con.= control, h = hours.

To further determine whether LPA stimulation only affects the developmental status of embryos on days 5 and 6 and is time-dependent, embryos were first cultured until day 5 in the absence of LPA; >8-cell stage embryos were then randomly selected and cultured in the presence of LPA. The blastocyst percentage from these >8-cell embryos was not significantly different between the control group (42.1%) and embryos stimulated with LPA for 2h (37.0%) or 4h (43.9%), whereas the blastocyst percentage was significantly higher ($p<0.05$) when the embryos were exposed to LPA for 24h (56.8%) (Figure 1D). These data indicate that LPA accelerates blastocyst formation at around day 5 and may therefore affect the first lineage segregation event.

Gene expression levels of LPA-cultured embryos

To evaluate how LPA accelerates blastocyst formation, we next quantified gene expression for *YAP*, *TAZ*, *TEAD4* and of the lineage specific genes *CDX2*, *OCT4* and *SOX2* in day 6 and day 8 embryos. Expression of all the selected genes was detected by quantitative RT-PCR in both LPA-stimulated and control embryos (Figure 2A-F). The *YAP* expression levels were similar between LPA-stimulated and control embryos at days 6 and 8 (Figure 2A). The expression of *TAZ* and *TEAD4* was significantly higher in day 6 LPA stimulated blastocysts than in control embryos, but there was no difference between-treatment difference in day 6 morulae and day 8 blastocysts (Figure 2B, C). No significant differences in expression of *CDX2*, *OCT4* and *SOX2* were detected between LPA-stimulated and control embryos at days 6 and 8 (Figure 2D, E).

Effect of LPA on YAP and CDX2 protein expression

To investigate the localization of YAP, whole mount immunofluorescence was performed on day 6 and day 8 bovine embryos. In agreement with the qRT-PCR results, YAP was detected in day 6 morulae and blastocysts, and in day 8 blastocysts (Figure 3). However, unlike in the mouse, we only detected nuclear YAP staining, even in cells spatially located in the inner part of the embryo (Figure 3). To assess the correlation between YAP and CDX2 localization and to evaluate YAP expression in ICM cells, embryos were simultaneously immunostained for CDX2. Interestingly, nuclear YAP was detected in both CDX2-positive and -negative cells in day 6 morulae and blastocysts (Figure 3), suggesting that nuclear YAP by alone is not sufficient to drive CDX2 expression.

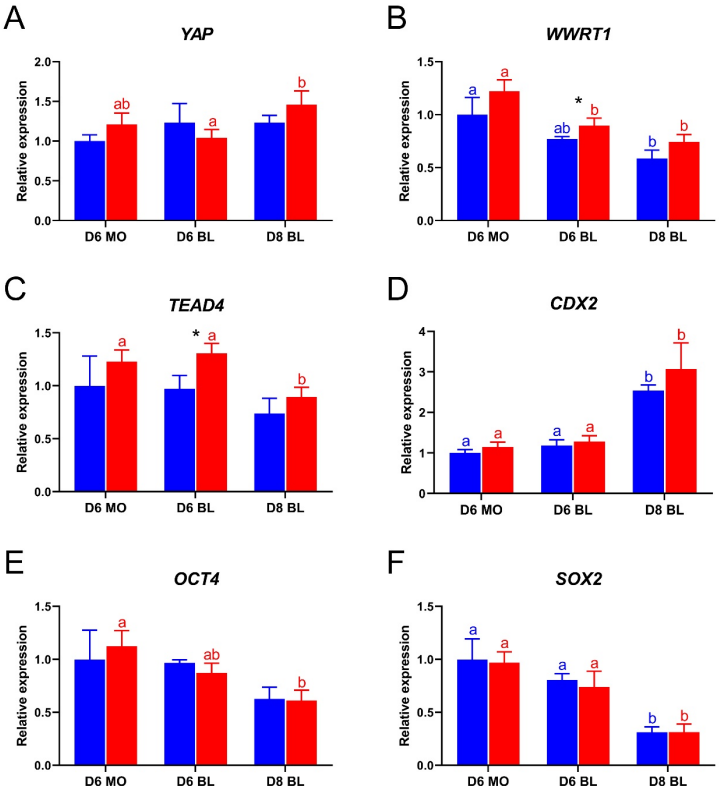

Figure 2. The relative expression of Hippo pathway and pluripotency genes in bovine embryos cultured in the absence of LPA (blue) and in the presence of 10^{-5} M LPA (red), as determined by quantitative RT-PCR. (A) *YAP*, (B) *TAZ*, (C) *TEAD4*, (D) *CDX2*, (E) *OCT4*, (F) *SOX2*. Relative expression from control embryos was set at 1; * ($p < 0.05$) indicates a significant difference between embryos cultured with and without LPA. Significant differences between developmental stages are indicated by different letters with the same color ($p < 0.05$). Error bars indicate standard deviations of three independent biological replicates. D = day, MO = morula, BL = blastocyst.

To examine whether LPA affects YAP expression, we determined the percentages of YAP expressing cells in day 6 and day 8 embryos. The total cell numbers were similar between embryos cultured with and without LPA for day 6 morulae, day 6 blastocysts and day 8 blastocysts (Figure 4A). A similar and high percentage of YAP positive cells was detected after culture with and without LPA in day 6 morulae (65.1% vs 62.8% respectively) and day 6 blastocysts (77.6% vs 78.1% respectively) (Figure 4B, C). By contrast, a significantly higher percentage of YAP positive cells was detected in day 8 blastocysts after LPA exposure

(75.2%) compared to control medium (61.7%) (Figure 4B, C). percentage of YAP positive cells was detected after culture with and without LPA in day 6 morulae

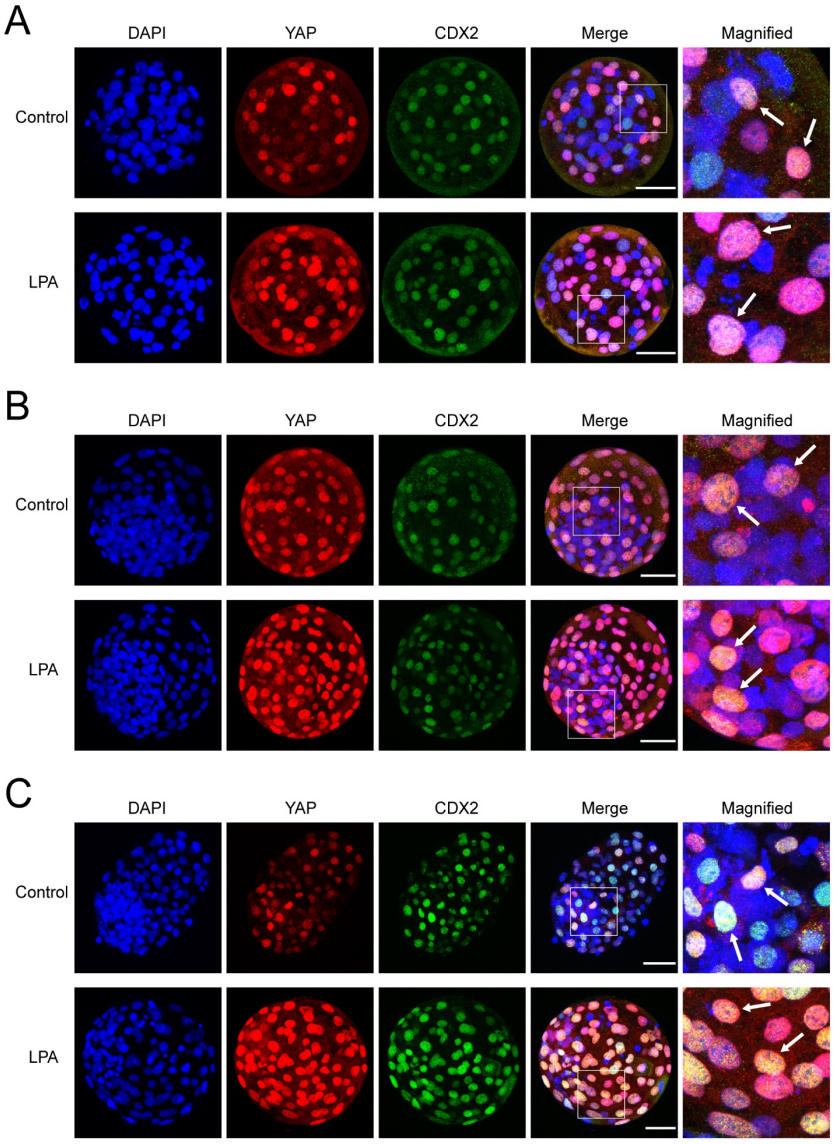

Figure 3. YAP and CDX2 immunofluorescence in bovine embryos cultured in the absence (control) or presence of 10^{-5} M LPA. Day 6 morula (A), day 6 blastocyst (B) and day 8 blastocyst (C). White boxes indicate areas presented in the right column at higher magnification. YAP and CDX2 colocalization is indicated (arrows). Scale bar = 50µm.

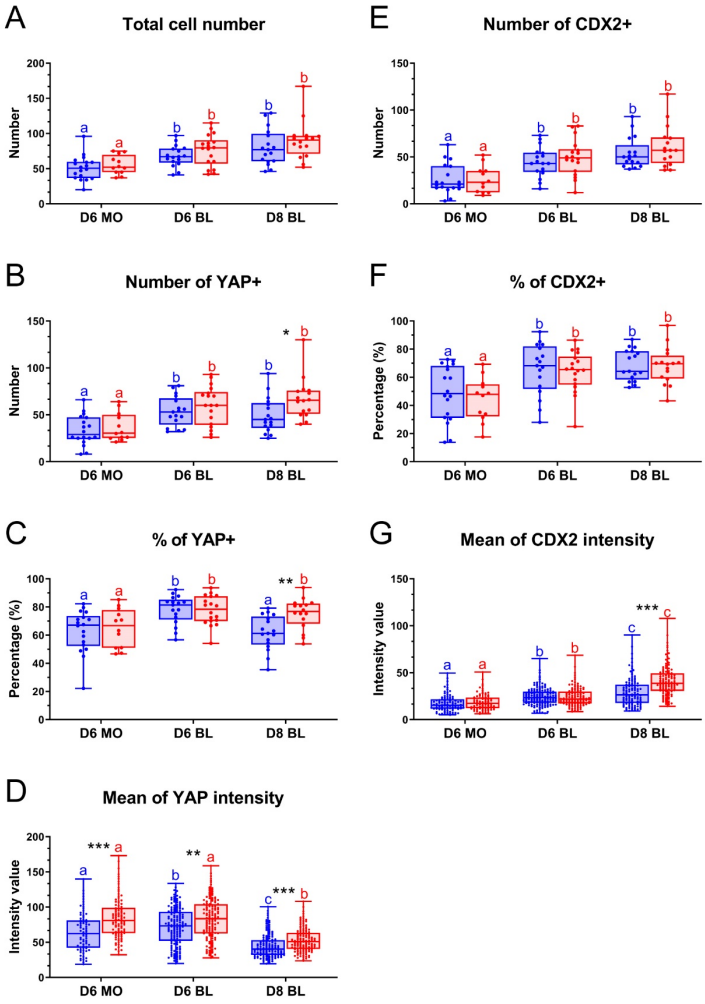

Figure 4. Effect of LPA on YAP and CDX2 expression in bovine embryos. Embryos were cultured in the absence of LPA (blue) or in the presence of 10^{-5} M LPA (red). Total cell number (A), number of YAP positive cells (B), percentage of YAP positives out of total cell population (C), Mean YAP intensity (RFU) in single nuclei (D), number of CDX2 positive cells (E), percentage of CDX2 positives of total cell population (F), Mean CDX2 intensity (RFU) in single nuclei (G). * ($p < 0.05$), ** ($p < 0.01$) and *** ($p<0.005$) indicate significant differences between embryos cultured with and without LPA. Significant differences among embryos cultured under the same conditions are indicated by different letters with the same color ($p < 0.05$). Error bars indicate standard deviations of embryos or single cells, collected from three independent biological replicates. D = day, MO = morula, BL = blastocyst.

(65.1% vs 62.8% respectively) and day 6 blastocysts (77.6% vs 78.1% respectively) (Figure 4B, C). By contrast, a significantly higher percentage of YAP positive cells was detected in day 8 blastocysts after LPA exposure (75.2%) compared to control medium (61.7%) (Figure 4B, C). The percentages of YAP positive cells were similar between day 6 and day 8 blastocysts after LPA exposure, but were significantly decreased from day 6 to day 8 in control conditions (Figure 4C), indicating that YAP degradation was inhibited by LPA exposure. To compare YAP expression in cells between embryos cultured with and without LPA, the average fluorescence intensity of a total of 5656 YAP positive cells from 98 embryos was analyzed. The fluorescence intensity, quantified as relative fluorescence units (RFU), was significantly higher when embryos were cultured with LPA, compared to control medium for day 6 morulae (83.5 RFU vs 52.0 RFU), day 6 blastocysts (82.7 RFU vs 72.2 RFU) and day 8 blastocysts (52.9 RFU vs 44.5 RFU) (Figure 4D).

Since absence of Hippo signaling can lead to CDX2 expression via YAP, we compared the percentages of CDX2 positive cells in day 6 and day 8 embryos cultured in the presence and absence of LPA. Contrary to expectations, the percentages of CDX2 positive cells were similar between embryos cultured with and without LPA for day 6 morulae (44.3% vs. 48.7%, respectively), day 6 blastocysts (63.9% vs. 65.7%, respectively) and day 8 blastocysts (68.2% vs. 68.7%, respectively) (Figure 4E,F). Moreover, the average CDX2 fluorescence intensity within nuclei were similar between embryos cultured with and without LPA for day 6 morulae (18.6 RFU vs. 15.8 RFU) and day 6 blastocysts (24.1 RFU vs. 23.8 RFU). However, the CDX2 intensity was significantly higher in day 8 blastocysts cultured in the presence of LPA (41.3 RFU), compared to control medium (24.9 RFU) (Figure 4G).

Colocalization of YAP and CDX2 in bovine embryos

We next focused on the relative localization of YAP and CDX2 in day 6 and day 8 embryos. A similar percentage of cells with colocalization of YAP and CDX2 was detected in embryos cultured, respectively, with or without LPA for day 6 morulae (43.3% vs 43.7%), day 6 blastocysts (62.0% vs 60.8%) and day 8 blastocysts (63.3% vs 56.7%) (Figure 5A, B). In addition, the percentages of cells positive for YAP but negative for CDX2 expression was similar between embryos cultured with and without LPA for day 6 morulae (20.8% vs 19.1%) and day 6 blastocysts (15.5% vs 18.0%). However, for day 8 blastocysts, a significantly higher percentage of YAP positive but CDX2 negative cells was detected when embryos were cultured in the presence of LPA (11.5%), compared to control

medium (4.9%) (Figure 5C, D). In addition, significantly lower percentages of CDX2 positive but YAP negative cells were present in embryos cultured with LPA, compared to control medium for day 6 morulae (1.1% vs 5.0%), day 6 blastocysts (1.9% vs 4.9%) and day 8 blastocysts (4.9% vs 10.6%) (Figure 5E, F). Combined, the data suggest that CDX2 expression in the nucleus lags behind the nuclear localization of YAP.

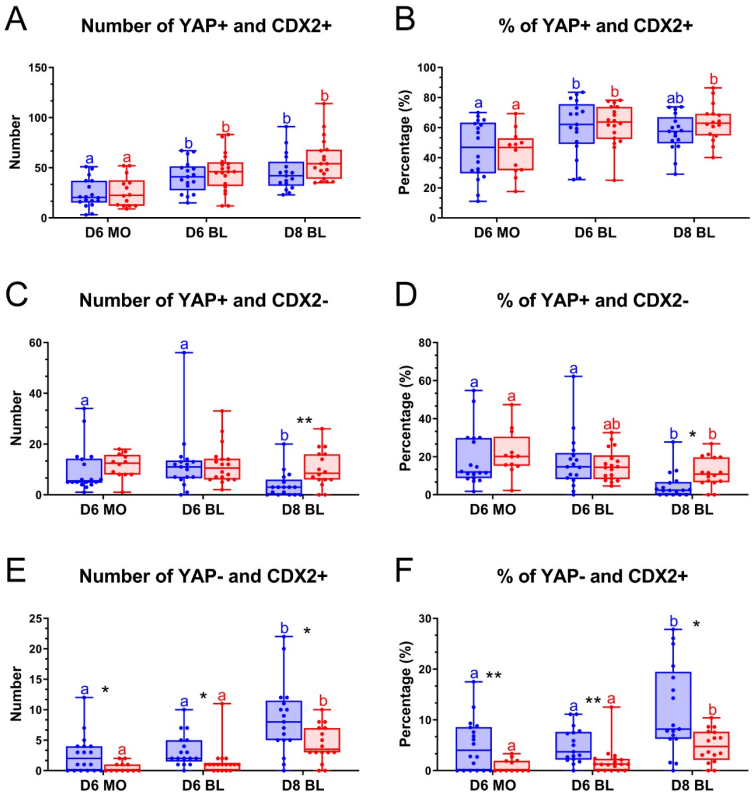

Figure 5. Effect of LPA on YAP and CDX2 localization in bovine embryos. Embryos were cultured in the absence of LPA (blue) or in the presence of 10^{-5} M LPA (red). Number of cells with colocalized YAP and CDX2 (A), percentage of YAP and CDX2 colocalization out of total cells (B), number of YAP positive (YAP+) but CDX2 negative (CDX2-) cells (C), percentage of YAP positive but CDX2 negative cells (D), number of YAP negative (YAP-) but CDX2 positive (CDX2+) cells (E), percentage of YAP negative but CDX2 positive cells (F). * ($p < 0.05$), ** ($p < 0.01$) and *** ($p<0.005$) indicate significant differences between embryos cultured with and without LPA. Significant differences among embryos cultured under the same conditions are indicated by different letters with the same color ($p < 0.05$). Error bars indicate standard deviations for embryos, collected from three independent biological replicates. D = day, MO = morula, BL = blastocyst.

Discussion

In mouse development, nuclear YAP is important for CDX2 expression and TE specification (Nishioka *et al.*, 2009). In human embryonic stem cells, however, YAP overexpression induces naïve pluripotency (Qin *et al.*, 2016), indicating that the role of YAP in early cell lineage segregation may not be conserved among mammals. Since YAP/TAZ signaling can be enhanced by LPA (Moroishi *et al.* , 2015, Qin *et al.*, 2016, Yu *et al.*, 2012), we studied the role of the Hippo/YAP pathway in embryonic development and lineage segregation by culturing bovine embryos in the presence of LPA.

LPA is present in all mammalian cells and tissues, and can induce a broad range of cellular effects, such as proliferation, survival, and migration (Kim *et al.* , 2019a, Lin *et al.*, 2010, Teo *et al.* , 2009). Our results demonstrate that LPA stimulation accelerates bovine blastocyst formation on days 5 and day 6 of in vitro culture, without changing the total cell number at day 6 or day 8. This indicates that YAP signaling does not affect the rate of cell division during bovine embryo development. In mouse embryos, similarly, LPA did not alter cleavage rates but increased the percentage of 2-cell stage embryos that developed to blastocysts (Kobayashi *et al.* , 1994). In porcine parthenogenetic embryos, LPA increased the cleavage and blastocyst rates and total cell numbers (Zhu *et al.* , 2018); all of which suggests that the function of LPA in embryos varies between different mammalian species.

In general, unphosphorylated YAP translocates to the nucleus, whereas phosphorylated YAP undergoes cytoplasmic inactivation (Karasek *et al.*, 2020, Nishioka *et al.*, 2009, Yao *et al.*, 2019). Here we detected YAP only in nuclei in day 6 and day 8 bovine embryos, when using an anti-YAP antibody that recognizes both phosphorylated and unphosphorylated YAP; it is possible that YAP is rapidly removed from the cytoplasm after phosphorylation.

LPA has been shown to increase YAP expression by inhibiting the Hippo pathway kinases LATS1/2 (Qin *et al.*, 2016, Yu *et al.*, 2012). Indeed, by comparing the intensity of fluorescence, we showed that YAP expression levels were higher in day 6 and 8 embryos cultured in the presence of LPA than in embryos cultured without LPA. No difference in *YAP* gene expression was detected between embryos cultured with and without LPA, indicating that LPA does not affect *YAP* transcription.

The transcription factor CDX2 is essential for TE specification and blastocyst formation (Wu *et al.* , 2010). Indeed, the percentage of CDX2 positive

cells, and average CDX2 intensity within single nuclei, were higher in day 6 blastocysts than day 6 morulae. In the presence of LPA, the percentage of embryos that had developed into blastocysts at day 6 was almost doubled, indicating that more cells within those individual embryos reached the CDX2 expression threshold for TE differentiation in the presence of LPA. However, the intensity of fluorescence after CDX2 immunostaining was not different in LPA-exposed embryos, suggesting other mechanisms are involved in maintaining CDX2 expression in a certain level. Of the embryos that had reached the blastocyst stage at day 6, no difference in the percentage of CDX2 -expressing cells was observed after LPA exposure, indicating that the TE/ICM ratio is not affected by the Hippo signaling pathway.

Materials and Methods

Chemicals

All chemicals were purchased from Sigma Aldrich (St. Louis, MO, USA), unless otherwise stated.

In vitro embryo production and LPA stimulation

Cumulus oocyte complexes (COCs) collection, oocyte recovery and in vitro fertilization were performed as described previously (Brinkhof *et al.*, 2015a). In short, COCs were aspirated from 2-8mm follicles from cattle ovaries, which were collected from a local slaughterhouse. the COCs were then cultured in maturation medium for 23 h at 38.5 °C, in an atmosphere of 5% CO_2-in-air, after which oocytes were fertilized with sperm for 20–22 h and fertilization day was considered as day 0 of embryo development. After removal of the cumulus cells, zygotes were randomly allocated to one of two experimental groups: (i) cultured in synthetic oviductal fluid (SOF) (Yu *et al.* , 2020); and (ii) LPA, cultured in SOF supplemented with 10^{-5} M LPA for further development at 38.5 °C, in a humidified atmosphere containing 5% CO_2 and 7% O_2. On day 5, embryos were transferred to fresh SOF or SOF supplemented with 10^{-5} M LPA respectively, and cultured until day 8.

Developmental stage on day 5 and blastocyst percentage from days 5 to 8 were analyzed by 2 independent researchers (double-blinded).

RNA Isolation, cDNA Generation and Quantitative Reverse Transcription-PCR

Groups of 20–22 embryos were collected and stored in 100 µL RLT buffer (Qiagen, Venlo, The Netherlands) at −80 °C until RNA isolation. Total RNA isolation and cDNA generation was performed as described previously (Yu *et al.*, 2020).

The quantitative reverse transcription PCR was performed as described previously (Yu *et al.*, 2020) using specific primer sequences and annealing temperatures for amplification (Table S1). Three independent biological cDNA samples were analyzed in duplicate. Expression of *RPL15*, *SDHA* and *YWHAZ* was used for normalization.

Immunofluorescence

Embryos were collected and fixed in 4% paraformaldehyde (PFA) for 15 min and then stored in 1% PFA at 4 °C until further use. After washing twice in PBST (1x PBS, 0.01% Triton X-100), samples were blocked in PBS with 5% goat serum and 0.3% Triton X-100 for 60 min. After three washes in PBST, samples were incubated with mouse monoclonal antibody against CDX2 (Biogenex, CA, USA; CDX2-88; 1:200) and rabbit monoclonal antibody against YAP (Cell signaling technologies, Leiden, The Netherlands; #14074; 1:100) in dilution buffer (1x PBS, 1% BSA, 0.3% Triton X-100) overnight. Following three washes in PBST, samples were incubated with the secondary antibodies: goat anti mouse Alexa488 (Invitrogen, Venlo, The Netherlands) and goat anti rabbit Alexa568 (Invitrogen) at 37 °C for 1 h. Subsequently, nuclei were stained with DAPI for 20 min in the dark. After three washes in PBST, samples were mounted with Vectashield (Brunschwig Chemie, Amsterdam, The Netherlands) on slides and stored at 4 °C in the dark before imaging. Fluorescent images were obtained using a confocal laser scanning microscope (SPE-II-DMI4000; Leica, Son, The Netherlands) with a Z-stack projection and were further analyzed using IMARIS software (Bitplane, Zürich, Switzerland).

Statistical analysis

Results are presented as means ± standard deviation in bar graphs. Statistical analysis was performed using Excel and GraphPad Prism 8 (https://www. graphpad.com/scientific-software/prism/). Pools of embryos from three biological replicates were analyzed for gene expression. Individual embryos from three biological replicates were analyzed after immunostaining. Differences between groups were analyzed by two-tailed unpaired Student's t-tests, and differences between multiple groups were examined by one-way ANOVA,

followed by a post-hoc Tukey test. Statistical significance was set at $p < 0.05$.

Author Contributions

Conceptualization, B.Y., H.T. and B.R.; methodology, B.Y., H.T., and B.R.; funding acquisition, B.R. and B.Y.; investigation, B.Y., H.T., and C.O.; resources, B.R.; data curation, B.Y.; writing—original draft preparation, B.Y.; writing—review and editing, T.S., and B.R.; visualization, B.Y.; supervision, T.S. and B.R..; project administration, B.R. All authors have read and agreed to the submitted version of the manuscript.

Acknowledgments

We thank Arend Rijneveld for assistance with oocyte recovery. The Center for Cell Imaging (CCI) of the Faculty of Veterinary Medicine is thanked for valuable assistance with microscopy.

Supplementals

Supplemental figures and tables in this chapter are available online at *internatio nal journal of molecular sciences* (https://www.mdpi.com/1422-0067/22/11/591 5/htm)

References

Bergsmedh A, Donohoe ME, Hughes RA, Hadjantonakis AK. Understanding the molecular circuitry of cell lineage specification in the early mouse embryo. *Genes* 2011;**2**:420-448.

Boyer LA, Lee TI, Cole MF, Johnstone SE, Levine SS, Zucker JP, Guenther MG, Kumar RM, Murray HL, Jenner RG *et al.* Core transcriptional regulatory circuitry in human embryonic stem cells. *Cell* 2005;**122**:947-956.

Brinkhof B, van Tol HT, Groot Koerkamp MJ, Riemers FM, SG IJ, Mashayekhi K, Haagsman HP, Roelen BA. A mRNA landscape of bovine embryos after standard and MAPK-inhibited culture conditions: a comparative analysis. *BMC Genomics* 2015;**16**:277.

Chen Y, Han H, Seo G, Vargas RE, Yang B, Chuc K, Zhao H, Wang W. Systematic analysis of the Hippo pathway organization and oncogenic alteration in evolution. *Scientific reports* 2020;**10**:3173.

Chen YA, Lu CY, Cheng TY, Pan SH, Chen HF, Chang NS. WW Domain-Containing Proteins YAP and TAZ in the Hippo Pathway as Key Regulators in Stemness Maintenance, Tissue Homeostasis, and Tumorigenesis. *Frontiers in oncology* 2019;**9**:60.

Felley-Bosco E, Stahel R. Hippo/YAP pathway for targeted therapy. *Translational lung cancer research* 2014;**3**:75-83.

Frisca F, Sabbadini RA, Goldshmit Y, Pébay A. Biological effects of lysophosphatidic acid in the nervous system. *International review of cell and molecular biology* 2012;**296**:273-322.

Frum T, Murphy TM, Ralston A. HIPPO signaling resolves embryonic cell fate conflicts during establishment of pluripotency in vivo. *eLife* 2018;**7**.

Hama K, Aoki J, Inoue A, Endo T, Amano T, Motoki R, Kanai M, Ye X, Chun J, Matsuki N *et al.* Embryo spacing and implantation timing are differentially regulated by LPA3-mediated lysophosphatidic acid signaling in mice. *Biology of reproduction* 2007;**77**:954-959.

Huang D, Guo G, Yuan P, Ralston A, Sun L, Huss M, Mistri T, Pinello L, Ng HH, Yuan G *et al.* The role of Cdx2 as a lineage specific transcriptional repressor for pluripotent network during the first developmental cell lineage segregation. *Scientific reports* 2017;**7**:17156.

Karasek C, Ashry M, Driscoll CS, Knott JG. A tale of two cell-fates: role of the Hippo signaling pathway and transcription factors in early lineage formation in mouse preimplantation embryos. *Molecular human reproduction* 2020;**26**:653-664.

Kim D, Li HY, Lee JH, Oh YS, Jun HS. Lysophosphatidic acid increases mesangial cell proliferation in models of diabetic nephropathy via Rac1/MAPK/KLF5 signaling. *Experimental & molecular medicine* 2019;**51**:1-10.

Kobayashi T, Yamano S, Murayama S, Ishikawa H, Tokumura A, Aono T. Effect of lysophosphatidic acid on the preimplantation development of mouse embryos. *FEBS letters* 1994;**351**:38-40.

Lin ME, Herr DR, Chun J. Lysophosphatidic acid (LPA) receptors: signaling properties and

disease relevance. *Prostaglandins & other lipid mediators* 2010;**91**:130-138.

Liu H, Du S, Lei T, Wang H, He X, Tong R, Wang Y. Multifaceted regulation and functions of YAP/TAZ in tumors (Review). *Oncology reports* 2018;**40**:16-28.

Lorthongpanich C, Issaragrisil S. Emerging Role of the Hippo Signaling Pathway in Position Sensing and Lineage Specification in Mammalian Preimplantation Embryos. *Biology of reproduction* 2015;**92**:143.

Moroishi T, Park HW, Qin B, Chen Q, Meng Z, Plouffe SW, Taniguchi K, Yu FX, Karin M, Pan D *et al.* A YAP/TAZ-induced feedback mechanism regulates Hippo pathway homeostasis. *Genes & development* 2015;**29**:1271-1284.

Nishioka N, Inoue K, Adachi K, Kiyonari H, Ota M, Ralston A, Yabuta N, Hirahara S, Stephenson RO, Ogonuki N *et al.* The Hippo signaling pathway components Lats and Yap pattern Tead4 activity to distinguish mouse trophectoderm from inner cell mass. *Developmental cell* 2009;**16**:398-410.

Nishioka N, Yamamoto S, Kiyonari H, Sato H, Sawada A, Ota M, Nakao K, Sasaki H. Tead4 is required for specification of trophectoderm in pre-implantation mouse embryos. *Mechanisms of development* 2008;**125**:270-283.

Qin H, Hejna M, Liu Y, Percharde M, Wossidlo M, Blouin L, Durruthy-Durruthy J, Wong P, Qi Z, Yu J *et al.* YAP Induces Human Naive Pluripotency. *Cell reports* 2016;**14**:2301-2312.

Sheng X, Yung YC, Chen A, Chun J. Lysophosphatidic acid signalling in development. *Development (Cambridge, England)* 2015;**142**:1390-1395.

Teo ST, Yung YC, Herr DR, Chun J. Lysophosphatidic acid in vascular development and disease. *IUBMB life* 2009;**61**:791-799.

Watt KI, Harvey KF, Gregorevic P. Regulation of Tissue Growth by the Mammalian Hippo Signaling Pathway. *Frontiers in physiology* 2017;**8**:942.

Wu G, Gentile L, Fuchikami T, Sutter J, Psathaki K, Esteves TC, Araúzo-Bravo MJ, Ortmeier C, Verberk G, Abe K *et al.* Initiation of trophectoderm lineage specification in mouse embryos is independent of Cdx2. *Development (Cambridge, England)* 2010;**137**:4159-4169.

Yao C, Zhang W, Shuai L. The first cell fate decision in pre-implantation mouse embryos. *Cell regeneration (London, England)* 2019;**8**:51-57.

Ye X, Hama K, Contos JJ, Anliker B, Inoue A, Skinner MK, Suzuki H, Amano T, Kennedy G, Arai H *et al.* LPA3-mediated lysophosphatidic acid signalling in embryo implantation and spacing. *Nature* 2005;**435**:104-108.

Yu B, van Tol HTA, Stout TAE, Roelen BAJ. Initiation of X Chromosome Inactivation during Bovine Embryo Development. *Cells* 2020;**9**:1016.

Yu FX, Zhao B, Panupinthu N, Jewell JL, Lian I, Wang LH, Zhao J, Yuan H, Tumaneng K, Li H *et al.* Regulation of the Hippo-YAP pathway by G-protein-coupled receptor signaling. *Cell* 2012;**150**:780-791.

Zhao B, Tumaneng K, Guan KL. The Hippo pathway in organ size control, tissue regeneration and stem cell self-renewal. *Nature cell biology* 2011;**13**:877-883.

Zheng Y, Pan D. The Hippo Signaling Pathway in Development and Disease. *Developmental cell* 2019;**50**:264-282.

Zhu X, Li L, Gao B, Zhang D, Ren Y, Zheng B, Li M, Shi D, Huang B. Early development of porcine parthenogenetic embryos and reduced expression of primed pluripotent marker genes under the effect of lysophosphatidic acid. *Reproduction in domestic animals = Zuchthygiene* 2018;**53**:1191-1199.

Chapter 5

Cellular fragments in the perivitelline space are not a predictor of expanded blastocyst quality

Bo Yu[1], Helena T. A. van Tol[1], Tom A.E. Stout[2] and Bernard A. J. Roelen[3]*

[1]Farm Animal Health; Department of Population Health Sciences, Faculty of Veterinary Medicine, Utrecht University, Utrecht, The Netherlands.

[2]Equine Sciences; Department Clinical Sciences, Faculty of Veterinary Medicine, Utrecht University, Utrecht, The Netherlands.

[3]Embryology, Anatomy and Physiology; Department Clinical Sciences, Faculty of Veterinary Medicine, Utrecht University, Utrecht, The Netherlands.

Adapted in *Frontiers in Cell and Developmental Biology. 2021 Jan 5;8:616801.*
Doi: 10.3389/fcell.2020.616801.

Abstract

The presence of cellular fragments in the perivitelline space is a commonly used parameter to determine quality before transfer of *in vitro* produced (IVP) embryos. However, this parameter is difficult to assess after blastocyst expansion. In this study, we used mechanical hatching to confirm the presence of cellular fragments in the perivitelline space of bovine IVP blastocysts. We further looked for associations between apoptosis within extruded cells/ cellular fragments and the quality of bovine blastocysts using quantitative RT-PCR and immunofluorescence. Surprisingly, more than 42% of expanded blastocysts had cellular fragments in the perivitelline space; however, more than 37% of extruded cells were TUNEL negative. We observed no significant difference in embryo quality between expanded blastocysts with and without cellular fragments in the perivitelline space. Overall, our data suggest that embryos extrude abnormal cells to maintain their developmental potential. The presence of fragmented cells is not an indicator of embryo quality.

Introduction

In the past 40 years, millions of human babies and bovine calves have been born with the help of *in vitro* fertilization (IVF) (Niederberger *et al.* , 2018, Sirard, 2018). Despite these numbers, the clinical pregnancy rate after embryo transfer is relatively low, at around 30-40%. It has however been established that transfer of embryos with good gross morphology results in higher pregnancy rates (Desai *et al.* , 2000, Lindner and Wright, 1983). Determination of embryo quality is challenging, however, because assessment of morphology is subjective and embryo grading results may vary between clinicians (Baxter Bendus *et al.*, 2006, Farin *et al.* , 1995, Lindner and Wright, 1983). In human IVF, it is common practice to transfer 4- to 8-cell stage embryos to the patient's uterus to shorten the *in vitro* embryo culture time. Currently, there is an increasing tendency to transfer at the blastocyst stage because this might improve implantation and clinical pregnancy rates (Gorodeckaja *et al.* , 2019, Papanikolaou *et al.*, 2005, Sciorio *et al.* , 2019). Indeed, in cattle and most domestic animals, only transfer of morulae-blastocysts reliably leads to pregnancy (Van Soom *et al.*, 2001). Therefore, a means to objectively assess the quality of blastocysts is of great importance for clinicians to aid selection of the best embryo to transfer.

There are two major approaches to evaluating blastocyst quality: invasive and non-invasive. Invasive evaluation of blastocyst quality mostly involves lysis

of the embryo for gene expression analysis, fixation for imaging or preimplantation genetic testing (PGT). The total cell number and the ratio of inner cell mass (ICM) to trophectoderm cells are directly correlated with blastocyst quality (Leppens *et al.* , 1996, Matsuura *et al.* , 2010) but because the ICM is highly compacted, it is difficult to accurately determine either total or ICM cell number using regular microscopy. Thus, staining of the nuclei together with a marker for the ICM and/or trophectoderm lineage after fixation can be a more accurate way to obtain information on blastocyst quality in an experimental setting. Another valuable indicator of blastocyst health is the percentage of cells undergoing apoptosis, which is often assessed using the terminal deoxynucleotidyl transferase (TdT) mediated dUTP nick-end labeling (TUNEL) assay (Neuber *et al.* , 2002). The disadvantage of these invasive evaluations of blastocyst quality is obvious, as these invasive procedures are not compatible with embryo survival. Therefore, in a clinical situation, embryo biopsy to remove a small number of cells for PGT is a more practical method to detect chromosomal or genetic abnormalities prior to embryo transfer, without the need to destroy the whole embryo. In commercial cattle breeding, analysis of cells to analyze for sex and assess genomic characteristics of the embryo is relatively common practice. However due to extra costs, risks of biopsy and of misdiagnosis because of the difficulty of extrapolating data from a small number of cells to the whole embryo (e.g. in the case of chromosomal mosaics), or because of the limited number of genes that can be analyzed on PGT samples (Cornelisse *et al.* , 2020, Kalfoglou *et al.* , 2005, Sermon *et al.* , 2016), non-invasive techniques based on gross morphological evaluation of embryos are still widely used in practice, particularly in human IVF (Bormann *et al.* , 2020, Farin *et al.*, 1995, Lindner and Wright, 1983).

An important parameter of non-invasive evaluation is the developmental stage in relation to time after fertilization. It has been shown that fast-cleaving embryos are of higher quality than slower-cleaving counterparts and expansion is considered to be an indicator of a ‘good’ blastocyst (Balaban *et al.* , 2006, van Soom *et al.*, 1997). Another emerging non-invasive embryo selection technique is time-lapse embryo imaging, which allows continuous observation of embryo morphology without taking the embryo from optimal culturing conditions (Kovacs, 2014). However, this technique is not ready for routine clinical application, as clinically meaningful outcome parameters of time-lapse embryo imaging have not been fully determined yet (Armstrong *et al.* , 2019).

One of the most commonly used parameters for assessing quality of

blastocysts is the presence of extruded blastomeres and the extent of cellular fragmentation in the perivitelline space. Embryos with extensive cellular fragmentation are considered as 'fair' or 'poor' embryos likely to result in a low likelihood of implantation (Racowsky *et al.* , 2010, Van Soom *et al.*, 2003).

Once a blastocyst expands, the perivitelline space becomes very small, which makes it difficult to identify cellular fragments. Thus, there is a lack of information about cellular fragments in the perivitelline space at the blastocyst stage and its relationship to embryo quality.

To investigate the correlation of the presence of cell fragments in the perivitelline space with blastocyst quality, we mechanically hatched the embryo from the zona pellucida of expanded blastocysts. Surprisingly, there was no significant difference in the quality of blastocysts with or without cells or cellular fragments in the perivitelline space of day 8 blastocysts. Our data confirmed that embryos can tolerate a certain level of apoptosis and still reach the blastocyst stage. It is concluded that apoptosis and fragmentation are methods to remove abnormal cells from the embryo, and thereby protect the developmental competence of the embryo.

Materials and Methods

In vitro embryo production

All chemicals were purchased from Sigma Aldrich (St. Louis, MO, USA), unless otherwise stated. Cattle ovaries were obtained from a local slaughterhouse within 2 h after slaughter. Cumulus-oocyte complexes (COCs) were aspirated from 2-8mm follicles using a winged infusion set (18G) connected to a vacuum aspiration system. COCs were isolated from the aspirated follicular fluid using a stereomicroscope. Groups of 40-60 oocytes were matured and fertilized in vitro as described previously (Brinkhof *et al.*, 2015a). In short, the oocytes were cultured in maturation medium: M199 (Life Technologies, Bleiswijk, The Netherlands) supplemented with 0.05 IU/mL recombinant hFSH (Organon, Oss, The Netherlands) and with 1% (v/v) penicillin-streptomycin (Life Technologies). Culture was for 23 h at 38.5 °C, in an atmosphere of 5% CO_2-in-air after which oocytes were fertilized by co-incubation with $1*10^6$/mL motile frozen/thawed sperm cells. The day on which COCs were co-incubated with sperm was considered as day 0 of embryo development. After incubation with sperm for 20-22 h, zygotes were denuded of their cumulus cells by vortexing for 3 min and then transferred to synthetic oviductal fluid (SOF) [107.63 mmol/L NaCl, 25

mmol/L $NaHCO_3$, 7.16 mmol/L KCl, 1.19 mmol/L KH_2PO_4, 1.78 mmol/L $CaCl_2 \cdot 2H_2O$, 3.20 mmol/L Sodium DL-lactate (60% syrup), 0.74 mmol/L $MgSO_4 \cdot 7H_2O$ (Merck Millipore, Billerica, MA, USA), 0.33 mmol/L Sodium pyruvate, 2.05 mmol/L L-Glutamine, 4 mg/mL BSA (Merck Millipore), 10 U/mL penicillin-streptomycin (Life Technologies), 1% MEM NEAA, 2% BME Amino Acids and 0.5 µL/mL Phenol Red 0.5% in LAL water (Lonza, Basel, Switzerland)] for further development at 38.5 °C, in a humidified atmosphere containing 5% CO_2 and 7% O_2. On day 5, embryos were transferred to fresh SOF and cultured until day 9 (Brinkhof *et al.*, 2017).

Mechanical separation

Day 7-9 expanded blastocysts were collected and placed in a washing medium composed of 6.66 mg/mL NaCl (Merck, Schiphol-Rijk, The Netherlands), 0.24 mg/mL KCl (Merck), 0.17 mg/mL $NaHCO_3$, 0.05 mg/mLNaH_2PO_4 (Merck), 0.22% (v/v) of a 60% sodium lactate solution, 2.38 mg/mL HEPES, 0.20% (v/v) phenol red, 0.39 mg/mL $CaCl_2 \cdot 2H_2O$, 0.10 mg/ mL $MgCl_2 \cdot 6H_2O$ (Merck), 0.11 mg/mL sodium pyruvate, 100U/mL penicillin-Streptomycin (Gibco, Paisley, UK) and 6.00 mg/mL bovine serum albumin fraction V (BSA) (MP Biomedicals, Santa Ana, CA, USA), set at an osmolality of 280±2 osmol/kg and pH 7.3±0.05. Embryos were mechanically separated from their zonae pellucida using tungsten needles in washing medium under a stereomicroscope. Isolated embryos and zonae pellucidae were rinsed in PBS before collection for quantitative reverse transcription PCR and immunofluorescence.

RNA isolation and cDNA generation

Groups of 47 to 55 zonae pellucidae containing obvious cell clumps or cellular fragments, and groups of 21-32 embryos were collected and stored in 100 µL RLT buffer (Qiagen, Venlo, The Netherlands) at -80ºC until RNA isolation. Total RNA extraction and genomic DNA digestion was performed using the RNeasy Micro Kit (Qiagen) according to the manufacturer's instructions. Complementary DNA (cDNA) was synthesized directly after RNA extraction. The mixture used for reverse transcription (RT) was made up of 10 µL of the RNA sample and 4 µL of 5 × RT buffer (Invitrogen, Breda, The Netherlands) in a total volume of 20 µL containing 10 mM DTT (Invitrogen), 0.5 mM dNTP (Promega, Leiden, the Netherlands), 8 units RNAse inhibitor (Promega) and 150 units Superscript III reverse transcriptase (Invitrogen). Minus-RT controls were prepared from 5 µL RNA sample using the same reagents as above, without the

reverse transcriptase. After incubation at 70 °C for 5 min, the mixtures were cooled down on ice for 5 min, followed by 1 h at 50 °C, and 5 min at 80 °C. cDNA samples were stored at -20 °C.

Quantitative reverse transcription-PCR

Primer pairs (Eurogentec, Maastricht, the Netherlands) were designed on Primer-Blast (http://www.ncbi.nlm.nih.gov/tools/primer-blast) according to *Bos taurus* mRNA (Genbank; http://www.ncbi.nlm.nih.gov/nucleotide). The quantitative reverse transcription PCR (qRT-PCR) mixture contained 10 µL iQ SYBR Green supermix (Bio-Rad, CA, USA), 9 µL RNAse-free and DNAse-free water (Invitrogen) and 1 µL cDNA with a final primer concentration of 500 nM. The specificity and annealing temperature of primers (Supplementary Table 1) were first established using a temperature gradient from 55 °C to 68 °C, and cDNA from 100 blastocysts as template. Reactions were performed on the CFX detection system (Bio-Rad) based on the manufacturer's protocol. Mixtures were kept at 95 °C for 3 min, followed by 40 cycles of denaturation at 95 °C for 20 sec, the primer specific annealing temperature for 20 sec and extension at 72 °C for 20 sec. To verify the purity of the amplified products, melting curves were generated after amplification with temperature increments of 0.5 °C from 65 °C to 95 °C for 5 sec each step. To calculate amplification efficiency, standard curves of primers were generated by 4-fold dilutions of cDNA from 100 blastocysts in each reaction. All the reactions were performed on three independent biological cDNA samples in duplicate. Expression of *RPL15*, *SDHA* and *YWHAZ* was used for normalization (Brinkhof *et al.*, 2015a).

Immunofluorescence

Blastocysts and zonae pellucidae with cellular fragments were collected and fixed in 4% paraformaldehyde (PFA) for 15 min and then stored in 1% PFA at 4 °C until further use. After washing twice in PBST (1x PBS, 0.01% Triton X-100), samples were blocked in PBS with 5% goat serum and 0.3% Triton X-100 for 60 min. Following three washes in PBST, samples were incubated with mouse monoclonal antibody against CDX2 (Biogenex, CA, USA; CDX2-88; 1:200) and Alexa Fluor™ 568 Phalloidin (Invitrogen; A12380; 1:100) in dilution buffer (1x PBS, 1% BSA, 0.3% Triton X-100) overnight. After three washes in PBST, secondary antibody incubation was performed with goat anti mouse Alexa488 (Invitrogen) for at least 1 h in the dark. Subsequently, nuclei were stained with DAPI (Sigma Aldrich) for 20 min in the dark. After three washes in PBST, samples were mounted with Vectashield (Brunschwig Chemie, Amsterdam, The

Netherlands) on slides and stored at 4 °C in the dark before imaging. Fluorescent images were obtained using a confocal laser scanning microscope (SPE-II-DMI4000; Leica, Son, The Netherlands) with a Z-stack projection and were further analyzed using IMARIS software (Bitplane, Zürich, Switzerland).

Combined TUNEL and immunofluorescence

Apoptotic cells were identified by terminal deoxynucleotidyl transferase dUTP nick end labeling (TUNEL) based on the Click-iT Plus TUNEL assay (Thermo Fisher Scientific, Carlsbad, CA, USA) with a few modifications. After fixation, samples were washed twice in PBST and incubated with 100 µL of TdT reaction buffer at 37 °C for 10 min, followed by incubation with TdT reaction mixture for 60 min at 37 °C. After two washes in Milli Q water, samples were incubated with 3% BSA and 0.1% Triton X-100 in PBS for 5 min at room temperature. Following two washes in PBST, samples were incubated with 100 µL of the Click-iT Plus TUNEL reaction cocktail for 30 min at 37 °C in the dark.

After three washes in PBST, immunofluorescence and imaging were performed as described above.

Statistical analysis

Statistical analysis was performed using Excel and GraphPad Prism 8 (https://www. graphpad.com/scientific-software/prism/). Pools of embryos or zonae with cellular fragments from three biological replicates were analyzed for gene expression. Individual embryos or zonae with cellular fragments from three biological replicates were analyzed after immunostaining. Differences between two groups were analyzed by two-tailed unpaired Student's t-tests, and differences between multiple groups were examined by one-way ANOVA, followed by a post-hoc Tukey test. A linear mixed model [SPSS (IBM, Amsterdam, Netherlands)] was used to investigate differences in the total cell number, CDX2 positive cell number and TUNEL positive cell number per blastocyst and cellular fragment comparison. The 'presence of cellular fragments' was used as fixed effect, and the 'IVF run' and 'IVF run by presence of cellular fragments interaction' were used as random effect due to random variability between batches of ovaries. Statistical significance was set at $P < 0.05$.

Result

The presence of cellular fragments in the perivitelline space of expanded blastocysts

As cellular fragments can be detected in the perivitelline space of day 9 hatching and hatched blastocysts (Figure 1), we presumed that fragmented cells would also be present in the zonae of expanded blastocysts but would not be visible due to the pressure of the expanding blastocyst against the zona pellucida. To preserve the integrity of blastocysts and zonae pellucidae, we examined the presence of cellular fragments following manual removal of the zona pellucida of a total number of 443 of day 7, 8 and 9 blastocysts (Supplementary Table 2). As expected, fragmented cells were also detected between the embryo and the zona pellucida of expanded blastocysts (Figure 2A, B). Note that the occurrence of fragmented cells in the perivitelline space is difficult to establish before mechanical separation (Figure 2A to 2D). To our surprise, more than 42% of expanded blastocysts demonstrated cells or cell fragments in the perivitelline space with no significant difference between day 7, day 8 and day 9 blastocysts (Figure 2E, Supplementary Table 2).

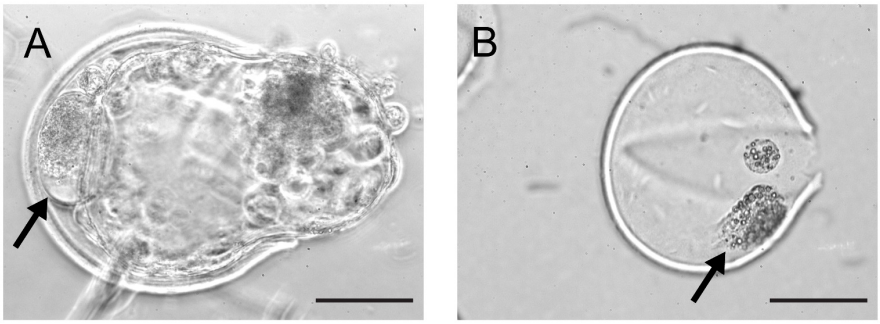

Figure 1. Cellular fragments in day 9 bovine blastocysts. Fragmented cells (arrows) in the perivitelline space of a day 9 hatching blastocyst (A) and within the zona pellucida of a hatched blastocyst (B). Scale bar = 50µm.

The level of apoptosis in cellular fragments

It has been suggested that cellular fragmentation in embryos is the result of elimination of abnormal cells (e.g. with chromosomal errors), and is closely related to apoptotic processes (Daughtry *et al.* , 2019, Haouzi and Hamamah, 2009). We first used DAPI to examine nuclear DNA in fragmented cells in the zona pellucida of day 9 blastocysts, with 16/25 (64%) containing DAPI positive fragments. We then evaluated the level of apoptosis-related changes in the cells and cellular fragments in the 11 zonae of day 9 blastocysts by means of the TUNEL assay. TUNEL positive cells were detected in the majority of cell clumps.

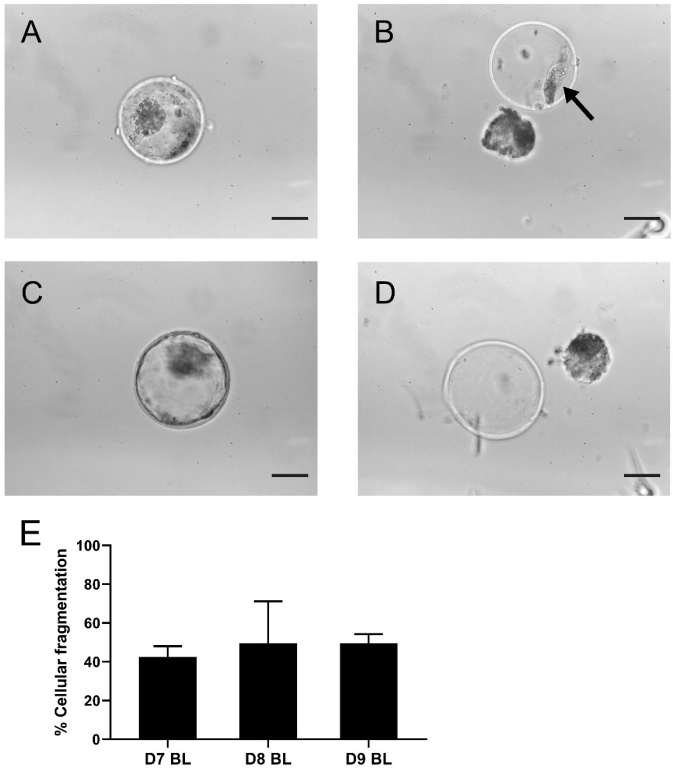

Figure 2. Cellular fragments in the zona pellucida of expanded blastocysts. Representative expanded blastocyst with cellular fragmentation before (A) and after (B) mechanically induced hatching. Representative expanded blastocyst without cellular fragments before (C) and after (D) mechanically induced hatching. Arrow indicates cell fragments. (E) Graph indicating percentages of blastocysts with cellular fragments in the zona pellucida after 7, 8, 9 days of in vitro culture. Error bars indicate standard deviation of three biological replicates. Scale bar = 50µm. D=day. BL=blastocyst.

Interestingly, we noticed that a mean of 37.4% of the extruded cells were TUNEL negative and contained morphologically normal nuclei as observed after DAPI staining (Figure 3A and Supplementary Table 3), indicating that a significant number of cells were extruded before apoptosis was initiated.

Since the cytoskeletal architecture plays a role as sensor and mediator of apoptosis (Desouza *et al.* , 2012), we reasoned the actin cytoskeleton presents in cellular fragments. We therefore analyzed the occurrence of actin cytoskeletal elements using phalloidin staining. We observed large phalloidin positive areas in fragmented cells of 10 day 9 blastocysts (Figure 3A; Supplementary Table 3),

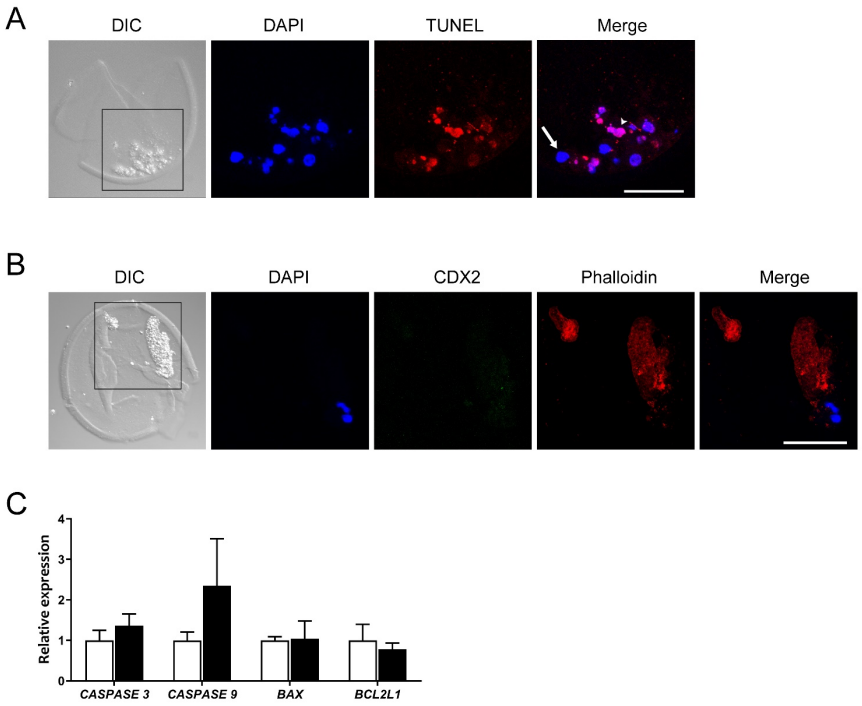

Figure 3. CDX2 and Phalloidin immunofluorescent staining, and apoptosis related gene expression in cellular fragments in the perivitelline space of a day 9 bovine blastocyst. (A) TUNEL positive (red, arrowhead) and negative cells (arrow) are indicated in a day 9 blastocyst. Blue represents DAPI staining. (B) CDX2 and Phalloidin staining of cellular fragments in a day 9 blastocyst. Black boxes in A and B indicate the areas presented in the right at higher magnification. Scale bar = 50µm. (C) Relative expression of apoptosis-related genes -in day 9 blastocysts (white bars) versus fragmented cells (black bars) as determined by qRT-PCR. Error bars indicate standard deviation of three biological replicates. DIC= differential interference contrast.

which further confirmed that fragmented cells were undergoing apoptotic processes. To examine whether the fragmented cells originated from the trophectoderm, cells were immunostained for CDX2 expression together with phalloidin. No CDX2 expression was detected in fragmented cells, including fragmented cells with an intact nucleus (Figure 3B). Together, these data suggest that either the cells were extruded by embryos before the differentiation of trophectoderm, or that trophectoderm cells rapidly lost CDX2 expression after exclusion from the embryo.

To evaluate the difference in apoptosis-related pathways between blastocysts and extruded cells of day 9 blastocysts, we next performed qRT-PCR to determine expression of genes in the caspase and Bcl-2 families (Brentnall *et al.* , 2013). Expression of *RPL15*, *SDHA* and *YWHAZ* was used as a reference for

quantification, and expression of these genes followed similar patterns in samples of blastocysts and extruded cells (data not shown). In contrast to expectations, the expression of caspase family genes was not statistically different between extruded cells and blastocysts (P>0.17 for *CASPASE 3* expression and P>0.11 for *CASPASE 9* expression). In addition, the expression levels of *BAX* (pro-apoptotic regulator) and *BCL2L1* (anti-apoptotic regulator) were similar in blastocysts and extruded cells (Figure 3C).

Blastocyst quality comparison

In order to determine whether the presence of cells in the perivitelline space is an indicator of reduced blastocyst quality, we compared the quality of a total number of 25 of day 8 blastocysts with and without cellular fragmentation using invasive methods.

To simultaneously investigate apoptosis and the ratio of ICM to trophectoderm cells at the single blastocyst level, we performed TUNEL staining combined with immunofluorescence staining for CDX2 (trophectoderm biomarker) and DAPI staining to label all nuclei (Figure 4A). The percentages of trophectoderm cells were similar between blastocysts with and without cells/cellular fragments in the perivitelline space, 64.6% and 67.0% CDX2 positive cells respectively (Figure 4B-D). A small but similar proportion of TUNEL positive cells was detected in blastocysts with (6.5%) and without (4.5%) fragmented cells (Figure 4E-F). TUNEL positive cells were also detected in presumptive ICM cells (CDX2 negative; Supplementary Tables 4, 5). Nevertheless, a similar and low percentage of TUNEL positive cells was found in presumptive ICM cells in blastocysts with (4.6%) and without (5.5%) cellular fragmentation (Figure 4G-H).

We further examined the expression of *CDX2* and *SOX2* (ICM biomarker) and apoptosis regulator genes in day 8 blastocysts. In agreement with the TUNEL/combined immunofluorescence results, there were no significant differences in the levels of *CDX2*, *SOX2*, *CASPASE 3*, *CASPASE 9*, *BAX* and *BCL2L1* expression between blastocysts with and without cellular fragmentation (Figure 4I).

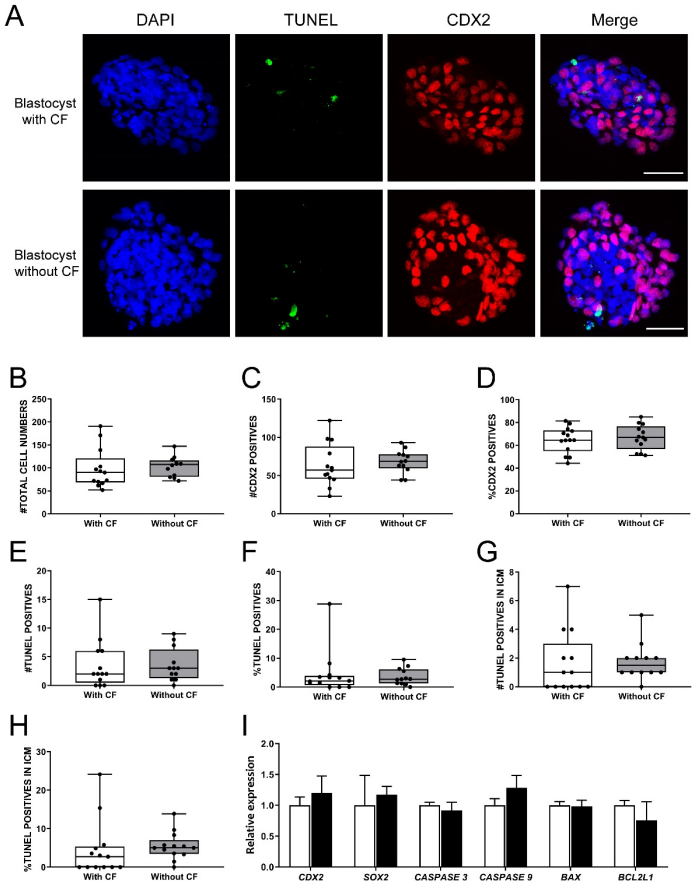

Figure 4. Frequency of apoptosis and ICM to trophectoderm ratio comparison between expanded bovine blastocysts with and without cellular fragments. (A) TUNEL (green) and CDX2 (red) immunofluorescence of day 8 blastocysts with and without cellular fragments. Scale bar = 50µm. Box-whisker plots of total cell number (B), CDX2 positive cells (C), percentage of CDX2 positive cells (D), total TUNEL positive cell number (E), percentage of TUNEL positive cells (F), TUNEL positive cell number in inner cell mass (ICM) (G), percentage of TUNEL positive cell number in ICM (H) in blastocysts with cellular fragments (white) or in blastocyst without (grey) fragmented cells in the perivitelline space. (I) Relative expression of genes in day 8 blastocysts with (white bars) or without (black bars) fragmented cells, as determined by qRT-PCR. Error bars indicate standard deviation of three biological replicates. BL=blastocyst. CF=cellular fragmentation.

Discussion

Despite being used in clinical practice for decades, embryo evaluation prior to transfer is a challenging and subjective procedure. The presence of cellular

fragments in the perivitelline space can be identified by clinicians, and is an important empirical criterion of embryo quality (Van Soom *et al.*, 2003). However, our data indicate that the presence of extruded or fragmented cells is common in expanded blastocysts and is not a reliable indicator of blastocyst quality.

Although cellular fragments can be often observed in the perivitelline space of cleavage stage embryos, their presence in the same location around expanded blastocysts is less easy to confirm by regular stereomicroscopy. To identify their presence in expanded blastocysts, we mechanically separated zonae pellucidae and embryos, which allowed examination of the cells detached from the embryo and attached to the zona pellucida. Using electron microscopy, several groups have previously identified fragmented cells or 'debris' in the perivitelline space (Fair *et al.* , 2001, Rizos *et al.* , 2002, Vajta *et al.* , 1997), but further examination of the cells was not possible.

Recently, it has been reported that cell fragments contain chromosomal material, possibly resulting from encapsulated micronuclei (Daughtry *et al.*, 2019). Indeed, we detected that more than half of cell fragments were DAPI positive and most of these DAPI positive cells were positive for TUNEL in day 9 blastocysts; nevertheless, we still found more than one third of cell fragments to be TUNEL negative.

In bovine embryos, cellular fragmentation has only been observed after the 8-cell stage, typically from the morula stage onwards (Gjorret *et al.* , 2003, Van Soom *et al.*, 2003). Similarly, apoptosis is also first observed after the 8-cell stage in bovine embryos (Byrne *et al.* , 1999, Gjorret *et al.*, 2003), coinciding with activation of the embryonic genome. Indeed, we found no CDX2 expression in the cellular fragments and there was no difference in the percentages of blastocysts with cellular fragments within the zona pellucida between days 7, 8 and 9 blastocysts, indicating that the cells were excluded from the embryo before the blastocyst stage. Possibly, embryos assess the genomic integrity of cells at around the time of embryonic genome activation, and extrusion and fragmentation of cells with chromosomal errors is initiated at this time. Alternatively, the cellular fragments observed at the blastocyst stage result from the progressive degeneration of cells excluded prior to blastocyst formation. This may explain why the majority of cellular fragments were TUNEL positive, i.e. programmed cell death may have started after cell exclusion. Removal of cells by programmed cell death within the developing embryos would mainly affect the cell that later form the fetus, i.e. the ICM (Leidenfrost *et al.* , 2011).

Interestingly, the detected mRNA levels in the cell fragments indicate that mRNA was not rapidly degraded. Indeed, the appearance of nuclear material within the fragments, as visualized using DAPI staining, suggested many nuclei were intact. In addition, the levels of caspase gene expression were not increased above those observed in the embryos themselves. These results indicate that not every extruded cell or cell fragment had undergone apoptosis, or that a portion of cellular fragments were at an early stage of apoptosis.

The technique of qRT-PCR does not allow determination of caspase protein activity, is partly dependent on post translational modification (Parrish *et al.* , 2013). Caspase mRNA can however be used as supplementary evidence of apoptosis (Krishnan *et al.* , 2005, Zhang *et al.* , 2019). Moreover, consistent with caspase gene expression, we did not find any significant differences in *BAX* (pro-apoptotic) and *BCL2L1* (anti-apoptotic) expression between day 9 blastocysts and day 9 zonae pellucidae with cellular fragments, or day 8 blastocysts with and without cellular fragments.

Generally, the presence of cellular fragments in the perivitelline space is considered as an indicator of poor embryo quality (Chi *et al.* , 2011, Jurisicova *et al.* , 1998, Maurer *et al.* , 2015), although it has also been proposed that low levels of fragmentation have no negative impact on implantation and pregnancy rates (Alikani *et al.*, 1999). In our study, there was no significant difference in embryo quality between day 8 blastocysts with cellular fragments and blastocysts without. Since in bovine IVF an average of only 30-40% of the embryos reach the blastocyst stage, it is possible that the embryos with high percentages of chromosomally abnormal cells were already arrested during early embryonic development, and the blastocysts we collected were of relatively high quality. Indeed, few TUNEL positive cell were detected in the blastocysts we collected.

To conclude, the presence of cellular fragments in the perivitelline space is common in expanded blastocysts. A limitation of this study is that even blastocysts with good morphology will not necessarily implant and give rise to healthy offspring. Blastocyst morphology is however a criterion used in practice to select or prioritize embryos for transfer. Although the most convincing demonstration of bovine blastocyst quality, i.e. birth of a healthy calf, has not been examined, we conclude that there is no correlation between the presence of cellular fragments in the perivitelline space and blastocyst quality.

Author Contributions

BY, HT, TS and BR conceived and designed the experiments. BY, HT and BR performed the experiments and collected the data. BY analysed the data. BR contributed the reagents, materials, and analysis tools. BY, TS and BR wrote the manuscript. All authors read and approved the manuscript.

Ackknowledge

We thank Arend Rijneveld and Christine Oei for assistance with oocyte recovery.

Supplementals

Supplemental figures and tables in this chapter are available at *Frontiers in cell and developmental biology* (https://www.frontiersin.org/articles/10.3389/fcell.2020.616801/full)

References

Alikani M, Cohen J, Tomkin G, Garrisi GJ, Mack C, Scott RT. Human embryo fragmentation in vitro and its implications for pregnancy and implantation. *Fertil Steril* 1999;**71**:836-842.

Armstrong S, Bhide P, Jordan V, Pacey A, Marjoribanks J, Farquhar C. Time-lapse systems for embryo incubation and assessment in assisted reproduction. *The Cochrane database of systematic reviews* 2019;**5**:Cd011320.

Balaban B, Yakin K, Urman B. Randomized comparison of two different blastocyst grading systems. *Fertil Steril* 2006;**85**:559-563.

Baxter Bendus AE, Mayer JF, Shipley SK, Catherino WH. Interobserver and intraobserver variation in day 3 embryo grading. *Fertil Steril* 2006;**86**:1608-1615.

Bormann CL, Kanakasabapathy MK, Thirumalaraju P, Gupta R, Pooniwala R, Kandula H, Hariton E, Souter I, Dimitriadis I, Ramirez LB *et al.* Performance of a deep learning based neural network in the selection of human blastocysts for implantation. *eLife* 2020;**9**.

Brentnall M, Rodriguez-Menocal L, De Guevara RL, Cepero E, Boise LH. Caspase-9, caspase-3 and caspase-7 have distinct roles during intrinsic apoptosis. *BMC cell biology* 2013;**14**:32.

Brinkhof B, van Tol HT, Groot Koerkamp MJ, Riemers FM, SG IJ, Mashayekhi K, Haagsman HP, Roelen BA. A mRNA landscape of bovine embryos after standard and MAPK-inhibited culture conditions: a comparative analysis. *BMC Genomics* 2015;**16**:277.

Brinkhof B, van Tol HT, Groot Koerkamp MJ, Wubbolts RW, Haagsman HP, Roelen BA. Characterization of bovine embryos cultured under conditions appropriate for sustaining human naive pluripotency. *PLoS One* 2017;**12**:e0172920.

Byrne AT, Southgate J, Brison DR, Leese HJ. Analysis of apoptosis in the preimplantation bovine embryo using TUNEL. *Journal of reproduction and fertility* 1999;**117**:97-105.

Chi HJ, Koo JJ, Choi SY, Jeong HJ, Roh SI. Fragmentation of embryos is associated with both necrosis and apoptosis. *Fertil Steril* 2011;**96**:187-192.

Cornelisse S, Zagers M, Kostova E, Fleischer K, van Wely M, Mastenbroek S. Preimplantation genetic testing for aneuploidies (abnormal number of chromosomes) in in vitro fertilisation. *The Cochrane database of systematic reviews* 2020;**9**:Cd005291.

Daughtry BL, Rosenkrantz JL, Lazar NH, Fei SS, Redmayne N, Torkenczy KA, Adey A, Yan M, Gao L, Park B *et al.* Single-cell sequencing of primate preimplantation embryos reveals chromosome elimination via cellular fragmentation and blastomere exclusion. *Genome research* 2019;**29**:367-382.

Desai NN, Goldstein J, Rowland DY, Goldfarb JM. Morphological evaluation of human embryos and derivation of an embryo quality scoring system specific for day 3 embryos: a preliminary study. *Hum Reprod* 2000;**15**:2190-2196.

Desouza M, Gunning PW, Stehn JR. The actin cytoskeleton as a sensor and mediator of apoptosis. *Bioarchitecture* 2012;**2**:75-87.

Fair T, Lonergan P, Dinnyes A, Cottell DC, Hyttel P, Ward FA, Boland MP. Ultrastructure of bovine blastocysts following cryopreservation: effect of method of blastocyst production. *Molecular reproduction and development* 2001;**58**:186-195.

Farin PW, Britt JH, Shaw DW, Slenning BD. Agreement among evaluators of bovine embryos produced in vivo or in vitro. *Theriogenology* 1995;**44**:339-349.

Gjorret JO, Knijn HM, Dieleman SJ, Avery B, Larsson LI, Maddox-Hyttel P. Chronology of apoptosis in bovine embryos produced in vivo and in vitro. *Biology of reproduction* 2003;**69**:1193-1200.

Gorodeckaja J, Neumann S, McCollin A, Ottolini CS, Wang J, Ahuja K, Handyside A, Summers M. High implantation and clinical pregnancy rates with single vitrified-warmed blastocyst transfer and optional aneuploidy testing for all patients. *Hum Fertil (Camb)* 2019:1-12.

Haouzi D, Hamamah S. Pertinence of apoptosis markers for the improvement of in vitro fertilization (IVF). *Current medicinal chemistry* 2009;**16**:1905-1916.

Jurisicova A, Latham KE, Casper RF, Casper RF, Varmuza SL. Expression and regulation of genes associated with cell death during murine preimplantation embryo development. *Molecular reproduction and development* 1998;**51**:243-253.

Kalfoglou AL, Scott J, Hudson K. PGD patients' and providers' attitudes to the use and regulation of preimplantation genetic diagnosis. *Reprod Biomed Online* 2005;**11**:486-496.

Kovacs P. Embryo selection: the role of time-lapse monitoring. *Reproductive biology and endocrinology : RB&E* 2014;**12**:124.

Krishnan S, Kiang JG, Fisher CU, Nambiar MP, Nguyen HT, Kyttaris VC, Chowdhury B, Rus V, Tsokos GC. Increased caspase-3 expression and activity contribute to reduced CD3zeta expression in systemic lupus erythematosus T cells. *Journal of immunology (Baltimore, Md : 1950)* 2005;**175**:3417-3423.

Leidenfrost S, Boelhauve M, Reichenbach M, Güngör T, Reichenbach HD, Sinowatz F, Wolf E, Habermann FA. Cell arrest and cell death in mammalian preimplantation development: lessons from the bovine model. *PloS one* 2011;**6**:e22121.

Leppens G, Gardner DK, Sakkas D. Co-culture of 1-cell outbred mouse embryos on bovine kidney epithelial cells: effect on development, glycolytic activity, inner cell mass:trophectoderm ratios and viability. *Hum Reprod* 1996;**11**:598-603.

Lindner GM, Wright RW, Jr. Bovine embryo morphology and evaluation. *Theriogenology* 1983;**20**:407-416.

Matsuura K, Hayashi N, Takiue C, Hirata R, Habara T, Naruse K. Blastocyst quality scoring based on morphologic grading correlates with cell number. *Fertil Steril* 2010;**94**:1135-1137.

Maurer M, Ebner T, Puchner M, Mayer RB, Shebl O, Oppelt P, Duba HC. Chromosomal Aneuploidies and Early Embryonic Developmental Arrest. *International journal of fertility & sterility* 2015;**9**:346-353.

Neuber E, Luetjens CM, Chan AW, Schatten GP. Analysis of DNA fragmentation of in vitro cultured bovine blastocysts using TUNEL. *Theriogenology* 2002;**57**:2193-2202.

Niederberger C, Pellicer A, Cohen J, Gardner DK, Palermo GD, O'Neill CL, Chow S, Rosenwaks Z, Cobo A, Swain JE *et al.* Forty years of IVF. *Fertil Steril* 2018;**110**:185-324 e185.

Papanikolaou EG, D'Haeseleer E, Verheyen G, Van de Velde H, Camus M, Van Steirteghem A, Devroey P, Tournaye H. Live birth rate is significantly higher after blastocyst transfer than after cleavage-stage embryo transfer when at least four embryos are available on day 3 of embryo culture. A randomized prospective study. *Hum Reprod* 2005;**20**:3198-3203.

Parrish AB, Freel CD, Kornbluth S. Cellular mechanisms controlling caspase activation and function. *Cold Spring Harbor perspectives in biology* 2013;**5**.

Racowsky C, Vernon M, Mayer J, Ball GD, Behr B, Pomeroy KO, Wininger D, Gibbons W, Conaghan J, Stern JE. Standardization of grading embryo morphology. *J Assist Reprod Genet* 2010;**27**:437-439.

Rizos D, Fair T, Papadopoulos S, Boland MP, Lonergan P. Developmental, qualitative, and ultrastructural differences between ovine and bovine embryos produced in vivo or in vitro. *Molecular reproduction and development* 2002;**62**:320-327.

Sciorio R, Thong KJ, Pickering SJ. Increased pregnancy outcome after day 5 versus day 6 transfers of human vitrified-warmed blastocysts. *Zygote* 2019;**27**:279-284.

Sermon K, Capalbo A, Cohen J, Coonen E, De Rycke M, De Vos A, Delhanty J, Fiorentino F, Gleicher N, Griesinger G *et al.* The why, the how and the when of PGS 2.0: current practices and expert opinions of fertility specialists, molecular biologists, and embryologists. *Molecular human reproduction* 2016;**22**:845-857.

Sirard MA. 40 years of bovine IVF in the new genomic selection context. *Reproduction* 2018;**156**:R1-R7.

Vajta G, Hyttel P, Callesen H. Morphological changes of in-vitro-produced bovine blastocysts after vitrification, in-straw direct rehydration, and culture. *Molecular reproduction and development* 1997;**48**:9-17.

Van Soom A, Mateusen B, Leroy J, De Kruif A. Assessment of mammalian embryo quality: what can we learn from embryo morphology? *Reprod Biomed Online* 2003;**7**:664-670.

Van Soom A, Vanroose G, de Kruif A. Blastocyst evaluation by means of differential staining: a practical approach. *Reprod Domest Anim* 2001;**36**:29-35.

van Soom A, Ysebaert MT, de Kruif A. Relationship between timing of development, morula morphology, and cell allocation to inner cell mass and trophectoderm in in vitro-produced bovine embryos. *Molecular reproduction and development* 1997;**47**:47-56.

Zhang X, Qin Y, Pan Z, Li M, Liu X, Chen X, Qu G, Zhou L, Xu M, Zheng Q *et al.* Cannabidiol Induces Cell Cycle Arrest and Cell Apoptosis in Human Gastric Cancer SGC-7901 Cells. *Biomolecules* 2019;**9**.

Chapter 6

General discussion

The human body is composed of around 300 different types of cell, each with a specialized shape, structure and function. All of these unique cell types have however developed from a single precursor cell, the fertilized egg or zygote. The zygote is considered to be a totipotent cell since it not only gives rise to all of the different cell types within our body, but also generates extraembryonic structures such as the fetal parts of the placenta and the umbilical cord. To generate billions of different cells from that one single progenitor cell, specific combinations of genes must be expressed within the daughter cells at the right time and place, and in the right concentration, via a process known as gene expression regulation. This process essentially controls all of the events that occur during oocyte maturation and early embryo development. Knowledge of how gene expression is regulated during embryonic development has come primarily from studies in model organisms such as *Drosophila*, *Xenopus* and the mouse. These studies have revealed both commonalities and differences in the regulation of gene expression. It has also become clear that for some aspects of embryonic gene expression regulation in the mouse is not representative of all mammalian species. In this thesis, gene expression regulation has been studied in bovine oocytes and embryos.

During late meiosis and early embryo development, changes in gene expression in oocytes and embryos are mostly dependent on post-transcriptional regulation of maternal mRNA. Since the length of the poly(A) tail is closely related to mRNA stability and translatability, gene expression at these stages is mainly regulated by controlling poly(A) tail length of maternal mRNAs. To examine gene expression levels, quantitative reverse transcription PCR (qRT-PCR) is often used to measure (maternal) mRNA abundance in oocytes and early embryos. However, most maternal mRNAs are not translated directly after synthesis, but are instead stored for later use. It is, therefore, possible that qRT-PCR in oocytes and zygotes may not reflect translation levels but simply give an overall idea of maternal mRNA stores. Furthermore, different methods for performing reverse transcription may lead to different results.

In **chapter 2**, complementary DNA (cDNA) was synthesized from bovine oocytes by two different reverse transcription strategies, (i) using random primers and (ii) oligo(dT) primers. In theory, oligo(dT) primers should only synthesize cDNA from mRNA with a poly(A) tail. For accurate gene expression measurement, data normalization is essential and this depends in part on the primers used for cDNA synthesis (Lovén *et al.* , 2012). In this thesis, the reference genes best suited for normalization of mRNA abundance in bovine oocytes were

first investigated using the GeNorm software package. The combination of *RPL15*, *SDHA* and *ACTB* was suitable for normalization in cDNA samples synthesized using random primers, whereas *HPRT1*, *YWHAZ* and *ACTB* was a better combination for cDNA samples synthesized using oligo(dT) primers. Reference gene selection for transcriptomic studies in oocytes has been investigated in various mammalian species, including the mouse, rabbit and pig (Kuijk *et al.*, 2007, Mamo *et al.*, 2007, Mamo *et al.* , 2008). However, the choice of reverse transcription priming strategy has been less well investigated. Since different methods for reverse transcription affect the optimal combination of reference genes for normalization, it is important to ensure that the same method for reverse transcription is used when deciding to select the reference genes from previous studies for normalization.

Cytoplasmic polyadenylation is regarded as the major mRNA regulator for translational control during oocyte maturation (Cui *et al.* , 2013, Radford *et al.* , 2008, Reyes and Ross, 2016). Therefore, regulation of the poly (A) tail of *GAPDH*, *CCNB1*, *CCNB2* and *HPRT1* during oocyte maturation was examined in **chapter 2**. Surprisingly, a decrease in poly(A) tail length was observed between GV and MII oocyte stages for *CCNB1*, *CCNB2* and *HPRT1*. By contrast, it has been reported that the length of the *CCNB2* poly(A) tail increases in *Xenopus* oocytes between these stages (Mendez and Richter, 2001) and the poly(A) tail of *CCNB1* is elongated in mouse, *Xenopus* and zebrafish oocytes (Kotani *et al.*, 2013). It is unknown whether these differences are because of different methods used for poly(A) tail detection, or because of differences in maternal mRNA regulation between species. Therefore, to understand the regulation of oocyte gene expression it is necessary to examine poly(A) tail changes during oocyte maturation in different species. Genome-wide analysis of mRNA poly(A) length as recently described (Yang *et al.*, 2020) will help to understand how poly(A) tail length is regulated for different genes.

In addition, in **chapter 2**, gene expression patterns during oocyte maturation were compared for cDNA samples synthesized using random primers and oligo(dT) primers. Indeed, the relative expression of *CCNB2* and *GAPDH* was different depending on whether cDNA from GV to MII oocytes was synthesized using random or oligo(dT) primers. Understandably, cDNA samples synthesized using either random or oligo(dT) primers cannot reflect translation levels in oocytes. It has been reported that the CCNB1 protein level increases from the GV to the MII stage and that the level of CCNB2 increases from GV to MI in bovine oocytes (Uzbekova *et al.* , 2008, Wu *et al.*, 1997). Interestingly, the gene

expression levels for *CCNB1* and *CCNB2* were stable from GV to MII and from GV to MI, respectively, in bovine oocytes (**chapter 2)**. In theory, the expression patterns in cDNA samples synthesized using random primers should indicate how the total amount of maternal mRNA changes during oocyte maturation. These expression patterns are not expected to change dramatically, since most maternal mRNA is degraded during the maternal to zygotic transition. Indeed, expression of every gene detected in **chapter 2** was very stable from GV to MII stage in oocytes. By definition, gene expression is the process of producing a gene product by transcribing information from the DNA code for that gene. In oocytes and early embryos, however, most gene information is not directly translated after transcription. One could argue that 'gene expression' in oocytes and early embryos is misleading because the information from that gene is stored as a form of maternal mRNA, waiting for the right moment to be translated.

During maternal to zygotic transition, maternal transcripts are largely degraded and embryos start to use their own genetic information to generate gene products. Not all the genes from the zygotic genome are expressed all the time. Embryonic cells coordinate gene activity and expression at the DNA level via epigenetic modifications. X chromosome inactivation (XCI) involves a series of epigenetic events designed to silence one of the two X chromosomes in female cells, a process intiatied during embryonic development.

In **chapter 3**, the timing of XCI in bovine embryos was examined by various methods: qRT-PCR, fluorescence in situ hybridization (FISH) and immunofluoresccence. The expression of *XIST* and the accumulation of *XIST* RNA were first deteced at around the morula stage in bovine embryos, which is different from the 4-cell stage in mouse and the 8-cell stage in human and rabbit embryos (Briggs *et al.* , 2015b, Okamoto *et al.*, 2011, van den Berg *et al.*, 2011a). Another epigenetic modification, trimethylation of lysine 27 of histone 3 (H3K27me3) was examined by immunofluorescence in **chapter 3**. This modification is involved in repression of nearby genes (Cai *et al.* , 2021). Indeed, strong expression of H3K27me3 was detected in a presumed X chromosome of day 7 bovine blastocysts, and was preceeded by *XIST* RNA accumulation. Interestingly, microarray data revealed that only 127 out of 930 X-linked genes were down-regulated in bovine embryos as they developed from morulae into blastocysts. This will in part be due to the fact that the microarray data were not sex-selected, but it will be interesting to observe how X-chromosome inactivation develops in gastrulation embryos. Therefore, future work could focus on which DNA sequences are modified by H3K27me3 after initiation of XCI during

embryonic development using chromatin immunoprecipitation. Together with gene expression analysis, it would be fascinating to know which genes escape from silencing despite H3K27me3 modification, and to understand the mechanisms that prevent the active X chromosome from inactivation.

Along with *XIST*, other candidate moelcules have been proposed to be involved in the process of XCI in the mouse (da Rocha and Heard, 2017, Pintacuda *et al.* , 2017). Gene expression for *HPRT1*, *EED*, *EZH2*, *HNRNPK*, *HNRNPU*, *RING1* and *JPX* in GV bovine oocytes and embryos up to the blastocyst stage was also determined in **chapter 3**. Interestingly, unlike expression of *XIST*, the expression of *EZH2*, *HNRNPU*, *RING1* and *JPX* was not up-regulated between the 8-cell embryo and morula stage, suggesting that the function of these candidates is not conserved across species. Therefore, it is necessary to look for other effectors of XCI that are more widely conserved.

One of the big mysteries in XCI research is how the active X chromosomes is protected from *XIST* activity. Compelling evidence suggests that repressors of *XIST* are encoded by an autosome (Migeon, 2019, 2021, Migeon *et al.* , 2017). This hypothesis is supported by the observation that 47, XXX diploid human cells have only a single active X chromosome, whereas most human triploid cells have two active X chromosomes (Migeon *et al.*, 2017). In this case, an extra copy of the autosome is possibly responsible to prevent inactivation of two X chromosomes. It has been suggested that the potential *XIST* repressors are located on chromosome 19 in man, which is similar to bovine chromosome 7. These chromosome regions harbor several candidate genes that might protect the active X from methylation, among which are *DNMT1*, *UHRF1*, *SAFB* and *SAFB2*. Therefore, the expression of *DNMT1* and *UHRF1* was examined in female and male bovine embryos between the 4-cell stage and day 8 blastocysts. Opposite to the expression of *XIST* (Figure 1A), the expression of *DNMT1* and *UHRF1* was significantly down-regulated between the 8-cell and morula stages (Figure 1B and 1C). This suggests that the expression of *XIST* might be suppressed by DNMT1 and/or UHRF1 before the morula stage, identifying DNMT1 and UHRF1 as candidate *XIST* repressors. To demonstrate that DNMT1 and UHRF1 are involved in *XIST* suppression, knockdown or knockout experiments need to be done in future studies. Interestingly, a down-regulation of *DNMT1* and *UHRF1* expression from 8-cell stage embryos to morulae was observed in both female and male embryos. This suggests that there must be other candidates involved in *XIST* suppression, at least in male embryos.

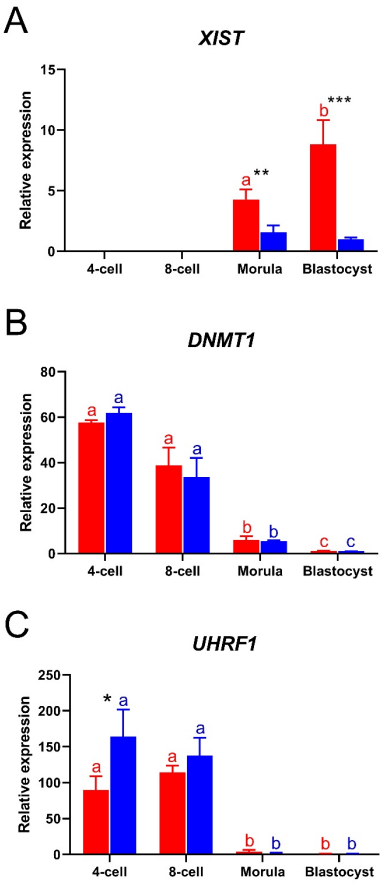

Figure 1. The relative expression of candidate *XIST* repressor genes in female (red bars) and male (blue bars) bovine embryos from 4-cell stage to day 8 blastocysts, as determined by quantitative RT-PCR. (A) *XIST*, (B) *DNMT1*, (C) *UHRF1*. Embryos were produced by fertilization with sex-sorted sperm. Relative expression from male blastocysts set at 1. Significant differences between females and males are indicated by * ($p < 0.05$), ** ($p < 0.01$) and *** ($p < 0.005$). Significant differences among embryos with the same gender are indicated by different letters with the same color ($p < 0.05$). Error bars indicate standard deviations of three independent biological replicates.

After several cycles of cell division, the embryo starts its first cell lineage determination when the blastomeres compact to form a morula. In general, the outer cells of the morula differentiate into the trophectoderm (TE) and the inner cells give rise to the inner cell mass (ICM). Differentiation is primarily driven by different combinations of transcription factors and the cells at these early stages are still very flexible with regard to their fate differentiation. Multiple key transcription factors in determining the first lineage segregation have been identified, for instance a crucial role for CDX2 has been identified for TE cell specification. However, how the key transcription factors are regulated during embryonic development is less well understood.

It has been reported that the Hippo/YAP signaling pathway is crucial for segregation of TE and ICM during mouse preimplantation development

(Nishioka *et al.*, 2009, Wu and Guan, 2021). However, the role of Hippo/YAP in cell lineage determination in other mammalian species has been less well studied. Recently, lysophosphatidic acid (LPA) has been demonstrated to activate YAP expression by inducing YAP dephosphorylation (Moroishi *et al.*, 2015, Yasuda *et al.* , 2019). To understand the role of YAP signaling in lineage segregation in bovine embryos, embryos were cultured in the presence of LPA and expression of Hippo/YAP signaling pathway candidates was examined in **chapter 4**. Indeed, YAP protein expression was increased in day 6 and 8 embryos cultured in the presence of LPA, compared to embryos cultured in control medium. This indicates that LPA can stimulate YAP expression in bovine embryos. Even though higher expression of CDX2 was observed only in day 8 blastocysts after LPA stimulation, the blastocyst percentage at day 6 was almost doubled by the addition of LPA compared to embryos cultured without LPA. Moreover, the number of CDX2 expressing cells was higher in day 6 blastocysts than in day 6 morulae. Overall, we showed that LPA stimulates CDX2 expression through the Hippo/YAP signaling pathway, indicating that the mechanisms of lineage segregation in bovine embryos are different to those of mouse embryos.

In **chapter 4**, LPA accelerated bovine blastocyst formation without changing the cell lineage constitution. Because in-vitro embryo culture conditions are different to in vivo conditions, blastocyst percentage and quality are far from optimal after in-vitro culture. Therefore, LPA could potentially be used to reduce in vitro culture time. Nevertheless, implantation rate and pregnancy rate, as well as post-transfer viability and proper fetal development need to be examined before LPA is used for commercial IVF embryo production.

After LPA exposure, YAP is dephosphorylated and transported to the nucleus to induce *CDX2* expression. It is, therefore, possible that the higher percentage of blastocyst development is due to more embryonic cells starting to express CDX2 to initiate TE differentiation after LPA exposure. However, the number and location of presumptive ICM cells were not altered after culture in the presence of LPA. Moreover, the expression patterns of *CDX2*, *SOX2* and *OCT4* were not changed by LPA stimulation, These results suggest that there are other mechnisms that maintain *CDX2* repression in the inner cells of morulae, where position or polarity of cells within the embryo could be the most importnat factor for the first cell determination (Jedrusik *et al.* , 2008). It is unknown whether *CDX2* can be expressed in the outer cells of morulae in the absence of YAP. Therefore, to better understand the importance of the Hippo/YAP signaling pathway in *CDX2* expression, knockdown or knockout of *YAP* should be

performed in embryos in future studies.

To ensure data reliability and stability in this thesis, bovine embryos with good quality according to the IETS manual (Bo and Mapletoft, 2013, Stringfellow *et al.* , 2010) were collected. Selecting embryos with good quality prior to transfer is also important for successful human IVF. One of most commonly used parameters for embryo quality evaluation is the presence of cellular fragments in the perivitelline space, which is considered to be an indicator of "fair" or "poor" embryos (Van Soom *et al.*, 2003). However, cellular fragments in the perivitelline space are very difficult to identify at the blastocyst stage, because the perivitelline space becomes small after blastocyst expansion. Thus, it is not known that whether cellular fragments in the perivitelline space are a predictor of embryo quality at the blastocyst stage.

To investigate any relationship with the integrity of blastocysts, the presence of cellular fragments in the perivitelline space was examined after mechanical hatching of blastocysts from their zonae pellucida in **chapter 5**. Surprisingly, almost 50% of expanded blastocysts contained cellular fragments in their perivitelline space. Such a high proportion of blastocysts with cellular fragments may be due to degradation of mixoploid or aneuploid cells during *in vitro* culture. Indeed, it has been reported that most bovine blastocysts produced *in vitro* contain mixoploid cells (Viuff *et al.* , 1999b). It is s not known whether *in vivo* produced blastocysts also have cellular fragments within the perivitelline space.

Quality of blastocysts with or without fragmented cells in the perivitelline space were compared on the basis of total cell number, pluripotent cell number and apoptosis levels in **chapter 5**. Overall, there was no difference in quality of blastocysts with or without fragmented cells on the basis of these parameters. It is possible that embryos can tolerate a certain level of abnormal cells and exclude/extrude them into the perivitelline space to maintain embryo viability and quality.

Precise regulation of gene expression ensures oocytes and embryos accomplish the dynamic events required for successful oocyte maturation and early embryo development. However, most studies of gene expression regulation have focused on the mouse. In this respect, we used the cow as an alternative mammalian model to study gene expression regulation during oocyte maturation and early embryo development. We described dynamic changes in gene expression and poly(A) tail length during bovine oocyte maturation and early embryo development. As a result of these changes, the reference genes most suitable for gene expression normalization are different when different reverse

transcription priming methods are employed. On the other hand, epigenetic alterations and differential regulation of transcription factors affect gene expression at the transcriptional level in embryos. One of the major epigenetic events-XCI, is initiated at morula stage in female bovine embryos. However, the initiation of XCI does not lead to complete down-regulation of all X-linked genes. The expression of the transcription factor CDX2 in bovine embryos is up regulated after exposure to LPA. But LPA stimulation does not change embryo constitution in terms of percentages of cells committed to one or another lineage. Overall, a better understanding of gene expression regulation during ocoyte maturation and early embryo development broadens our fundamental knowledge of mammalian embryonic development and will improve our understanding of the requirements for cell lineage determination and pluripotency, and the short and longer term consequences of epigenetic disturbances resulting from sub-optimal maternal health and nutrition or *in vitro* fertilization and embryo culture conditions.

References

Bo G, Mapletoft R. Evaluation and classification of bovine embryos. *Animal reproduction* 2013;**10**:344-348.

Briggs SF, Dominguez AA, Chavez SL, Reijo Pera RA. Single-Cell XIST Expression in Human Preimplantation Embryos and Newly Reprogrammed Female Induced Pluripotent Stem Cells. *Stem cells (Dayton, Ohio)* 2015;**33**:1771-1781.

Cai Y, Zhang Y, Loh YP, Tng JQ, Lim MC, Cao Z, Raju A, Lieberman Aiden E, Li S, Manikandan L *et al.* H3K27me3-rich genomic regions can function as silencers to repress gene expression via chromatin interactions. *Nature communications* 2021;**12**:719.

Cui J, Sartain CV, Pleiss JA, Wolfner MF. Cytoplasmic polyadenylation is a major mRNA regulator during oogenesis and egg activation in *Drosophila*. *Developmental biology* 2013;**383**:121-131.

da Rocha ST, Heard E. Novel players in X inactivation: insights into Xist-mediated gene silencing and chromosome conformation. *Nature structural & molecular biology* 2017;**24**:197-204.

Jedrusik A, Parfitt D-E, Guo G, Skamagki M, Grabarek JB, Johnson MH, Robson P, Zernicka-Goetz M. Role of Cdx2 and cell polarity in cell allocation and specification of trophectoderm and inner cell mass in the mouse embryo. *Genes & development* 2008;**22**:2692-2706.

Kotani T, Yasuda K, Ota R, Yamashita M. Cyclin B1 mRNA translation is temporally controlled through formation and disassembly of RNA granules. *The Journal of cell biology* 2013;**202**:1041-1055.

Kuijk EW, du Puy L, van Tol HT, Haagsman HP, Colenbrander B, Roelen BA. Validation of reference genes for quantitative RT-PCR studies in porcine oocytes and preimplantation embryos. *BMC developmental biology* 2007;**7**:58.

Lovén J, Orlando DA, Sigova AA, Lin CY, Rahl PB, Burge CB, Levens DL, Lee TI, Young RA. Revisiting global gene expression analysis. *Cell* 2012;**151**:476-482.

Mamo S, Gal AB, Bodo S, Dinnyes A. Quantitative evaluation and selection of reference genes in mouse oocytes and embryos cultured in vivo and in vitro. *BMC developmental biology* 2007;**7**:14.

Mamo S, Gal AB, Polgar Z, Dinnyes A. Expression profiles of the pluripotency marker gene POU5F1 and validation of reference genes in rabbit oocytes and preimplantation stage embryos. *BMC molecular biology* 2008;**9**:67.

Mendez R, Richter JD. Translational control by CPEB: a means to the end. *Nature reviews Molecular cell biology* 2001;**2**:521-529.

Migeon BR. The Non-random Location of Autosomal Genes That Participate in X Inactivation. *Frontiers in cell and developmental biology* 2019;**7**:144.

Migeon BR. Stochastic gene expression and chromosome interactions in protecting the human

active X from silencing by XIST. *Nucleus (Austin, Tex)* 2021;**12**:1-5.

Migeon BR, Beer MA, Bjornsson HT. Embryonic loss of human females with partial trisomy 19 identifies region critical for the single active X. *PloS one* 2017;**12**:e0170403.

Moroishi T, Park HW, Qin B, Chen Q, Meng Z, Plouffe SW, Taniguchi K, Yu FX, Karin M, Pan D *et al.* A YAP/TAZ-induced feedback mechanism regulates Hippo pathway homeostasis. *Genes & development* 2015;**29**:1271-1284.

Nishioka N, Inoue K, Adachi K, Kiyonari H, Ota M, Ralston A, Yabuta N, Hirahara S, Stephenson RO, Ogonuki N *et al.* The Hippo signaling pathway components Lats and Yap pattern Tead4 activity to distinguish mouse trophectoderm from inner cell mass. *Developmental cell* 2009;**16**:398-410.

Okamoto I, Patrat C, Thépot D, Peynot N, Fauque P, Daniel N, Diabangouaya P, Wolf JP, Renard JP, Duranthon V *et al.* Eutherian mammals use diverse strategies to initiate X-chromosome inactivation during development. *Nature* 2011;**472**:370-374.

Pintacuda G, Wei G, Roustan C, Kirmizitas BA, Solcan N, Cerase A, Castello A, Mohammed S, Moindrot B, Nesterova TB *et al.* hnRNPK Recruits PCGF3/5-PRC1 to the Xist RNA B-Repeat to Establish Polycomb-Mediated Chromosomal Silencing. *Mol Cell* 2017;**68**:955-969.e910.

Radford HE, Meijer HA, de Moor CH. Translational control by cytoplasmic polyadenylation in Xenopus oocytes. *Biochim Biophys Acta* 2008;**1779**:217-229.

Reyes JM, Ross PJ. Cytoplasmic polyadenylation in mammalian oocyte maturation. *Wiley interdisciplinary reviews RNA* 2016;**7**:71-89.

Stringfellow DA, Givens MD, Society IET. *Manual of the International Embryo Transfer Society: a procedural guide and general information for the use of embryo transfer technology emphasizing sanitary procedures*. 2010. The Society.

Uzbekova S, Arlot-Bonnemains Y, Dupont J, Dalbiès-Tran R, Papillier P, Pennetier S, Thélie A, Perreau C, Mermillod P, Prigent C *et al.* Spatio-temporal expression patterns of aurora kinases a, B, and C and cytoplasmic polyadenylation-element-binding protein in bovine oocytes during meiotic maturation. *Biology of reproduction* 2008;**78**:218-233.

van den Berg IM, Galjaard RJ, Laven JS, van Doorninck JH. XCI in preimplantation mouse and human embryos: first there is remodelling…. *Human genetics* 2011;**130**:203-215.

Van Soom A, Mateusen B, Leroy J, De Kruif A. Assessment of mammalian embryo quality: what can we learn from embryo morphology? *Reproductive biomedicine online* 2003;**7**:664-670.

Viuff D, Rickords L, Offenberg H, Hyttel P, Avery B, Greve T, Olsaker I, Williams JL, Callesen H, Thomsen PD. A high proportion of bovine blastocysts produced in vitro are mixoploid. *Biology of reproduction* 1999;**60**:1273-1278.

Wu B, Ignotz G, Currie WB, Yang X. Dynamics of maturation-promoting factor and its constituent proteins during in vitro maturation of bovine oocytes. *Biology of reproduction*

1997;**56**:253-259.

Wu Z, Guan KL. Hippo Signaling in Embryogenesis and Development. *Trends in biochemical sciences* 2021;**46**:51-63.

Yang F, Wang W, Cetinbas M, Sadreyev RI, Blower MD. Genome-wide analysis identifies cis-acting elements regulating mRNA polyadenylation and translation during vertebrate oocyte maturation. *RNA (New York, NY)* 2020;**26**:324-344.

Yasuda D, Kobayashi D, Akahoshi N, Ohto-Nakanishi T, Yoshioka K, Takuwa Y, Mizuno S, Takahashi S, Ishii S. Lysophosphatidic acid-induced YAP/TAZ activation promotes developmental angiogenesis by repressing Notch ligand Dll4. *The Journal of clinical investigation* 2019;**129**:4332-4349.

Chapter 7

Summary

English Summary

When an oocyte is successfully fertilized by a spermatozoon, the totipotent cell known as the zygote is formed and a new life begins. Through the process of mitosis, the zygote undergoes a series of rapid cell divisions to form a blastocyst. The outer cells of the blastocyst are required for implantation and give rise to part of the placenta, while the inside cells give rise to the yolk sac and the embryo proper, which will eventually become the fetus. In other words, billions of differentiated and specialized cells in our body originate from that single cell-zygote. To achieve this, specific combinations of genes and their products need to be expressed at the right time and place. Gene expression regulation is crucial for proper early embryo development. However, much of the detail of how gene expression is regulated during embryonic development, particularly in mammals such as man, are still unknown

The cow has several advantages as a model to study human reproduction. First, women and cows are both mono-ovulatory, and the duration of oocyte maturation and preimplantation development is very similar. Secondly, large numbers of bovine oocytes can be obtained from slaughterhouse ovaries and can be efficiently fertilized and cultured in vitro to the blastocyst stage.

Since oocytes and early embryos are transcriptionally silent from the germinal vesicle breakdown (GVBD) stage until zygotic genome activation, gene expression regulation in oocytes and early embryos is mainly achieved through post-transcriptional regulation of maternal mRNAs. The length of the poly(A) tail of maternal mRNAs is adapted before and after mRNA recruitment for translation. Reverse transcription using oligo(dT) primers is based on the presence of a poly(A) tail, whereas reverse transcription using random primers is not. Therefore, it is possible that different methods for reverse transcription result in different estimations of gene expression in oocytes. In **chapter 2**, samples from oocytes were split into two equal parts after RNA isolation, for reverse transcription using either random or oligo(dT) primers. The reference genes most suitable for normalization were *RPL15*, *SDHA* and *ACTB* when random primers were used for reverse transcription, whereas *HPRT1*, *YWHAZ* and *ACTB* were the optimal reference genes for normalization if cDNA samples had been synthesized using oligo(dT) primers. Moreover, measured gene expression levels for *CCNB2* and *GAPDH* were different during oocyte maturation when different methods for reverse transcription were used. To determine whether gene expression patterns are coordinated by regulation of mRNA poly(A) tail size during oocyte maturation, the size of the poly(A) tail was determined by sequencing. It was

found that the poly(A) tails of *GAPDH*, *CCNB1* and *CCNB2* were shorter in MII oocytes than GV oocytes.

During zygotic genome activation, maternal transcripts are largely degraded, and embryonic cells start to use their own genomes as the blueprint to generate gene products. Therefore, gene expression in embryonic cells is increasingly regulated at the transcription level and epigenetic changes are initiated. X-chromosome inactivation (XCI) is an epigenetic phenomenon that balances the dosage of X-linked gene products between XY males and XX females, and is initiated during early embryonic development. However, the timing of XCI and regulation of X-linked gene expression after XCI are different between species, even within the mammalians. To determine the timing of XCI initiation in cattle embryos, changes in the expression of XCI related genes were examined in oocytes from germinal vesicle (GV) oocytes up to embryos at the blastocyst stage **(chapter 3)**. The expression of the noncoding RNA, *XIST,* was significantly increased, but the expression of *HPRT1* was down-regulated from the 8-cell to the morula stages. Moreover, *XIST* RNA localization first observed in the nuclei of female morulae, whereas co-localization of *XIST* RNA and histone H3 lysine 27 trimethylation was first detected in female day 7 blastocysts. These data indicate that XCI is initiated at the morula stage during bovine embryo development. To determine the degree to which initiation of XCI down-regulates expression of X-linked genes, published microarray data were analyzed. Unexpectedly, these data did not show a global downregulation of X-lined genes between bovine morulae and blastocysts.

After several rounds of cleavage divisions, the inner cells of the embryo develop into the inner cell mass (ICM) and the outer cells differentiate into the trophectoderm (TE); this is considered the first cell fate decision. It has previously been determined that the transcription factor CDX2 is essential for TE cell specification. Recent studies have shown that expression of CDX2 is regulated by the Hippo-YAP signaling pathway in the mouse. However, it was not known whether the Hippo-YAP signaling pathway was important for the activation of CDX2 expression in other mammalian embryos. In **chapter 3**, bovine embryos were cultured in the presence of Lysophosphatidic Acid (LPA), which maintains YAP expression by inhibiting its degradation. The onset of blastocyst formation on days 5 and 6 was accelerated when bovine embryos were cultured in the presence of LPA, but LPA did not affect the TE/ICM constitution of embryos. YAP was localized in nuclei in both morulae and blastocysts. The expression of *TAZ* and *TEAD4* was up-regulated in day 6 blastocysts after LPA

exposure compared to control culture medium. Expression of YAP was increased in LPA-treated day 6 and day 8 embryos, but expression of CDX2 was up-regulated only in day 8 embryos. Together these data indicate that, in bovine embryos, the TE/ICM ratio is not affected by the Hippo/YAP signaling pathway but blastocyst formation is accelerated.

Accurate assessment of the quality of embryos is important for clinicians to select the best embryo for transfer. Selecting embryos with good quality is also valuable for researchers to obtain reliable data. Embryo quality is mainly evaluated by morphological observation using conventional microscopy. Abundant cellular fragments in the perivitelline space of cleavage stage embryos is commonly used as an indicator of poor embryo quality. However, cellular fragments are difficult to identify once the blastocyst has expanded and the perivitelline space has become too small to identify cells. To assess the presence of cellular fragments after blastocyst expansion, embryos were mechanically hatched from their zona pellucidae in **chapter 4**, and the numbers of cells outside the embryo were determined. Nearly half of the expanded blastocysts examined had cellular fragments in the perivitelline space. To compare embryo quality between expanded blastocysts with and without cellular fragments in the perivitelline space, total cell number, ICM to TE ratio and percentage of apoptotic cells were determined. There was no significant difference in embryo quality between expanded blastocysts with and without cellular fragments. These data indicate that embryos shed cells, possibly those with abnormal chromosome numbers, during development, but that this does not necessarily compromise the viability of the embryos or indicate an embryo of poor quality.

A correct regulation of gene expression is essential during early embryonic development. Gene expression regulation in oocytes and embryos differs between different mammalian species. However, most of our knowledge about gene expression regulation has been derived from the mouse. In this thesis, we describe maternal mRNA regulation in bovine oocytes, initiation of XCI and regulation of transcription factors in bovine embryos. These data are important to increase our fundamental knowledge on mammalian early development and may be useful to improve reproductive technologies such as in vitro fertilization, both in the veterinary and in the human field.

Dutch Summary

Na bevruchting van een eicel door een spermacel wordt de totipotente zygoot gevormd, waarmee een nieuw leven begint. De zygoot start een serie van klievingsdelingen en eerste differentiatieprocessen en vormt een zogenaamde blastocyst. De buitenste cellen van een blastocyst, trofectoderm (TE) zijn noodzakelijk voor innesteling in de baarmoeder en vorming van de placenta, terwijl de binnenste cellen van een blastocyst, (binnenste celmassa of ICM) de eigenlijke foetus vormen en de dooierzak. Met andere woorden, miljoenen gedifferentieerde en gespecialiseerde cellen worden allemaal gevormd vanuit de eencellige zygoot. Om dit te bereiken dienen specifieke combinaties van genen en genproducten op het juiste moment en op de juiste locatie tot expressie worden gebracht. Regulering van genexpressie is cruciaal voor een goede embryonale ontwikkeling. Hoe de genexpressie specifiek is gereguleerd gedurende de embryogenese is niet goed bekend, en dit geldt met name voor de humane embryonale ontwikkeling.

De embryonale ontwikkeling van het rund is in verschillende aspecten vergelijkbaar met humane embryonale ontwikkeling; runderembryo's kunnen daarom gebruikt worden als model voor humane embryo's. Zowel koeien als vrouwen zijn mono-ovulatoir, en de tijdsduur van eicelrijping en pre-implantatie ontwikkeling is vergelijkbaar tussen de soorten. Van het rund kunnen relatief grote hoeveelheden ovaria verkregen worden van slachthuizen, en eicellen verkregen uit deze ovaria kunnen in vitro worden gerijpt, bevrucht en gekweekt tot een blastocyst.

Omdat de transcriptie van eicellen en embryo's vrijwel stil ligt vanaf *germinal vesicle breakdown* (GVBD) in de eicel tot de activatie van het embryonale genoom, wordt de genexpressie van eicellen en vroege embryo's voornamelijk bereikt door post-transcriptionele regulatie van maternale RNA's. De lengte van de poly(A) staart van maternale RNA's wordt gemodificeerd voor en na de selectie van mRNA's voor translatie. Om mRNA expressie te onderzoeken wordt veelal gebruik gemaakt van *reverse transcription polymerase chain reaction* (RT-PCR). *Reverse transcription* gebruik makende van oligo(dT) *primers* berust op de aanwezigheid van een poly(A) staart, terwijl *reverse transcription* met behulp van *random primers* daar niet van afhankelijk is. Het is derhalve mogelijk dat de verschillende methodes voor *reverse transcription* resulteren in verschillende meetbare niveaus van genexpressie. In **hoofdstuk 2** zijn rundereicellen verdeeld in twee gelijke groepen na de isolatie van RNA

waarna *reverse transcription* is gedaan gebruik makend van of *random*, of oligo(dT) *primers*. De (referentie)genen die het meest geschikt bleken voor normalisatie van genexpressie waren *RPL15*, *SDHA* en *ACTB* voor random primers, terwijl *HPRT1*, *YWHAZ* en *ACTB* het meest geschikt waren als referentiegenen wanneer de cDNA monsters geproduceerd waren met behulp van oligo(d) *primers*.

De gemeten niveaus van genexpressie bleken voor zowel *CCNB2* als *GAPDH* verschillend, afhankelijk van de methode van *reverse transcription*. Om er achter te komen of de niveaus van genexpressie onder andere worden veroorzaakt door de lengte van de poly(A) staart van mRNA, werd deze lengte bepaald door middel van *sequencing*. Gevonden werd dat de poly(A) staarten van *GAPDH*, *CCNB1* en *CCNB2* korter waren in eicellen van het metafase II (MII) stadium (rijpe eicellen) dan van onrijpe eicellen op het *germinal vesicle* stadium.

Gedurende de periode van activatie van het embryonale genoom worden maternale transcripten afgebroken, en starten de embryonale cellen met transcriptie van het eigen genoom. Genexpressie in embryonale cellen wordt dan gereguleerd op het niveau van transcriptie en epigenetische modificaties worden aangebracht. Inactivatie van het X-chromosoom (XCI) wordt epigenetisch bewerkstelligd en zorgt voor de juiste balans in X-chromosomale genexpressie tussen XY mannen en XX vrouwen. Dit proces wordt gestart gedurende de vroege embryonale ontwikkeling. De initiatie van XCI kan verschillende tussen zoogdiersoorten, zowel qua tijdspunt en regulering. Om te achterhalen op welk ontwikkelingstijdspunt XCI wordt gestart in runderembryo's werd de expressie van X-chromosoom gerelateerde genen onderzocht in eicellen van het GV stadium tot aan embryo's op het blastocyst stadium (**hoofdstuk 3**). Het expressieniveau van *XIST*, een *non-coding* RNA, werd verhoogd, maar het expressieniveau van *HPRT1* werd verlaagd van het 8-cellig stadium tot het moerbei stadium. Het eerste ontwikkelingsstadium waarop *XIST* werd gedetecteerd in de celkern was in vrouwelijke embryo's van het moerbei stadium, terwijl co-expressie van XIST en histon 3 lysine 27 trimethylatie voor het eerst werd geobserveerd in vrouwelijke blastocysten van dag 7. Deze data tonen aan dat XCI wordt geïnitieerd op het moerbeistadium van het rund. Om te bepalen in hoeverre XCI leidt tot vermindering van genen op het X-chromosoom werd de expressie geanalyseerd van gepubliceerde *micro-array* data. Hier werd uit geconcludeerd dat expressie van genen op het X-chromosoom niet globaal werd verminderd tussen het moerbei (*morula*) en blastocyst-stadium in rund.

Nadat het embryo enkele klievingsdelingen heeft ondergaan differentiëren

cellen tot een buitenste laag van trofectoderm (TE) en een binnenste celmassa (*inner cell mass*, ICM). De transcriptiefactor CDX2 is belangrijk voor differentiatie tot TE. De expressie van CDX2 wordt in embryo's van de muis gereguleerd door HIPPO-YAP signalering. Of deze signaaltransductieroute ook van belang is voor de expressie van CDX2 in andere zoogdieren is niet bekend. Daarom werden, zoals beschreven in **hoofdstuk 3**, runderembryo's gekweekt in aanwezigheid van Lysophosphatidic Acid (LPA), dat zorgt voor behoudt van YAP expressie door de degradatie van dit eiwit te verhinderen. In aanwezigheid van LPA werd de vorming van blastocysten op dagen 5 en 6 versneld, maar de verhouding van TE en ICM was niet anders dan deze verhouding in controle embryo's. *YAP* expressie werd gezien in de kernen van zowel *morulae* and blastocysten. Er werd een verhoogde expressie gevonden van *TAZ* en *TEAD* in dag 6 blastocysten na blootstelling aan LPA in vergelijking met controle blastocysten. De expressie van *YAP* was verhoogd in dag 6 en dag 8 embryo's na blootstelling aan LPA, maar de expressie van *CDX2* was alleen verhoogd op dag 8. Samengevoegd suggereren deze data dat in runderembryo's de TE-ICM ratio niet wordt bepaald door de HIPPO signaaltransductieroute, maar dar dat deze wel zorgt voor de snelheid waarop blastocysten worden gevormd.

Een juiste bepaling van embryokwaliteit is belangrijk voor fertiliteitsartsen om het beste embryo te selecteren voor terugplaatsing. Het selecteren van embryo's van goede kwaliteit is ook belangrijk voor onderzoekers om betrouwbare data te genereren. Embryokwaliteit wordt voornamelijk bepaald door morfologie met gebruik van conventionele microscopie. De aanwezigheid van celfragmenten in de perivitelline ruimte van embryo's gedurende de klievingsstadia wordt gezien als een indicator van een slechte kwaliteit. Deze celfragmenten zijn echter lastig te zien als de embryo's expanderen en de perivitelline ruimte te klein wordt om hierin celfragmenten te kunnen zien. Om de aanwezigheid van celfragmenten te bepalen bij geëxpandeerde blastocysten zijn, beschreven in **hoofdstuk 4**, embryo's mechanisch gekipt van de zona pellucida, en de aantallen cellen buiten de embryo's geteld. In bijna de helft van het aantal geëxpandeerde blastocysten werden celfragmenten aangetroffen in de perivitelline ruimte. Om embryokwaliteit van geëxpandeerde blastocysten te vergelijken tussen embryo's met en zonder celfragmenten werden totale celaantallen, ICM/TE ratio en percentages apoptotische cellen bepaald. Er werden geen significante verschillen gevonden in deze embryo kwaliteitsparameters tussen embryo's met en zonder celfragmenten. Deze data suggereren dat embryo's cellen, mogelijk met abnormale chromosoomaantallen, afscheiden gedurende de ontwikkeling, maar dat dit de kwaliteit van de embryo's

niet beïnvloedt.

Een correcte regulatie van genexpressie is essentieel gedurende de vroegembryonale ontwikkeling. De routes waarop deze regulatie plaatsvindt verschillen tussen de zoogdiersoorten, maar de meeste informatie die we hierover hebben is afkomstig van experimenten met muizen. In dit proefschrift wordt de regulatie van mRNA expressie, de start van X-chromosoominactivatie en de regulatie van expressie van transcriptiefactoren beschreven in runderembryo's. Deze data zijn belangrijk om onze kennis over vroegembryonale ontwikkeling van zoogdieren te vergroten en kunnen nuttig zijn voor reproductietechnieken zoals reageerbuisbevruchting, zowel in het veterinaire als in het humane veld.

Appendices

Acknowledgement

Looking back on the past five years as a PhD student at Utrecht University, I have received a lot of help, support and care from many people. It is my luck to have all those fantastic people who made this thesis possible. Here, I would like to thank to all the people around me thoughout my wonderful journey in the Netherlands.

First and foremost, I am deeply grateful to have you as my supervisors, Professor Tom Stout and Dr. Bernard Roelen. Tom, thank you for all the support, encouragement and patience you have provided during my scientific journey. Although we sometimes end up with disagreement, I still really enjoy all the constructive discussions and thought exchanges during our Thursday meeting. Hi, Bernard, thank you so much for everything. You are more like a problem solving machine and a lighthouse during my PhD time. Each time I met problem, I always tell myself 'Do not worry, I have Bernard with me'. This confidence I built with you is more valuable than knowledge I have learnd. Additionally, your passion in science always inspired me to move forward and go deeper.

I also would like to thank to my colleagues at the Department of Farm Animal Health, JDV building. Leni, thanks for your constant patience and help whenever I needed. I still remember that you tried to use Google Translate and drawing to make your idea clear, because of my bad English in the first year of my PhD. Arend, I wish your piano skill improves everyday and I believe that you will hold a personal concert one day. Christine, I really appreciate that you always share some traditional Chinese food with me during Chinese festivals. The moon cake you made is indeed amazing. Sometimes, people prefer to speak, but Elly, you always translate Dutch into English for me. Thank you. Also Eric, you like to teach me some Dutch and still now I can pronounce phases like 'oede morgen' and 'fijn weekend'. Besides, I would like express my thanks to Hilde, Mabel, Claudia, Marilena, Kaatje and Marcia for helping me in the lab.

My special thanks to Richard Wubbolts from Center for Cellular Imaging for teaching me fluorescence image analysis.

I am very thankful to my former colleagues for all the happy time in and outside the lab. Bart, you always tell me that I will become the president of China one day, hopefully, it will come true one day. Joesphin and Paula, I really missed the 'annoying time' we had togather. Nadia, Ivana, Kees, Raydian and Philippo, I really appreciate the unforgettable eating, driking and gaming time we have had.

I also take this opportunity to thank all the friends I met in the Netherlands. Chenyu, thanks for the companionship and the entertainment time for almost four years. Tianshu and Muge, still miss the days we had bear and we were hanging around. Min, special thanks for sharing your Chinese food for so many times. Wen, I miss the football matches we had watched togather. I am particularly grateful to Shuxian, You make me feel that Groningen is my second hometown in the Netherlands.

My heartfelt thanks to my dear Mengying. Thank you for your companionship you had offered during my writing time. You make my life much more colorful.

Finally, I want to take this opportunity to express my deepest gratitude to my beloved parents. You unconditionally support me during my five years in the Netherlands, both emotionally and financially. You came to the Netherlands to visit me, even though you two can only speak a few words in English. I am so proud and happy to be your son!

Curriculum Vitae

Bo Yu was born on October 3rd 1990 in Wuhan, China. After obtaining his bachelor of science in 2013, at Wuhan Polytechnic University (China), he started his veterinary medicine study at Northwest A&F University (China) and obtained his master degree of agriculture in 2016. In 2016, he started to his PhD research at Faculty of Veterinary Medicine, Utrecht University (the Netherlands). This thesis in the dissertation of his PhD research, which is funded by the China Scholarship Council (CSC).

List of Publications

1. Yu B, van Tol HTA, Oei CHY, Stout TAE, Roelen BAJ. Lysophosphatidic Acid Accelerates Bovine In Vitro-Produced Blastocyst Formation through the Hippo/YAP Pathway. *International journal of molecular sciences* 2021a;**22**.

2. Yu B, van Tol HTA, Stout TAE, Roelen BAJ. Cellular Fragments in the Perivitelline Space Are Not a Predictor of Expanded Blastocyst Quality. *Frontiers in cell and developmental biology* 2020a;**8**:616801.

3. Yu B, van Tol HTA, Stout TAE, Roelen BAJ. Initiation of X Chromosome Inactivation during Bovine Embryo Development. *Cells* 2020b;**9**.

4. Yu B, van Tol HTA, Stout TAE, Roelen BAJ. Reverse transcription priming methods affect normalisation choices for gene expression levels in oocytes and early embryos. *Molecular human reproduction* 2021b;**27**.